Department of Radio Science and Engineering

Solutions to electromagnetic integral equations exploiting addition theorems

Tommi Dufva

Aalto University

DOCTORAL DISSERTATIONS

Aalto University publication series
DOCTORAL DISSERTATIONS 89/2011

Solutions to electromagnetic integral equations exploiting addition theorems

Tommi Dufva

Doctoral dissertation for the degree of Doctor of Science in Technology to be presented with due permission of the School of Electrical Engineering for public examination and debate in Auditorium S1 at the Aalto University School of Electrical Engineering (Espoo, Finland) on the 21th of October 2011 at 12 o'clock.

Aalto University
School of Electrical Engineering
Department of Radio Science and Engineering
Electromagnetics

Supervisors
Prof. Jukka Sarvas
Prof. Keijo Nikoskinen

Instructor
Dr. Johan Sten

Preliminary examiners
Dr. Ignace Bogaert, Ghent University, Belgium
Prof. Karri Muinonen, University of Helsinki, Finland

Opponent
Assoc. Prof. Vladimir Okhmatovski, University of Manitoba, Canada

Aalto University publication series
DOCTORAL DISSERTATIONS 89/2011

ISBN 978-952-60-4301-2 (pdf)
ISBN 978-952-60-4300-5 (printed)
ISSN-L 1799-4934
ISSN 1799-4942 (pdf)
ISSN 1799-4934 (printed)

Aalto Print
Helsinki 2011

Finland

The dissertation can be read at http://lib.tkk.fi/Diss/

Aalto University

Abstract

Aalto University, P.O. Box 11000, FI-00076 Aalto www.aalto.fi

Author
Tommi Dufva

Name of the doctoral dissertation
Solutions to electromagnetic integral equations exploiting addition theorems

Publisher School of Electrical Engineering

Unit Department of Radio Science and Engineering

Series Aalto University publication series DOCTORAL DISSERTATIONS 89/2011

Field of research Electromagnetics

Manuscript submitted 6 April 2011 **Manuscript revised** 22 August 2011

Date of the defence 21 October 2011 **Language** English

☐ **Monograph** ☒ **Article dissertation (summary + original articles)**

Abstract

A variety of electromagnetic field problems can be most elegantly formulated by integral equations. A common way to search for a solution to such an integral equation is the method of moments (MoM) where the equation is discretised by expanding the unknown function in basis functions and forcing the error in the approximation to be orthogonal to test functions. Many times, the method can be enhanced by exploiting wave functions together with addition theorems for them.

The thesis treats three electromagnetic field problems formulated by integral equations: one electrostatic, one magnetostatic and one time-harmonic. The geometry in the static problems consists of ring conductors, and the solution can be constructed by using sophisticated entire-domain basis functions and Galerkin's method. The geometry in the time-harmonic problem is an extremely complex model of a pine tree, and therefore, the solution must be formed by using simple sub-domain basis functions and point matching.

In each of the above solutions, wave functions together with addition theorems for them are exploited. In the static problems, the Green's function is expanded in cylindrical wave functions, the MoM matrix terms are formulated partly in the spectral domain using addition theorems for the cylindrical wave functions, and certain integral results are derived from addition theorems for ultra-spherical wave functions. In the time-harmonic problem, the discretised problem is solved by using an iterative scheme and the calculation is accelerated by using the Multilevel fast multipole algorithm (MLFMA) which is based on addition theorems for spherical wave functions.

The thesis is based upon five publications. The first two publications present an efficient and accurate method for calculating the capacitances and inductances of ring conductors in a layered medium. The third publication gives a unified and transparent derivation of translational addition theorems for spherical wave functions. The last two publications concern the MLFMA. The former one describes a broadband version of the MLFMA with some novel ideas, and the latter one applies the algorithm in calculating the scattering of an electromagnetic plane wave by a pine tree.

Keywords integral equations, method of moments, wave equation, wave functions, addition theorems, Multilevel fast multipole algorithm, capacitance, inductance, scattering

ISBN (printed) 978-952-60-4300-5 **ISBN (pdf)** 978-952-60-4301-2

ISSN-L 1799-4934 **ISSN (printed)** 1799-4934 **ISSN (pdf)** 1799-4942

Location of publisher Espoo **Location of printing** Helsinki **Year** 2011

Pages 191 **The dissertation can be read at** http://lib.tkk.fi/Diss/

Aalto-yliopisto

Tiivistelmä

Aalto-yliopisto, PL 11000, 00076 Aalto www.aalto.fi

Tekijä
Tommi Dufva

Väitöskirjan nimi
Ratkaisuja sähkömagnetiikan integraaliyhtälöihin lisäysteoreemoja hyödyntäen

Julkaisija Sähkötekniikan korkeakoulu

Yksikkö Radiotieteen ja -tekniikan laitos

Sarja Aalto University publication series DOCTORAL DISSERTATIONS 89/2011

Tutkimusala Sähkömagnetiikka

Käsikirjoituksen pvm 06.04.2011 **Korjatun käsikirjoituksen pvm** 22.08.2011

Väitöspäivä 21.10.2011 **Kieli** Englanti

☐ **Monografia** ☒ **Yhdistelmäväitöskirja (yhteenveto-osa + erillisartikkelit)**

Tiivistelmä

Moni sähkömagnetiikan ongelma on formuloitavissa kaikkein näppärimmin integraaliyhtälöiden avulla. Tavallinen tapa hakea ratkaisua tällaiselle integraaliyhtälölle on momenttimenetelmä (MoM), jossa yhtälö diskretoidaan kehittämällä tuntematon funktio summaksi kantafunktioita ja pakottamalla approksimaation virhe ortogonaaliseksi testifunktioihin nähden. Monesti menetelmää on mahdollista tehostaa hyödyntämällä aaltofunktioita ja niiden lisäysteoreemoja.

Väitöstyö käsittelee kolmea integraaliyhtälöiden avulla formuloitua sähkömagnetiikan ongelmaa: yhtä sähköstaattista, yhtä magnetostaattista ja yhtä aikaharmonista. Staattisissa ongelmissa geometria muodostuu rengasmaisista johtimista ja ratkaisut voidaan rakentaa käyttämällä erityisiä kokoalueen kantafunktioita ja Galerkinin menetelmää. Aikaharmonisessa ongelmassa geometriana on erittäin pikkutarkka malli männystä, mistä johtuen ratkaisu täytyy muodostaa käyttämällä yksinkertaisia osa-alueen kantafunktioita ja pistesovitusta.

Kussakin yllä mainitussa ratkaisussa hyödynnetään aaltofunktioita sekä niiden lisäysteoreemoja. Staattisissa ongelmissa Greenin funktio kehitetään summaksi sylinteriaaltofunktioita, momenttimenetelmän matriisialkiot formuloidaan osittain spektraaliavaruudessa hyödyntäen sylinteriaaltofunktioiden lisäysteoreemoja ja tietyt integraalitulokset johdetaan ultra-palloaaltofunktioiden lisäysteoreemoista. Aikaharmonisessa ongelmassa diskretoitu ongelma ratkaistaa käyttämällä iteratiivista menetelmää ja laskentaa nopeutetaan käyttämällä Monitasoista nopeaa multipolialgoritmia (MLFMA), joka perustuu palloaaltofunktioiden lisäysteoreemoihin.

Väitöstyö perustuu viiten julkaisuun. Kaksi ensimmäistä julkaisua esittelevät nopean ja tarkan menetelmän, jolla voi laskea kerroksellisessa väliaineessa sijaitsevien rengasmaisten johtimien kapasitanssit ja induktanssit. Kolmas julkaisu esittää yhtenäisen ja selkeän johdon palloaaltofunktioiden lisäysteoreemoille. Kaksi viimeistä julkaisua käsittelevät MLFMA:ta. Näistä ensimmäinen kuvailee laajakaistaisen version MLFMA:sta muutaman uuden idean kera ja jälkimmäinen soveltaa menetelmää laskettaessa sähkömagneettisen aallon sirontaa männystä.

Avainsanat integraaliyhtälöt, momenttimenetelmä, aaltoyhtälö, aaltofunktiot, lisäysteoreemat, Monitasoinen nopea multipolialgoritmi, kapasitanssi, induktanssi, sironta

ISBN (painettu) 978-952-60-4300-5 **ISBN (pdf)** 978-952-60-4301-2

ISSN-L 1799-4934 **ISSN (painettu)** 1799-4934 **ISSN (pdf)** 1799-4942

Julkaisupaikka Espoo **Painopaikka** Helsinki **Vuosi** 2011

Sivumäärä 191 **Luettavissa verkossa osoitteessa** http://lib.tkk.fi/Diss/

Preface

When I finished my Master's thesis at VTT, Dr. Johan Sten pushed me to continue with postgraduate studies straight away. Heeding the advice, I took some courses, and during one Tekes project I wrote with Johan the first publication of the thesis.

While writing the second publication, we applied for funding from the Academy of Finland in collaboration with Prof. Jukka Sarvas' group at TKK. We had no luck with the application, but yet Jukka wanted to help me with my studies and arranged for me a postgraduate position at TKK. During the next three years I wrote with Jukka, Johan, Jaan Praks and Dr. Seppo Järvenpää the last three publications of the thesis.

I felt lucky to have two different mentors, one specialised in theoretical, the other in computational electromagnetics. I thank both Johan and Jukka. I also thank Jaan and Seppo for collaboration in writing the fifth publication.

I thank Prof. Keijo Nikoskinen for acting as the custos in the public defense of the thesis. I also thank Jouko Aurinsalo for taking care of my interests at VTT.

At this point, I want to thank the whole staff of the former Electromagnetics laboratory at TKK for the enthusiastic atmosphere and excellent teaching — two of the reasons why I got interested in electromagnetics in the first place. I also thank my colleagues at VTT for a more practical viewpoint to electromagnetic problems.

Finally, I thank Riina for English help in finishing the thesis and for company in other things. My parents I thank for all the help and else.

Helsinki, September 26, 2011,

Tommi Dufva

Contents

Preface 1

Contents 3

List of Publications 5

Author's Contribution 7

List of Figures 9

List of Abbreviations 11

List of Symbols 13

1 Introduction 17

2 Basics of the electromagnetic field 21

2.1 Maxwell's equations 21

2.2 Conditions at interfaces and boundaries 23

2.3 Potential functions 23

2.4 Separation of time dependency 24

2.5 Solution of field for a given source 25

2.6 Static field 26

3 Selected electromagnetic problems formulated by integral equations 29

3.1 Capacitances of conductors 29

3.2 Inductances of conductors 30

3.3 Scattering of electromagnetic plane wave by a dielectric object 32

4 Method of moments 35

4.1 Overview of method 35

4.2 Variational principle 36
4.3 Definitions of original and adjoint problems 37
4.4 Choice of basis and test functions 40
4.5 Solution of discretised problem 42

5 Wave functions and translational addition theorems for them 43
5.1 In an arbitrary separable system of co-ordinates 43
5.2 In rectangular system of co-ordinates 46
5.3 In cylindrical system of co-ordinates 48
5.4 In spherical system of co-ordinates 50
5.5 In ultra-spherical system of co-ordinates 58

6 Spatial-spectral hybrid method in cylindrical system of co-ordinates 59
6.1 Hankel transforms 59
6.2 Static Green's function in layered medium 60
6.3 MoM system matrix terms in hybrid method 61
6.4 Charge and current on ring conductor 63
6.5 Application to an LC-model of a spiral inductor 66

7 Multilevel fast multipole algorithm 69
7.1 Overview of algorithm with expansions in wave functions . . 69
7.2 Diagonal translations with wave patterns 75
7.3 Interpolation and anterpolation 78
7.4 Alternative expansions enabling full use of the FFT 80
7.5 Error control 82
7.6 Application to a scattering model of a pine tree 83

8 Conclusions 85

Bibliography 89

Publications 93

List of Publications

This thesis consists of an overview and of the following publications which are referred to in the text by their Roman numerals.

I T. J. Dufva and J. C.-E. Sten. Quasi-static variational analysis of planar spiral conductors. *J. of Electromagn. Waves and Appl.*, Vol. 16, No. 7, 957–976, 2002.

II T. J. Dufva and J. C.-E. Sten. Calculation of capacitances and inductances of ring conductors in a stratified medium. *Electromagn.*, Vol. 26, No. 8, 581–599, 2006.

III T. J. Dufva, J. Sarvas and J. C.-E. Sten. Unified derivation of the translational addition theorems for the spherical scalar and vector wave functions. *Progress In Electromagnetics Research B*, Vol. 4, 79–99, 2008.

IV T. Dufva and J. Sarvas. Broadband MLFMA with plane wave expansions and optimal memory demand. *IEEE Trans. Antennas Propag.*, Vol. 57, No. 3, 742–753, 2009.

V T. Dufva, J. Praks, S. Järvenpää and J. Sarvas. Scattering model for a pine tree employing VIE with a broadband MLFMA and comparison to ICA. *IEEE Trans. Geosci. Remote Sens.*, Vol. 48, No. 3, 1119–1127, 2010.

Author's Contribution

Publication I: "Quasi-static variational analysis of planar spiral conductors"

Publication I is a continuation to the author's Master's thesis on a similar method applied to straight strip conductors. Dr. Johan Sten found the idea of approximating a spiral by concentric rings and the references providing the needed integral transforms. Otherwise, the theory and equations were formulated, the computer program was coded, and the numerical examples were computed by the author. The text was written in collaboration.

Publication II: "Calculation of capacitances and inductances of ring conductors in a stratified medium"

Publication II is a continuation to Publication I. Dr. Johan Sten found the reference providing some of the needed integral transforms. Prof. Jukka Sarvas gave a hint on numerical integration. Otherwise, the theory and equations were formulated, the computer program was coded, and the numerical examples were computed by the author. The text was written in collaboration between the author and Dr. Johan Sten.

Publication III: "Unified derivation of the translational addition theorems for the spherical scalar and vector wave functions"

The idea of writting Publication III came from Prof. Jukka Sarvas after an extensive study on the subject by the author. The theory and equations were formulated mostly by the author under the guidance of Prof. Jukka

Sarvas. The text was written in collaboration between the author and Prof. Jukka Sarvas, with comments and advice by Dr. Johan Sten.

Publication IV: "Broadband MLFMA with plane wave expansions and optimal memory demand"

Prof. Jukka Sarvas introduced the author to the subject of Publication IV. The ideas, theory, equations and text were all results of collaboration. The computer program was coded, and the numerical examples were computed by the author.

Publication V: "Scattering model for a pine tree employing VIE with a broadband MLFMA and comparison to ICA"

Publication V reports testing the method presented in Publication IV in the solution of a volume integral equation (VIE) and comparing it with the infinite cylinder approximation (ICA) studied by Prof. Jukka Sarvas and Jaan Praks. The theory and equations were formulated mainly by the author. The discussion on the results of the two methods was provided mainly by Jaan Praks. The computer program for the VIE was first coded in Matlab by the author and then in C language by Dr. Seppo Järvenpää. The numerical examples for the VIE were computed by Dr. Seppo Järvenpää and for the ICA by Jaan Praks. The combination of the results of the two methods was done by the author. The whole work was guided by Prof. Jukka Sarvas.

List of Figures

3.1 Conductors, the ground and a dielectric medium. 30
3.2 Loop conductors and magnetic fluxes. 31
3.3 An incident electric field, a scatterer and a scattered electric field. 33

4.1 Example of constructing the electric charge on an indefinitely thin strip conductor. 41

5.1 Translation of origin. 44
5.2 Translation of origin in the cylindrical system of co-ordinates. 49

6.1 System of co-ordinates and layered medium. 61
6.2 Ring conductors in a layered medium. 62
6.3 Spiral conductor. 67
6.4 Steps in approximating a spiral conductor and charge/current on it. 67
6.5 LC-model for a spiral conductor. 68

7.1 Example of the hierarchical system of the MLFMA. 71
7.2 Examples of translations in the MLFMA hierarchical system. 73
7.3 Illustrative paths on the complex α-plane defined by $\cos\alpha = \varrho e^{i\gamma}$ in comparison to Γ. 82

List of Abbreviations

FFT	Fast Fourier transform
GMRES	Generalized Minimal Residual method
MLFMA	Multilevel fast multipole algorithm
MoM	Method of moments

List of Symbols

i	Imaginary unit equal to $\sqrt{-1}$
$\mathbf{v}$	Vector
$\hat{v}$	Unit vector into the direction of $\mathbf{v}$
f	Scalar function
$\mathbf{F}$	Vector function
$\mathbb{F}$	Dyadic function
$\mathbf{E}$	Electric field
$\mathbf{B}$	Magnetic induction
$\mathbf{D}$	Electric displacement
$\mathbf{H}$	Magnetic field
$\mathbf{J}$	Electric current
ϱ	Electric charge
$\mathbf{P}$	Polarisation
$\mathbf{M}$	Magnetisation
$\mathbf{A}$	Vector potential
Φ	Scalar potential
G	Green's function
$\mathbb{G}$	Green's dyadic
c	Speed of light
ϵ	Electric permittivity

μ	Magnetic permeability
σ	Conductivity
Q	Total electric charge
U	Voltage
C	Capacitance
I	Total electric current
Ψ	Magnetic flux
L	Inductance
$\mathbf{E}_\infty$	Radiation pattern of $\mathbf{E}$
$\mathbf{E}_0$	Incoming wave pattern of $\mathbf{E}$
t	Time
ω	Angular frequency of oscillation
$\mathbf{r}$	Position vector
$\mathbf{k}$	Wave vector
x, y, z	Spatial co-ordinates in a rectangular system
k_x, k_y, k_z	Spectral co-ordinates in a rectangular system
ρ, ϕ, z	Spatial co-ordinates in a cylindrical system
k_ρ, β, k_z	Spectral co-ordinates in a cylindrical system
r, θ, ϕ	Spatial co-ordinates in a spherical system
k, α, β	Spectral co-ordinates in a spherical system
ψ_n	Scalar wave function
$\mathbf{L}_n$, $\mathbf{M}_n$, $\mathbf{N}_n$	Vector wave functions
J_m	Bessel function of the first kind
j_l	Spherical Bessel function of the first kind
$h_l^{(1)}$	Spherical Hankel function of the first kind
$Y_{l,m}$	Scalar spherical harmonic

$\mathbf{U}_{l,m}$, $\mathbf{V}_{l,m}$	Vector spherical harmonics
P_l^m	Associate Legendre function
$C_n^{(\alpha)}$	Gegenbauer polynomial
T_n	Chebyshev polynomial of the first kind

1. Introduction

In general, there are two ways to formulate an electromagnetic field problem: either by a differential equation for a field function or by an integral equation for a source function. One of the differences between the two formulations is that a field function spreads out over all the space within the boundaries, while a source function is confined inside or on the surfaces of material objects. Consequently, differential equation formulations are best suited for bounded problems but without further restrictions for the geometry and the matter. On the other hand, integral equation formulations are well suited for unbounded as well as bounded problems, as long as there are separate material objects and a simple background.

In order to find an accurate solution to any practical electromagnetic field problem, formulated either by a differential equation or an integral equation, the problem needs to be discretised, meaning that the unknown function is expanded in a suitable set of building blocks, called basis functions. In consequence, the original problem is transformed into finding such values for the expansion coefficients that the expansion approximates the unknown function well. One way to accomplish this is the method of moments (MoM), which adjusts the values of the expansion coefficients through the moments of the responses to the basis functions with respect to another set of functions, called test functions.

The choices of the basis and test functions determine the characters of the discretised problem, while the geometry and other properties of the original problem confine the choices of the basis and test functions. If the geometry is complicated, the unknown function is typically constructed out of simple sub-domain basis functions. This often leads to an elaborate and difficult discretised problem. However, if the geometry is such that it aligns with one of the separable systems of co-ordinates, the unknown function can usually be constructed out of more sophisticated and physical

entire-domain basis functions. This often leads to a compact and easy discretised problem. The test functions determine the measure for the error in the approximation or, in other words, the distance of the approximate solution to the exact solution.

Regarding the differences in discretising differential and integral equations, the advantage of differential equations is that the discretisation leads to a sparse system matrix while with integral equations the system matrix is full. On the other hand, the advantage of integral equations is that, since the unknown function is usually confined into a smaller region, the system matrix is smaller, too.

In this thesis, two topics will be highlighted. As the first one, the thesis treats three selected electromagnetic problems formulated by integral equations: one electrostatic problem, one magnetostatic problem and one time-harmonic electromagnetic problem. The geometry considered in both static problems consists of ring conductors and is such that the unknown source functions can be expanded in the most sophisticated entire-domain basis functions, resulting in a compact and easy discretised problem. In contrast, the geometry considered in the time-harmonic problem is an extremely complex geometry model for a pine tree and, consequently, the unknown function is expanded in the simplest sub-domain basis functions, resulting in a more challenging discretised problem.

The second highlighted topic of the thesis is the translational addition theorems for wave functions. Even when solving an integral equation with a source function, it is often useful also to expand auxiliary field functions, such as the Green's function, in basis functions, for instance, in wave functions, which are characteristic solutions of wave equations resulting from Maxwell's equations. Expansions in wave functions are limited to the particular system of co-ordinates; if the system is changed, the coefficients of the expansion are changed as well. One possible change of the system is a translation of the origin. In that case, the coefficients in the translated system are found with the aid of translational addition theorems for wave functions. The theorems give a wave function in the translated system in terms of the wave functions in the initial system.

One important application for the translational addition theorems is the Multilevel fast multipole algorithm (MLFMA), which is a method for speeding up a matrix-vector multiplication needed in an iterative solution of an integral equation discretised by the MoM. The matrix-vector multiplication equals to a calculation of interactions between sources rep-

resented by the basis and test functions. The MLFMA arranges these sources into groups and calculates far interactions between these groups collectively. This procedure takes advantage of the translation addition theorems or, to be more precise, diagonal forms of them. In the thesis, some novel ideas are introduced to the MLFMA and the resulting algorithm is applied to the solution of the pine tree problem mentioned above.

Besides their primary purposes, addition theorems serve also as sources of various useful integral results involving wave functions. In the thesis, such results are exploited in the solution of the conducting ring problems mentioned above.

The thesis is based upon five publications written and published during the years 2002–2010. Publications I and II present an efficient and accurate method for calculating the capacitances and inductances of ring conductors in a layered medium. The former one introduces the method for thin conductors, and the latter one generalises it for thick conductors. Publication III gives a unified and transparent derivation of translational addition theorems for spherical wave functions. Publications IV and V concern the MLFMA. The former one describes a broadband version of the MLFMA with some novel ideas, and the latter one applies the algorithm in calculating the scattering of an electromagnetic plane wave by a pine tree.

The objectives of this synopsis are to establish the context for the publications and to place them into the vast scope of electromagnetic theory and computing, to show the connections between the publications and the two highlighted topics mentioned above, and to revise some details of the methods and results presented in the publications.

The synopsis is organised as follows: Section 2 reviews the basics of the electromagnetic theory in the extent required by the subsequent topics. In Section 3, the selected electromagnetic problems treated in Publications I, II and V are formulated by integral equations. Section 4 reviews the principles of the MoM considering also the variational principle, which gives another point of view to the method. Thereafter, the definitions of the electromagnetic problems formulated in Section 3 are specified to match with the mathematical theory of the MoM and the variational principle. Also, the choices of the basis and test functions, in particular for the selected problems, are discussed. Section 5 discusses wave functions and translational addition theorems for them. The discussion is started with formal definitions of the wave functions and the theorems in an arbitrary

system of co-ordinates and is continued with specific definitions in the rectangular and cylindrical system of co-ordinates. Next, the wave functions and the theorems are given in the spherical systems of co-ordinates as presented in Publication III. At the end, one special case of the theorem is given in an ultra-spherical system of co-ordinates, which is utilised later. Section 6 gives an overview of the spatial-spectral hybrid method in the cylindrical system of co-ordinates that is presented in Publications I and II to calculate capacitances and inductances of ring conductors. These capacitances and inductances can be used to construct equivalent circuit models for inductors, transformers, split-ring resonators, etc., as illustrated with an example at the end of the section. Section 7 discusses the MLFMA, first giving a brief overview of the algorithm and then describing the advantages of the more advanced methods presented in Publication IV. At the end of the section, an introduction is given for Publication V, in which the MLFMA is applied in an MoM solution of a volume integral equation related to scattering of an electromagnetic plane wave by a pine tree. Finally, some conclusions of the thesis are made in Section 8.

Since the publications of the thesis were written over quite a long period of time and under the influence of two different mentors, the notation varies slightly from one publication to another. In order to have a consistent notation throughout the synopsis, the notation has been adjusted and consequently it differs in places from that in the publications. Also, some details are revised. The author apologises for any possible inconvenience.

2. Basics of the electromagnetic field

2.1 Maxwell's equations

According to Maxwell's electromagnetic theory, see e.g. [1], [2], [3], [4] and [5], the electromagnetic field is described by the electric field $\mathbf{E}$ (measured in V/m), the magnetic induction $\mathbf{B}$ (Vs/m^2), the electric displacement $\mathbf{D}$ (As/m^2) and the magnetic field $\mathbf{H}$ (A/m); the source of the field is described by the electric current $\mathbf{J}$ (A/m^2) and the electric charge ϱ (As/m^3); and the field is related to the source by Maxwell's equations

$$\nabla \times \mathbf{E} = -\frac{\partial \mathbf{B}}{\partial t}, \tag{2.1}$$

$$\nabla \times \mathbf{H} = \mathbf{J} + \frac{\partial \mathbf{D}}{\partial t}, \tag{2.2}$$

$$\nabla \cdot \mathbf{D} = \varrho, \tag{2.3}$$

$$\nabla \cdot \mathbf{B} = 0. \tag{2.4}$$

The source complies with the fundamental equation of continuity,

$$\nabla \cdot \mathbf{J} = -\frac{\partial \varrho}{\partial t}, \tag{2.5}$$

which is inbuilt in the pair (2.2) and (2.3).

In a vacuum,

$$\mathbf{D} = \epsilon_0 \mathbf{E}, \tag{2.6}$$

$$\mathbf{H} = \frac{1}{\mu_0} \mathbf{B}, \tag{2.7}$$

where $\mu_0 = 4\pi \cdot 10^{-7}$ Vs/Am is the magnetic permeability and $\epsilon_0 \approx 8.854 \cdot 10^{-12}$ As/Vm is the electric permittivity so that $(\mu_0 \epsilon_0)^{-1/2}$ equals exactly $c = 299792458$ m/s, which is the speed of light. With (2.6) and (2.7), (2.2) and (2.3), respectively, read

$$\nabla \times \mathbf{B} = \mu_0 \mathbf{J} + \frac{1}{c^2} \frac{\partial \mathbf{E}}{\partial t}, \tag{2.8}$$

$$\nabla \cdot \mathbf{E} = \frac{1}{\epsilon_0} \varrho. \tag{2.9}$$

In a medium, the field interferes with the electric equilibrium in atoms and molecules inducing electric dipoles and arranges permanent electric and magnetic dipoles. On a macroscopic scale, the effect of those dipoles can be described through average quantities, the polarisation $\mathbf{P}$ (As/m^2) and the magnetisation $\mathbf{M}$ (A/m), which can, as explained e.g. in [5, Sec. 9.2], be added as additional sources to the right-hand-sides of (2.8) and (2.9) as

$$\nabla \times \mathbf{B} = \mu_0 \left(\mathbf{J} + \epsilon_0 \frac{\partial \mathbf{E}}{\partial t} + \frac{\partial \mathbf{P}}{\partial t} + \nabla \times \mathbf{M} \right), \tag{2.10}$$

$$\nabla \cdot \mathbf{E} = \frac{1}{\epsilon_0} (\varrho - \nabla \cdot \mathbf{P}). \tag{2.11}$$

Then, defining

$$\mathbf{D} = \epsilon_0 \mathbf{E} + \mathbf{P}, \tag{2.12}$$

$$\mathbf{H} = \frac{1}{\mu_0} \mathbf{B} - \mathbf{M}, \tag{2.13}$$

(2.10) and (2.11) are compressed to (2.2) and (2.3), respectively.

In an arbitrary medium, the dependence of $\mathbf{P}$ and $\mathbf{M}$ on the field can be quite complex. In a linear, isotropic, non-dispersive medium, however, the relations can be formulated as

$$\mathbf{P} = \epsilon_0 \chi_\mathrm{e} \mathbf{E}, \tag{2.14}$$

$$\mathbf{M} = \chi_\mathrm{m} \mathbf{H}, \tag{2.15}$$

where χ_e and χ_m are the electric and magnetic susceptibilities, respectively. Then, (2.12) and (2.13) are compressed to

$$\mathbf{D} = \epsilon \mathbf{E}, \tag{2.16}$$

$$\mathbf{H} = \frac{1}{\mu} \mathbf{B}, \tag{2.17}$$

with the electric permittivity ϵ and the magnetic permeability μ being given by

$$\epsilon = (1 + \chi_\mathrm{e}) \epsilon_0, \tag{2.18}$$

$$\mu = (1 + \chi_\mathrm{m}) \mu_0, \tag{2.19}$$

respectively.

In addition to the electric and magnetic dipoles, the medium may contain free electric charge carriers, which, in the presence of an electric field, give rise to a conductivity current. In a linear, isotropic and non-dispersive case, this current is given by

$$\mathbf{J}_\mathrm{c} = \sigma \mathbf{E}, \tag{2.20}$$

where σ (A/Vm) is the conductivity in the medium.

2.2 Conditions at interfaces and boundaries

The differential forms (2.1)–(2.4) of Maxwell's equations are not valid at an interface where the medium, and hence the field, too, is discontinuous. By examining the integral forms of Maxwell's equations near the interface, see e.g. [3, Sec. 1.13] or [4, Sec. I.5], the following conditions can be derived: If two regions separated by an interface are denoted by 1 and 2 and fields in the regions by corresponding subscripts, and if $\hat{n}$ is a unit vector normal to the interface and directed into region 2, the fields on the two sides of the interface are related as

$$\hat{n} \times (\mathbf{E}_2 - \mathbf{E}_1) = 0, \tag{2.21}$$

$$\hat{n} \times (\mathbf{H}_2 - \mathbf{H}_1) = \mathbf{J}_\mathrm{s}, \tag{2.22}$$

$$\hat{n} \cdot (\mathbf{D}_2 - \mathbf{D}_1) = \varrho_\mathrm{s}, \tag{2.23}$$

$$\hat{n} \cdot (\mathbf{B}_2 - \mathbf{B}_1) = 0, \tag{2.24}$$

where $\mathbf{J}_\mathrm{s}$ (A/m) and ϱ_s (As/m^2), respectively, are a surface current and charge at the interface.

An interface becomes a boundary if the field on either side vanishes. This happens, for example, if region 1 is filled with the perfect electric conductor, i.e., $\sigma_1 \to \infty$. Then, $\mathbf{E}_1 \to 0$ in order to prevent $\mathbf{J}_{\mathrm{c},1}$ given by (2.20) from becoming infinite. Conditions at such a boundary are obtained from (2.21)–(2.24) by setting the field in region 1 to zero.

2.3 Potential functions

The description of the electromagnetic field can be compacted into one vector function and one scalar function in the following manner.

By virtue of (2.4), $\mathbf{B}$ is solenoidal and can be represented as a curl of another vector function:

$$\mathbf{B} = \nabla \times \mathbf{A}. \tag{2.25}$$

If (2.25) is substituted into (2.1), it is found that $\mathbf{E} + \partial\mathbf{A}/\partial t$ is irrotational and can be set to equal the gradient of a scalar function, say $-\Phi$. Consequently, $\mathbf{E}$ can be represented as

$$\mathbf{E} = -\frac{\partial \mathbf{A}}{\partial t} - \nabla\Phi. \tag{2.26}$$

The auxiliary functions $\mathbf{A}$ (Vs/m) and Φ (V) are called the vector and scalar potentials, respectively.

In a linear, isotropic, non-dispersive, homogeneous, lossless medium with ϵ and μ constants and $\sigma = 0$, substitutions of (2.25) and (2.26) into the remaining equations (2.2) and (2.3), respectively, yields

$$\nabla^2 \mathbf{A} - \mu\epsilon \frac{\partial^2 \mathbf{A}}{\partial t^2} - \nabla\left(\nabla \cdot \mathbf{A} + \mu\epsilon \frac{\partial \Phi}{\partial t}\right) = -\mu \mathbf{J}, \tag{2.27}$$

$$\nabla^2 \Phi + \frac{\partial (\nabla \cdot \mathbf{A})}{\partial t} = -\frac{1}{\epsilon}\varrho. \tag{2.28}$$

The divergence of $\mathbf{A}$ can be freely chosen since (2.25) defines only the curl. A common choice is the Lorenz condition,

$$\nabla \cdot \mathbf{A} = -\mu\epsilon \frac{\partial \Phi}{\partial t}, \tag{2.29}$$

in which case (2.27) and (2.28), respectively, reduce to

$$\nabla^2 \mathbf{A} - \mu\epsilon \frac{\partial^2 \mathbf{A}}{\partial t^2} = -\mu \mathbf{J}, \tag{2.30}$$

$$\nabla^2 \Phi - \mu\epsilon \frac{\partial^2 \Phi}{\partial t^2} = -\frac{1}{\epsilon}\varrho. \tag{2.31}$$

These are the Helmholtz equations for the vector and scalar potentials.

2.4 Separation of time dependency

Solving (2.30) and (2.31) is often started by separating the time dependency. Separation of variables in the homogeneous equations shows that the time dependency of the field is of the form $e^{-i\omega t}$ where ω is the angular frequency of oscillation. This suggests that the field and the source can be expanded as

$$F(\mathbf{r}, t) = \frac{1}{2\pi} \int_{-\infty}^{\infty} f(\mathbf{r}, \omega) e^{-i\omega t}\, d\omega, \tag{2.32}$$

where F is a field or source component in the time-domain and f is its Fourier transform in the frequency-domain given by

$$f(\mathbf{r}, \omega) = \int_{-\infty}^{\infty} F(\mathbf{r}, t) e^{i\omega t}\, dt. \tag{2.33}$$

As is seen from (2.32), a derivation of F with respect to time equals a multiplication of f by $-i\omega$. Applying (2.32) on both sides of (2.30) and (2.31) yields, respectively,

$$\nabla^2 \mathbf{A} + k^2 \mathbf{A} = -\mu \mathbf{J}, \tag{2.34}$$

$$\nabla^2 \Phi + k^2 \Phi = -\frac{1}{\epsilon}\varrho, \tag{2.35}$$

where $k^2 = \omega^2 \mu\epsilon$. Here and henceforth, the functions in the frequency-domain are denoted with the same symbols as in the time-domain.

Besides the Helmholtz equations, all the above equations written in the time-domain can be rewritten in the frequency-domain by replacing the time derivations with multiplications by $-i\omega$. In particular, consider (2.8) and (2.9). In the frequency-domain, also the conductivity current defined in (2.20) can be added as an additional source to the right-hand-sides of the equations as

$$\nabla \times \mathbf{B} = \mu_0(\mathbf{J} - i\omega\epsilon_0\mathbf{E} - i\omega\mathbf{P} + \nabla \times \mathbf{M} + \sigma\mathbf{E}), \tag{2.36}$$

$$\nabla \cdot \mathbf{E} = \frac{1}{\epsilon_0}\left(\varrho - \nabla \cdot \mathbf{P} + \frac{\sigma}{i\omega}\nabla \cdot \mathbf{E}\right). \tag{2.37}$$

Now, by defining

$$\mathbf{D} = \epsilon_0\mathbf{E} + \mathbf{P} - \frac{\sigma}{i\omega}\mathbf{E}, \tag{2.38}$$

(2.36) and (2.37) are compressed to the frequency-domain forms of (2.2) and (2.3), respectively. Furthermore, in a linear, isotropic, spatially non-dispersive medium, by defining

$$\epsilon = (1 + \chi_\mathrm{e})\epsilon_0 - \frac{\sigma}{i\omega}, \tag{2.39}$$

(2.38) is compressed to (2.16). In the frequency-domain the temporal non-dispersivity is not required for (2.16), (2.17) and (2.20) to hold and ϵ, μ and σ may vary with the frequency.

2.5 Solution of field for a given source

Consider the scalar Helmholtz equation (2.35) with a normalised point source written as

$$(\nabla^2 + k^2)G(\mathbf{r}, \mathbf{r}') = -\delta(\mathbf{r} - \mathbf{r}'). \tag{2.40}$$

Here, the solution G is called a Green's function and is given by

$$G(\mathbf{r}, \mathbf{r}') = \frac{e^{ik|\mathbf{r}-\mathbf{r}'|}}{4\pi|\mathbf{r} - \mathbf{r}'|}. \tag{2.41}$$

The other independent solution, i.e., the one with a negative imaginary exponent, is rejected as it is not representing a field radiating outwards from the source. G in (2.41) is the Green's function for an unbounded space; the Green's function for a bounded space can be formulated as

$$G(\mathbf{r}, \mathbf{r}') = \frac{e^{ik|\mathbf{r}-\mathbf{r}'|}}{4\pi|\mathbf{r} - \mathbf{r}'|} + H(\mathbf{r}, \mathbf{r}') \tag{2.42}$$

where H is a solution of the homogeneous equation adjusting G to satisfy the required conditions at the boundary. Since the operator $\nabla^2 + k^2$

in (2.35) is linear, the solution for an arbitrary source in a volume V is obtained by superposing the solutions for point sources as

$$\Phi(\mathbf{r}) = \frac{1}{\epsilon} \int_V G(\mathbf{r}, \mathbf{r}') \varrho(\mathbf{r}') \, dV'. \tag{2.43}$$

By decomposing $\mathbf{A}$ and $\mathbf{J}$ into the three cartesian components, the vector Helmholtz equation (2.34) is decomposed into three scalar equations similar to (2.35). Consequently, G given by (2.41) or a variant of (2.42) applies also for (2.34) and the solution for an arbitrary source in a volume V is obtained as

$$\mathbf{A}(\mathbf{r}) = \mu \int_V G(\mathbf{r}, \mathbf{r}') \mathbf{J}(\mathbf{r}') \, dV'. \tag{2.44}$$

The field quantities can be obtained through (2.25) and the frequency-domain form of (2.26). For example, an explicit formula for $\mathbf{E}$ in terms of $\mathbf{J}$ is obtained by combining (2.44) and (2.43) according to (2.26) and using the frequency-domain form of (2.5) and the divergence theorem, see e.g. [3, Sec. 1.2, Eq. (8)], yielding

$$\mathbf{E}(\mathbf{r}) = \left(i\omega\mu\mathbb{I} - \frac{1}{i\omega\epsilon} \nabla\nabla \right) \cdot \int_V G(\mathbf{r}, \mathbf{r}') \mathbf{J}(\mathbf{r}') \, dV', \tag{2.45}$$

where $\mathbb{I}$ denotes a unit dyadic. If $\mathbf{r} \notin V$, (2.45) can be further compacted to

$$\mathbf{E}(\mathbf{r}) = i\omega\mu \int_V \mathbb{G}(\mathbf{r}, \mathbf{r}') \cdot \mathbf{J}(\mathbf{r}') \, dV' \tag{2.46}$$

by introducing the dyadic Green's function

$$\mathbb{G}(\mathbf{r}, \mathbf{r}') = \left(\mathbb{I} + \frac{1}{k^2} \nabla\nabla \right) G(\mathbf{r}, \mathbf{r}'). \tag{2.47}$$

2.6 Static field

In contrast to a dynamic field, a field is called static if it does not vary in time. A static field can be thought as an approximation to a dynamic field varying slowly in time; slowly meaning that, for instance, in the case of a time-harmonic field, $kd \ll 1$ where d is the diameter of the space of interest.

In statics, $\mathbf{E}$ and $\mathbf{D}$ are no longer connected to $\mathbf{B}$ and $\mathbf{H}$ through (2.1) and (2.2). In fact, as $kd \to 0$, usually either $\mathbf{B}$ and $\mathbf{H}$ or $\mathbf{E}$ and $\mathbf{D}$ vanish. In the former case, the remaining field is called electrostatic, in the latter case magnetostatic.

An electrostatic field is irrotational and, thus, can be expressed through the scalar potential alone. The source of an electrostatic field is a static

electric charge. Like $\mathbf{B}$ and $\mathbf{H}$ of any electromagnetic field, a magnetostatic field is solenoidal and can be expressed through the vector potential alone. The source of a magnetostatic field is a static electric current, which is solenoidal.

All the above equations written for a dynamic field can be rewritten for a static field by setting derivations with respect to time to zero or $\omega = 0$.

3. Selected electromagnetic problems formulated by integral equations

3.1 Capacitances of conductors

Consider an electrostatic field in the presence of P conductors, the ground and a dielectric medium illustrated in Fig. 3.1. Denote the surfaces of the conductors by $S_1, \ldots, S_P$. Let the electrostatic field be due to the electric charges $Q_1, \ldots, Q_P$ carried by the conductors. Inside the conductors the field vanishes and the scalar potential Φ gets constant values. Denote those values, i.e., the voltages representing the potential differences between the conductors and the ground, by $U_1, \ldots, U_P$. Relations between the charges and the voltages are given by capacitances (measured in F=As/V), which are parameters of the geometry and the medium. By introducing a matrix C consisting of those capacitances and compacting the charges and voltages in vectors Q and U, respectively, the relations read

$$Q = CU. \tag{3.1}$$

Let the problem be to find C.

The vanishing of the electric field inside a conductor is a result of the settling of the charge onto the surface of the conductor. Denote the surface charge distribution on the pth conductor by ϱ_p. Because the field is zero inside the conductor, the conductor can be removed, as long as the surface charge is kept intact. Then, by (2.43), the scalar potential Φ outside of the conductors can be evaluated from

$$\Phi(\mathbf{r}) = \sum_{p'=1}^{P} \int_{S_{p'}} G(\mathbf{r}, \mathbf{r}') \varrho_{p'}(\mathbf{r}') \, dS', \tag{3.2}$$

where G is the Green's function for a space including the ground and the dielectric medium. By requiring Φ to equal U_p on S_p, and similarly on the other conductors, a set of surface integral equations is obtained for

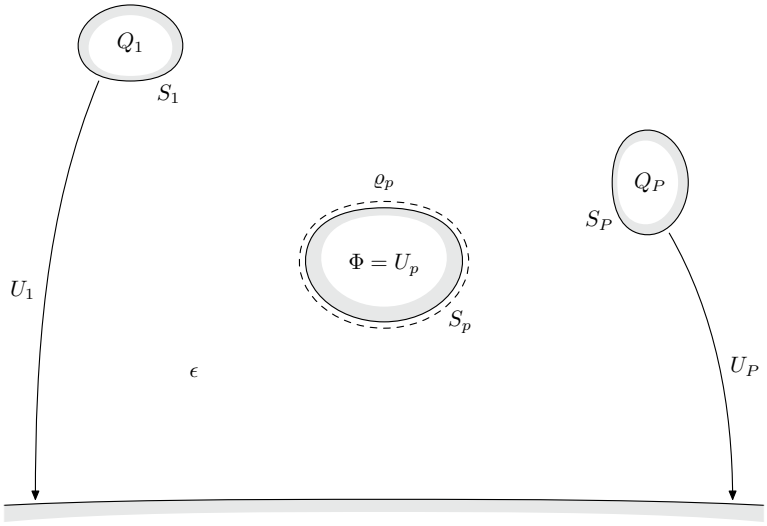

Figure 3.1. Conductors, the ground and a dielectric medium.

$\varrho_1, \ldots, \varrho_P$:

$$\sum_{p'=1}^{P} \int_{S_{p'}} G(\mathbf{r}, \mathbf{r}') \varrho_{p'}(\mathbf{r}') \, dS' = U_p, \quad \mathbf{r} \in S_p, \quad p = 1, \ldots, P. \tag{3.3}$$

The capacitance matrix C can be found by solving (3.3) with different vectors U. The most straightforward approach is to set $U_p = 1$ V, keep the other conductors grounded and solve the set of equations for $\varrho_1, \ldots, \varrho_P$. Then, the pth column of C is obtained from the values of $Q_1, \ldots, Q_P$ given by

$$Q_p = \int_{S_p} \varrho_p(\mathbf{r}) \, dS. \tag{3.4}$$

The capacitances can also be found from the electrostatic energy

$$W_\mathrm{e} = \frac{1}{2} U^\mathrm{T} Q = \frac{1}{2} U^\mathrm{T} C U, \tag{3.5}$$

which relates them to a certain functional discussed together with a variational principle in Section 4.

In Publications I and II, the above formulation is used in a calculation of capacitances of ring conductors.

3.2 Inductances of conductors

Consider a magnetostatic field in the presence of P loop conductors illustrated in Fig. 3.2. Denote the surfaces of the conductors by $S_1, \ldots, S_P$.

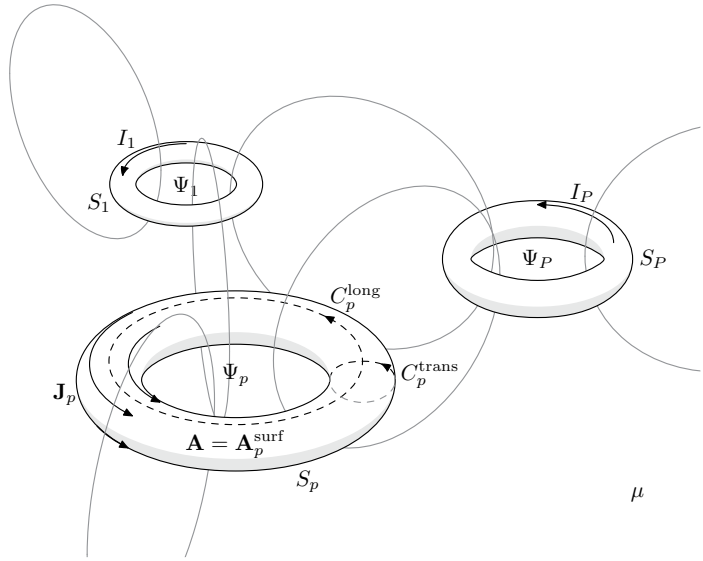

Figure 3.2. Loop conductors and magnetic fluxes.

Let the magnetostatic field be due to electric currents $I_1, \ldots, I_P$ circulating along the conductors. Assume that the field does not penetrate inside the conductors, so that the field is tangential on $S_1, \ldots, S_P$. Denote the magnetic fluxes encircled by the loops by $\Psi_1, \ldots, \Psi_P$. Relations between the fluxes and the currents are given by inductances (H=Vs/A), which are parameters of the geometry and the medium. By introducing a matrix L consisting of those inductances and compacting the fluxes and currents in vectors Ψ and I, respectively, the relations read

$$\Psi = LI. \tag{3.6}$$

Let the problem be to find L.

Since it is assumed that the field vanishes inside a conductor, the current must be settled onto the surface. Denote the surface current distribution on the pth conductor by $\mathbf{J}_p$. Moreover, the conductor can be removed, as long as the surface current is kept intact. Then, by (2.44), the vector potential $\mathbf{A}$ outside the conductors can be evaluated from

$$\mathbf{A}(\mathbf{r}) = \sum_{p'=1}^{P} \int_{S_{p'}} G(\mathbf{r}, \mathbf{r}') \mathbf{J}_{p'}(\mathbf{r}') \, dS', \tag{3.7}$$

where the Green's function G includes the effect of the surroundings. On the surface of a conductor the vector potential must satisfy

$$\int_{C_p^{\text{long}}} \hat{l} \cdot \mathbf{A}_p^{\text{surf}}(\mathbf{r}) \, dl = \Psi_p, \tag{3.8}$$

where C_p^{long} is a closed curve on S_p that goes longitudinally around the conductor and $\hat{l}$ is a unit vector in direction of C_p^{long}. Notice that the conductor has not necessarily to be circular but can be formed by any double connected volume. By requiring $\mathbf{A}$ to equal $\mathbf{A}_p^{\text{surf}}$ on S_p, and similarly on the other conductors, a set of surface integral equations is obtained for $J_1, \ldots, J_P$:

$$\sum_{p'=1}^{P} \int_{S_{p'}} G(\mathbf{r}, \mathbf{r}') \mathbf{J}_{p'}(\mathbf{r}')\, dS' = \mathbf{A}_p^{\text{surf}}(\mathbf{r}), \quad \mathbf{r} \in S_p, \quad p = 1, \ldots, P. \tag{3.9}$$

The inductance matrix L can be found by solving (3.9) with different vectors Ψ. The straightforward approach is to set $\Psi_p = 1$ Vs, keep the fluxes through the other loops zero and solve the set of equations for $J_1, \ldots, J_P$. Then, the pth column of the inverse matrix L^{-1} is obtained from the values of $I_1, \ldots, I_P$ given by

$$I_p = \int_{C_p^{\text{trans}}} \hat{l} \cdot \mathbf{J}_p(\mathbf{r})\, dl, \tag{3.10}$$

where C_p^{trans} is a closed curve on S_p that goes transversally around the cross-section of the conductor. The inductances can also be found from the magnetostatic energy

$$W_{\text{m}} = \frac{1}{2} \Psi^{\text{T}} I = \frac{1}{2} \Psi^{\text{T}} L^{-1} \Psi. \tag{3.11}$$

In Publications I and II, the above formulation is used in a calculation of inductances of ring conductors.

3.3 Scattering of electromagnetic plane wave by a dielectric object

Consider the scattering of an electromagnetic plane wave by a dielectric object illustrated in Fig. 3.3. Let the shape of the object be defined by V and assume that V is filled with an isotropic dielectric medium with an electric susceptibility χ. To incorporate losses, χ can be defined complex as suggested by (2.39). Examine the electric field $\mathbf{E}$, which now consists of a given incident field $\mathbf{E}^{\text{inc}}$ and an unknown scattered field $\mathbf{E}^{\text{sca}}$ as

$$\mathbf{E} = \mathbf{E}^{\text{inc}} + \mathbf{E}^{\text{sca}}. \tag{3.12}$$

Define $\mathbf{E}^{\text{inc}}$ as a plane wave

$$\mathbf{E}^{\text{inc}}(\mathbf{r}) = \mathbf{E}_0^{\text{inc}} e^{ik\hat{k}\cdot\mathbf{r}}, \tag{3.13}$$

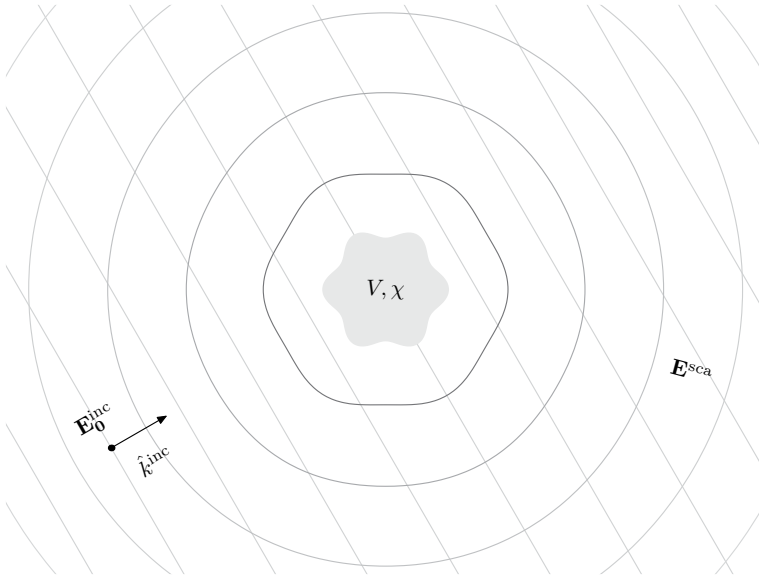

Figure 3.3. An incident electric field, a scatterer and a scattered electric field. The straight lines represent equiphase surfaces of the incident field and the annular lines represent equiphase surfaces of the scattered field.

where $\hat{k}$ is a unit vector in the direction of propagation and $\mathbf{E}_0^{\text{inc}}$ is an amplitude vector with $\hat{k} \cdot \mathbf{E}_0^{\text{inc}} = 0$. Since the source of $\mathbf{E}^{\text{sca}}$ is contained in V, $\mathbf{E}^{\text{sca}}$ is such that in a far zone with $kr \gg 1$ it can be approximated as

$$\mathbf{E}^{\text{sca}}(\mathbf{r}) \approx \frac{e^{ikr}}{ikr}\mathbf{E}_\infty^{\text{sca}}(\hat{r}), \tag{3.14}$$

where $r = |\mathbf{r}|$, $\hat{r} = \mathbf{r}/r$ and $\mathbf{E}_\infty^{\text{sca}}$ is a scattering pattern defined as

$$\mathbf{E}_\infty^{\text{sca}}(\hat{r}) = \lim_{kr\to\infty} \frac{ikr}{e^{ikr}}\mathbf{E}^{\text{sca}}(\mathbf{r}). \tag{3.15}$$

Let the problem be to find $\mathbf{E}_\infty^{\text{sca}}$.

In a deterministic scenario, the source of the scattered field $\mathbf{E}^{\text{sca}}$ is a polarisation current $\mathbf{J}^{\text{pol}}$, which, in turn, is induced by the total field $\mathbf{E}$ as $\mathbf{J}^{\text{pol}} = -i\omega\epsilon_0\chi\mathbf{E}$. Using this quantity as a source function in (2.45) yields

$$\mathbf{E}^{\text{sca}}(\mathbf{r}) = (k^2\mathbb{I} + \nabla\nabla) \cdot \int_V G(\mathbf{r}, \mathbf{r}')\chi(\mathbf{r}')\mathbf{E}(\mathbf{r}')\, dV', \tag{3.16}$$

and substituting (3.16) into (3.12) results a volume integral equation for $\mathbf{E}$:

$$\mathbf{E}(\mathbf{r}) - (k^2\mathbb{I} + \nabla\nabla) \cdot \int_V G(\mathbf{r}, \mathbf{r}')\chi(\mathbf{r}')\mathbf{E}(\mathbf{r}')\, dV' = \mathbf{E}^{\text{inc}}(\mathbf{r}). \tag{3.17}$$

The integral equation (3.17) can also be reformulated for the polarisation $\mathbf{P} = \epsilon_0\chi\mathbf{E}$ as

$$\mathbf{P}(\mathbf{r}) - \chi(\mathbf{r})(k^2\mathbb{I} + \nabla\nabla) \cdot \int_V G(\mathbf{r}, \mathbf{r}')\mathbf{P}(\mathbf{r}')\, dV' = \epsilon_0\chi(\mathbf{r})\mathbf{E}^{\text{inc}}(\mathbf{r}). \tag{3.18}$$

After finding $\mathbf{E}$ that solves (3.17), $\mathbf{E}_\infty^{\mathrm{sca}}$ is obtained from

$$\mathbf{E}_\infty^{\mathrm{sca}}(\hat{r}) = \frac{(ik)^3}{4\pi}(\mathbb{I} - \hat{r}\hat{r}) \cdot \int_V e^{-ik\hat{r}\cdot\mathbf{r}'} \chi(\mathbf{r}')\mathbf{E}(\mathbf{r}')\, dV', \tag{3.19}$$

which is the far field limit of (3.16) according to (3.15).

In Publication V, the formulation by (3.17) is used in a calculation of the scattering of an electromagnetic plane wave by the top of a pine tree.

4. Method of moments

4.1 Overview of method

Consider a linear problem

$$Lf = u, \tag{4.1}$$

where L is a linear operator, f is an unknown function, and u is a given function. Assume that f belongs to a Hilbert space F, u belongs to another Hilbert space U, and $L\colon F \to U$. Denote the inner product on F by $\langle f, g\rangle_F$ where $f, g \in F$, and the inner product on U by $\langle u, v\rangle_U$ where $u, v \in U$. For more on Hilbert spaces and the definition of the inner product, see [6, Sec. 3.1]. Along with many other integral equations in electromagnetics, (3.3), (3.9) and (3.17) are of the form of (4.1).

The method of moments (MoM), described in [7], is a method for searching an approximate solution to (4.1) through an equivalent discretised problem. The discretisation is performed as follows: First, choose a linearly independent set of basis functions $b_1, \ldots, b_N$ that spans a subspace $B_N \subset F$ and construct an approximative solution $\tilde{f}_N$ to (4.1) as

$$\tilde{f}_N = \sum_{n'=1}^{N} c_{n'} b_{n'}, \tag{4.2}$$

where $c_1, \ldots, c_N$ are unknown coefficients. Then, take a linearly independent set of test functions $t_1, \ldots, t_N$ that spans another subspace $T_N \subset U$ and require that the remainder

$$R_N = u - L\tilde{f}_N, \tag{4.3}$$

while using (4.2) to approximate f in (4.1), is orthogonal to T_N. This results in a set of equations

$$\sum_{n'=1}^{N} \langle t_n, Lb_{n'}\rangle_U c_{n'} = \langle t_n, u\rangle_U, \quad n = 1, \ldots, N, \tag{4.4}$$

from which $c_1, \ldots, c_N$ can be solved. In matrix notation (4.4) reads

$$Ax = y, \tag{4.5}$$

where the entries of the system matrix A and the vectors x and y, respectively, are

$$a_{n,n'} = \langle t_n, Lb_{n'} \rangle_U, \tag{4.6}$$

$$x_{n'} = c_{n'}, \tag{4.7}$$

$$y_n = \langle t_n, u \rangle_U. \tag{4.8}$$

4.2 Variational principle

The so-called variational principle gives another point of view to the MoM and yields some nice additional results. The discussion below follows loosely the discussions in [8], [9, Sec. 3], [10], [11] and [12].

Besides the original problem (4.1), consider an adjoint problem

$$L^{\mathrm{a}} v = g, \tag{4.9}$$

where L^{a} is an adjoint linear operator of L, v is an unknown function, and g is a given function. Assume that $v \in U$, $g \in F$, and $L^{\mathrm{a}} \colon U \to F$. By definition, L^{a} is related to L through $\langle Lf, v \rangle_U = \langle f, L^{\mathrm{a}} v \rangle_F$. If $L^{\mathrm{a}} = L$, the operator is called self-adjoint.

As suggested in [8, Eq. (33)], [10, Eq. (5)] and [11, Eq. (25)], introduce a bilinear functional

$$J(h, w) = \langle h, g \rangle_F + \langle u, w \rangle_U - \langle Lh, w \rangle_U, \tag{4.10}$$

where $h \in F$ and $w \in U$. If $h = f$ and $w = v$, i.e., h equals the solution of (4.1) and w equals the solution of (4.9), J receives the value

$$J_0 = J(f, v) = \langle f, g \rangle_F = \langle u, v \rangle_U. \tag{4.11}$$

In many cases, J_0 is exactly the quantity of interest. If small variations δf and δv are introduced to f and v, respectively, the corresponding variation δJ of J is

$$\delta J = J(f + \delta f, v + \delta v) - J(f, v) = -\langle L\delta f, \delta v \rangle_U = -\langle \delta f, L^{\mathrm{a}} \delta v \rangle_F. \tag{4.12}$$

It is seen that small variations in the input functions introduce a second-order variation in the value of the functional. Roughly speaking, the

above means that moderately accurate approximations of f and v result in a highly accurate approximation of J_0. If L is self-adjoint and the adjoint problem is defined similarly as the original problem, J becomes a quadratic functional of h. Then, it is said that J is stationary at f and that J_0 is the stationary value of J. Moreover, in some cases δJ can be confirmed to be either positive or negative for all δf. Consequently, it is known that J_0 is either the minimum or the maximum of J and the estimation is always greater or smaller than that value, respectively.

In addition to obtaining a second-order estimate of some interesting quantity, the functional (4.10) can be exploited to derive the discretisation (4.4) of the original problem (4.1) and a similar discretisation of the adjoint problem (4.9). The derivation goes as follows: First, approximate f by using the basis functions $b_1, \ldots, b_N$ as in (4.2) and v by using the test functions $t_1, \ldots, t_N$ as

$$\tilde{v}_N = \sum_{n'=1}^{N} d_{n'} t_{n'}, \tag{4.13}$$

where $d_1, \ldots, d_N$ are unknown coefficients. Then, following the Rayleigh-Ritz procedure, discussed e.g. in [9, Sec. 3.2], substitute (4.2) and (4.13) into (4.10), differentiate with respect to $c_1, \ldots, c_N$ and $d_1, \ldots, d_N$ and equate the derivatives to zero to get two sets of equations

$$\frac{\partial}{\partial c_n} J\left(\sum_{n'=1}^{N} c_{n'} b_{n'}, \sum_{n'=1}^{N} d_{n'} t_{n'} \right) = 0, \quad n = 1, \ldots, N, \tag{4.14}$$

$$\frac{\partial}{\partial d_n} J\left(\sum_{n'=1}^{N} c_{n'} b_{n'}, \sum_{n'=1}^{N} d_{n'} t_{n'} \right) = 0, \quad n = 1, \ldots, N. \tag{4.15}$$

Finally, apply the inner products and derivatives to get

$$\sum_{n'=1}^{N} \langle t_n, L b_{n'} \rangle_U c_{n'} = \langle t_n, u \rangle_U, \quad n = 1, \ldots, N, \tag{4.16}$$

$$\sum_{n'=1}^{N} \langle b_n, L^{\mathrm{a}} t_{n'} \rangle_F d_{n'} = \langle b_n, g \rangle_F, \quad n = 1, \ldots, N. \tag{4.17}$$

The set of equations (4.16) is the same as (4.4); the set (4.17) is for the adjoint problem (4.9).

4.3 Definitions of original and adjoint problems

With careful definitions of the original and adjoint problems, the above mathematical theory can be nicely linked to the physical problems formulated by (3.3), (3.9) and (3.17).

As the first example, consider the electrostatic problem formulated by (3.3) when there is only one conductor. The most obvious choice for the definition of the operator L is

$$L\colon f \to \int_S G(\mathbf{r}, \mathbf{r}') f(\mathbf{r}')\, dS', \tag{4.18}$$

in which case $f \equiv \varrho$ and $u \equiv U$. Since the problem is real-valued, the inner product $\langle f, g \rangle_F$ can be defined as

$$\langle f, g \rangle_F = \int_S f(\mathbf{r}) g(\mathbf{r})\, dS \tag{4.19}$$

and $\langle u, v \rangle_U$ similarly. Then, by a change of the order of integration it can be shown that $L^{\mathrm{a}} = L$. Moreover, defining $v \equiv f$ and $g \equiv u$,

$$J_0 = \langle f, g \rangle_F = \langle u, v \rangle_U = U \int_S \varrho(\mathbf{r})\, dS = UQ. \tag{4.20}$$

This equals two times the electrostatic energy in (3.5) and is thus also proportional to the capacitance. Moreover, by examining δJ in (4.12) it is found that the variation is negative for all $\delta\varrho$. Hence, it can be concluded that with the above definitions of the original and adjoint problems, the functional J in (4.10) yields an estimated value for the capacitance, the error of which is of second-order and which is always smaller than the exact value. The above formulation can be generalised for any number of conductors.

Reconsider the above electrostatic problem when the conductor is an indefinitely thin strip with $S = \{\, (x, y) \mid x \in [-1, 1],\, y = 0 \,\}$. The surface charge distribution on such a strip is known to grow like the inverse square root of the distance to the edge when approaching the edge; see e.g. [4, Sec. 2.11], [13], [14, Ch. 4] or [15]. Then, the most rigorous formulation of the problem is obtained by introducing a weight function w that exactly matches with the edge singularity, namely,

$$w(x) = \frac{1}{\sqrt{1 - x^2}}, \tag{4.21}$$

and attaching w to the operator and the inner products so that

$$L\colon f \to \int_{-1}^{1} G(x, y; x', 0) w(x') f(x')\, dx', \tag{4.22}$$

$$\langle f, g \rangle_F = \int_{-1}^{1} w(x) f(x) g(x)\, dx \tag{4.23}$$

and similarly for $\langle u, v \rangle_U$. Then, the unknown function f of the resulting modified problem must be smooth and expressible with a plain polynomial of x.

Next, consider the magnetostatic problem formulated by (3.9) when there is only one conductor. The operator of the problem can be defined as

$$L\colon \mathbf{f} \to \int_S G(\mathbf{r}, \mathbf{r}')\mathbf{f}(\mathbf{r}')\, dS', \tag{4.24}$$

in which case $\mathbf{f} \equiv \mathbf{J}$ and $\mathbf{u} \equiv \mathbf{A}^{\text{surf}}$. Since the problem is real-valued, the inner product $\langle \mathbf{f}, \mathbf{g} \rangle_F$ can be defined as

$$\langle \mathbf{f}, \mathbf{g} \rangle_F = \int_S \mathbf{f}(\mathbf{r}) \cdot \mathbf{g}(\mathbf{r})\, dS \tag{4.25}$$

and similarly for $\langle \mathbf{u}, \mathbf{v} \rangle_U$. Then, by a change of the order of integration it can be shown that $L^{\text{a}} = L$. Moreover, defining $\mathbf{v} \equiv \mathbf{f}$ and $\mathbf{g} \equiv \mathbf{u}$,

$$J_0 = \langle \mathbf{f}, \mathbf{g} \rangle_F = \langle \mathbf{u}, \mathbf{v} \rangle_U = \int_S \mathbf{J}(\mathbf{r}) \cdot \mathbf{A}^{\text{surf}}(\mathbf{r})\, dS = \Psi I. \tag{4.26}$$

This equals two times the magnetostatic energy in (3.11) and is thus also inversely proportional to the inductance. Moreover, by examining δJ in (4.12) it is found that the variation is negative for all $\delta\mathbf{J}$. Therefore, it can be concluded that with the above definitions of the original and adjoint problems, the functional J in (4.10) yields an estimated value for the inductance, the error of which is of second-order and which is always greater than the exact value. The above formulation can be generalised for any number of conductors.

If the conductor in the above magnetostatic problem is, for instance, an indefinitely thin strip, the edge singularity of the surface current can be embedded in the operator and the inner product just like in the electrostatic problem.

As a final example, consider the scattering problem formulated by (3.17). The operator of the problem can be defined as

$$L\colon \mathbf{f} \to \mathbf{f}(\mathbf{r}) - (k^2\mathbb{I} + \nabla\nabla) \cdot \int_V G(\mathbf{r}, \mathbf{r}')\chi(\mathbf{r}')\mathbf{f}(\mathbf{r}')\, dV', \tag{4.27}$$

in which case $\mathbf{f} \equiv \mathbf{E}$ and $\mathbf{u} \equiv \mathbf{E}^{\text{inc}}$. If the inner product $\langle \mathbf{f}, \mathbf{g} \rangle_F$ is defined as

$$\langle \mathbf{f}, \mathbf{g} \rangle_F = \int_V \mathbf{f}^*(\mathbf{r}) \cdot \mathbf{g}(\mathbf{r})\, dV \tag{4.28}$$

and similarly for $\langle \mathbf{u}, \mathbf{v} \rangle_U$, the adjoint operator turns out to be

$$L^{\text{a}}\colon \mathbf{v} \to \mathbf{v}(\mathbf{r}) - \chi^*(\mathbf{r})(k^2\mathbb{I} + \nabla\nabla) \cdot \int_V G^*(\mathbf{r}, \mathbf{r}')\mathbf{v}(\mathbf{r}')\, dV'. \tag{4.29}$$

This suggests that the adjoint problem of (3.17) is of the form of the complex conjugate of (3.18). Moreover, defining $\mathbf{v}^* \equiv \mathbf{P}'$ and $\mathbf{g}^* \equiv \epsilon_0\chi\mathbf{E}_0^{\text{inc}\prime}e^{-ik\hat{\mathbf{k}}\cdot\mathbf{r}}$,

$$J_0{}^* = \langle \mathbf{f}, \mathbf{g} \rangle_F = \epsilon_0\mathbf{E}_0^{\text{inc}\prime} \cdot \int_V e^{-ik\hat{\mathbf{k}}\cdot\mathbf{r}}\chi(\mathbf{r})\mathbf{E}(\mathbf{r})\, dV. \tag{4.30}$$

Now, by choosing $\mathbf{E}_0^{\mathrm{inc}\prime}$ properly, the right-hand-side of (4.30) can be set proportional to a component of the scattering pattern in (3.19). Hence, it can be concluded that with the above definitions of the original and adjoint problems, the functional J in (4.10) yields an estimated value for the scattering pattern, the error of which is of second-order.

4.4 Choice of basis and test functions

Quite an obvious criterion in choosing the basis functions is that they should approximate the unknown function of the original problem (4.1) well. More precisely, B_N should be such that f is close to it when N is finite and is captured in it at the latest when $N \to \infty$. In addition, B_N may be chosen so that it excludes functions with unwanted properties.

Take, for example, the electrostatic problem with an indefinitely thin strip conductor discussed earlier. If the problem is defined with the weight function defined as in (4.21), the natural choice for the basis functions is

$$b_n(x) = T_{n-1}(x), \tag{4.31}$$

where T_{n-1} is Chebyshev polynomial of the first kind, which with $n = 1, 2, \ldots$ constitute an orthonormal set with the inner product defined as in (4.23). These polynomials are eigenfunctions of the operator in (4.22). If the problem is defined without the weight function, the basis functions can be defined as

$$b_n(x) = \frac{T_{n-1}(x)}{\sqrt{1-x^2}}. \tag{4.32}$$

This leads to the same numerical results, only not through as a rigorous formulation. In Fig. 4.1, there are examples of expansions without and with the weight function. Other planar geometries, for which the edge singularity of the surface charge and current distributions can be analytically formulated, include at least a circular disk, an elliptic disk and a circular ring. In Publications I and II, electro- and magnetostatic problems consisting of circular ring conductors are solved by using similar entire-domain basis functions with analytical and exact edge singularities. Some details are revised in Section 6.

If the geometry is more complex, B_N must be constructed out of simpler sub-domain basis functions. Common choices are piecewise constant functions, rooftop functions on quadrilateral supports and the so-called RWG functions on triangular supports, introduced in [16]. The advantages of

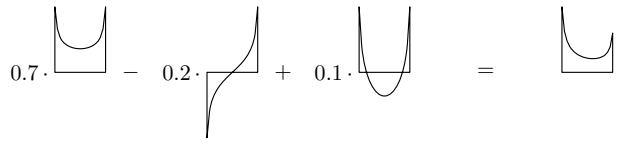

(a)

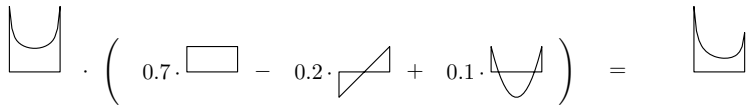

(b)

Figure 4.1. Example of constructing the electric charge on an indefinitely thin strip conductor (a) when the edge singularity is left embedded in the unknown function and (b) when it is extracted into a separate weight function. In the latter case, the basis functions are Chebyshev polynomials.

this kind of an approach are that it is applicable to arbitrary geometries and that the entries of the system matrix A in (4.6) are sufficiently easy to evaluate. The disadvantage is that N might get large, which brings more challenges to the solution of the discretised problem (4.5). In Publication V, the scattering of an electromagnetic plane wave by the top of a pine tree is solved by using the most simple piecewise constant subdomain basis functions. A short introduction of the problem is given in Section 7.6.

Criteria for choosing the test functions do not at first seem as obvious as in choosing the basis functions. However, one criterion is suggested by the variational principle: if the best estimation is desired for the stationary value of the functional in (4.10), the result of the variation in (4.12) suggests that the test functions should be chosen so that they approximate the unknown function of the adjoint problem (4.9) well. If the operator is self-adjoint and the adjoint problem is defined similarly as the original problem, the above criterion defines the test functions to be the same as the basis functions. This leads to Galerkin's method with

$$t_n = b_n. \tag{4.33}$$

Even if the operator is not self-adjoint and the adjoint problem is not exactly the same as the original problem, still many times the adjoint problem is similar to the original problem to such a degree that the well-chosen basis functions approximate also the unknown function of the adjoint problem well. Then, Galerkin's method is an easy choice, even though

a similar accuracy can be achieved with different choices as well, as noted and demonstrated in [11]. In addition, if the operator L is self-adjoint, Galerkin's method leads to a hermitian system matrix A, which might ease the solution of the discretised problem. The solutions presented in Publications I and II apply Galerkin's method.

Sometimes Galerkin's method leads to difficult integrals in the evaluation of the entries (4.6) of the system matrix A. The most simple evaluation of the entries is obtained if the test functions are chosen to be Dirac delta functions as

$$t_n(\mathbf{r}) = \delta(\mathbf{r} - \mathbf{r}_n), \tag{4.34}$$

where $\mathbf{r}_n$ are, for instance, the midpoints of the support of the basis functions. The procedure is called point matching because it nails the approximation $\tilde{f}_N$ exactly to f at $\mathbf{r} = \mathbf{r}_1, \ldots, \mathbf{r}_N$. Elsewhere, however, $\tilde{f}_N$ can be almost anything. This suggests that, since δv in (4.12) is greater than with the choice (4.33), the estimation for the stationary value of the functional might not be as accurate as with Galerkin's method. Also, with the point matching, the system matrix A is not hermitian, which might make the solution of the discretised problem more difficult. The solution presented in Publication V applies the point matching.

4.5 Solution of discretised problem

If N is small, the discretised problem (4.5) can be solved simply by the Gaussian elimination. This requires a numerical work proportional to N^3, which grows fast with N. So, if N is large, (4.5) must be solved by using an iterative scheme, such as Generalized minimal residual method (GMRES), explained e.g. in [17, Lecture 35]. This lowers the numerical work to be proportional to MN^2 if M is the number of iterations. If N is very large, even this might be too much. Iterative schemes repeatedly apply a multiplication of the coefficient vector x by the system matrix A. This matrix-vector multiplication can be accelerated by using the MLFMA, for instance, the version of the algorithm presented in Publication IV, reviewed in Section 7 and applied in Publication V. This lowers the numerical work further so that it becomes proportional to $MN \log N$.

5. Wave functions and translational addition theorems for them

5.1 In an arbitrary separable system of co-ordinates

Consider the scalar Helmholtz equation (2.35) in an empty space, i.e.,

$$(\nabla^2 + k_0^2)\Phi = 0, \tag{5.1}$$

where $k_0 = \omega\sqrt{\mu_0\epsilon_0}$. The solutions of (5.1) obtained through the process of separation of variables in a separable system of co-ordinates are called scalar wave functions. Denote them by ψ_n. The wave functions form an orthogonal set: $\langle\psi_n, \psi_{n'}\rangle = 0$ if $n \neq n'$. Above, the inner product is taken over a surface with respect to two of the co-ordinates, the dependency of ψ_n on the third co-ordinate being fixed through a separation equation $\mathrm{k}\cdot\mathrm{k} = k_0^2$ where k is the wave vector. An arbitrary solution of (5.1) can be expanded in wave functions as

$$\Phi(\mathbf{r}) = \sum_n a_n\psi_n(\mathbf{r}), \tag{5.2}$$

where a_n are expansion coefficients. They are determined through the orthogonality of ψ_n.

The expansion in (5.2) is limited to the particular system of co-ordinates; if the system is changed, the coefficients of the expansion are changed as well. In particular, consider a translation of the origin illustrated in Fig. 5.1. To that end, denote the field expressed in the initial and translated systems by Φ^{init} and Φ^{trans}, respectively, and the origin of the translated system with respect to the initial system by t. Then,

$$\Phi^{\mathrm{trans}}(\mathbf{r}) = \Phi^{\mathrm{init}}(\mathbf{t} + \mathbf{r}). \tag{5.3}$$

Now, the question is: what are the coefficients a_n^{trans} of Φ^{trans} in terms of the coefficients a_n^{init} of Φ^{init}? The answer is found with the aid of a translational addition theorem for the scalar wave functions. The theorem gives

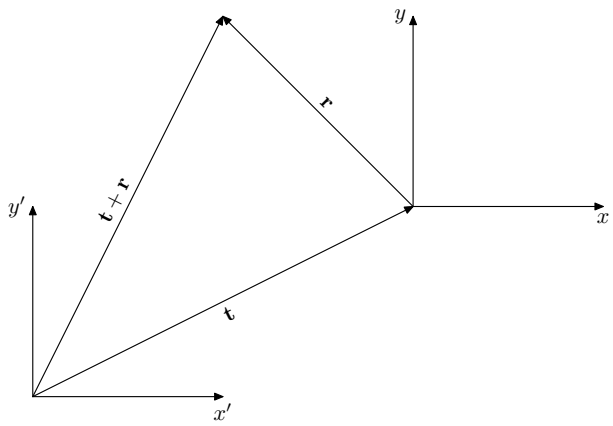

Figure 5.1. Translation of origin. The initial system is defined by x' and y' and the translated system by x and y.

a wave function in the translated system in terms of the wave functions in the initial system as

$$\psi_{n'}(\mathbf{t}+\mathbf{r}) = \sum_n \alpha_{n,n'}(\mathbf{t})\psi_n(\mathbf{r}), \tag{5.4}$$

where $\alpha_{n,n'}$ are scalar translation coefficients. Notice that since the wave function on the left-hand-side of (5.4) must satisfy the wave equation also as a function t, the translation coefficients on the right-hand-side must satisfy the wave equation and, consequently, be expressible in terms of the wave functions. By substituting (5.4) into the expansion of Φ^{init} and interchanging the order of summations, it is found that the coefficients of Φ^{trans} are given by

$$a_n^{\text{trans}} = \sum_{n'} \alpha_{n,n'}(\mathbf{t}) a_{n'}^{\text{init}}. \tag{5.5}$$

Next, consider the vector Helmholtz equation (2.34) in an empty space, i.e.,

$$(\nabla^2 + k_0^2)\mathbf{A} = 0. \tag{5.6}$$

An arbitrary solution of (5.6) could be decomposed into three rectangular components, each of which could then be expanded in scalar wave functions as a scalar field in (5.2). However, as presented e.g. in [3, Sec. 7.1], there is a certain advantage in introducing vector wave functions $\mathbf{L}_n$, $\mathbf{M}_n$

and $\mathbf{N}_n$ defined here as

$$\mathbf{L}_n(\mathbf{r}) = \frac{1}{k_0}\nabla\psi_n(\mathbf{r}), \tag{5.7}$$

$$\mathbf{M}_n(\mathbf{r}) = \mathbf{L}_n(\mathbf{r}) \times \mathbf{p}, \tag{5.8}$$

$$\mathbf{N}_n(\mathbf{r}) = \frac{1}{k_0}\nabla \times \mathbf{M}_n(\mathbf{r}), \tag{5.9}$$

where $\mathbf{p}$ is called a pilot vector. With a proper choice of $\mathbf{p}$, all the vector wave functions of one type are orthogonal to the vector wave functions of another type: $\langle \mathbf{L}_n, \mathbf{M}_{n'} \rangle = 0$, $\langle \mathbf{L}_n, \mathbf{N}_{n'} \rangle = 0$ and $\langle \mathbf{M}_n, \mathbf{N}_{n'} \rangle = 0$ for all n, n'; and the vector wave functions of the same type are orthogonal to each other: $\langle \mathbf{L}_n, \mathbf{L}_{n'} \rangle = 0$ if $n \neq n'$, etc. Also, out of the three types of the vector wave functions, one is irrotational: $\nabla \times \mathbf{L}_n = 0$; while the other two are solenoidal: $\nabla \cdot \mathbf{M}_n = 0$, $\nabla \cdot \mathbf{N}_n = 0$; and besides (5.9), $k_0\mathbf{M}_n = \nabla \times \mathbf{N}_n$. Now, the advantage in introducing the vector wave functions is that if Φ is expanded as in (5.2) and $\mathbf{A}$ is expanded as

$$\mathbf{A}(\mathbf{r}) = \frac{k_0}{i\omega}\sum_n [a_n\mathbf{L}_n(\mathbf{r}) + b_n\mathbf{M}_n(\mathbf{r}) + c_n\mathbf{N}_n(\mathbf{r})], \tag{5.10}$$

substitutions of these expansions into the frequency-domain forms of (2.26) and (2.25) with (2.7) imply that the electric and magnetic fields are expanded in terms of only $\mathbf{M}_n$ and $\mathbf{N}_n$ as

$$\mathbf{E}(\mathbf{r}) = k_0\sum_n [b_n\mathbf{M}_n(\mathbf{r}) + c_n\mathbf{N}_n(\mathbf{r})], \tag{5.11}$$

$$\mathbf{H}(\mathbf{r}) = -i\omega\epsilon_0\sum_n [c_n\mathbf{M}_n(\mathbf{r}) + b_n\mathbf{N}_n(\mathbf{r})]. \tag{5.12}$$

So, one set of coefficients is saved in contrast to using three expansions for the rectangular components of $\mathbf{E}$ and $\mathbf{H}$.

Now, consider the translation of the origin formulated similarly as in the scalar case so that

$$\mathbf{A}^{\text{trans}}(\mathbf{r}) = \mathbf{A}^{\text{init}}(\mathbf{t} + \mathbf{r}). \tag{5.13}$$

While the translation of the irrotational part is already given by (5.4), the translation of the solenoidal part is enabled by the translation addition theorems for the vector wave functions, which are of the form

$$\mathbf{M}_{n'}(\mathbf{t} + \mathbf{r}) = \sum_n [\beta_{n,n'}(\mathbf{t})\mathbf{M}_n(\mathbf{r}) + \gamma_{n,n'}(\mathbf{t})\mathbf{N}_n(\mathbf{r})], \tag{5.14}$$

$$\mathbf{N}_{n'}(\mathbf{t} + \mathbf{r}) = \sum_n [\gamma_{n,n'}(\mathbf{t})\mathbf{M}_n(\mathbf{r}) + \beta_{n,n'}(\mathbf{t})\mathbf{N}_n(\mathbf{r})], \tag{5.15}$$

where $\beta_{n,n'}$ and $\gamma_{n,n'}$ are vector translation coefficients. Notice that the vector wave functions on the left-hand-sides of (5.14) and (5.15) must satisfy the vector wave equation also as a function of $\mathbf{t}$. Then, it follows

that the translation coefficients on the right-hand-sides must satisfy the scalar wave equation. By substituting (5.14) and (5.15) into the expansion of $\mathbf{A}^{\text{init}}$, interchanging the order of summation and collecting the terms, it is found that the coefficients of $\mathbf{A}^{\text{trans}}$ are given by

$$b_n^{\text{trans}} = \sum_{n'} [\beta_{n,n'}(\mathbf{t}) b_{n'}^{\text{init}} + \gamma_{n,n'}(\mathbf{t}) c_{n'}^{\text{init}}], \tag{5.16}$$

$$c_n^{\text{trans}} = \sum_{n'} [\gamma_{n,n'}(\mathbf{t}) b_{n'}^{\text{init}} + \beta_{n,n'}(\mathbf{t}) c_{n'}^{\text{init}}]. \tag{5.17}$$

5.2 In rectangular system of co-ordinates

In the rectangular system of co-ordinates, the separation of variables in (5.1) shows that the scalar wave functions are composed of trigonometric and exponential functions. One possible form is a plane wave

$$\psi(\mathbf{k}_\rho, \mathbf{r}) = e^{i\mathbf{k}\cdot\mathbf{r}} \tag{5.18}$$

with $\mathbf{k} = \mathbf{k}_\rho + \hat{z}k_z$ where $\mathbf{k}_\rho$ is taken as an independent variable, k_z being fixed through the separation equation $\mathbf{k}_\rho \cdot \mathbf{k}_\rho + k_z^2 = k_0^2$. The wave functions defined as in (5.18) are orthogonal on any plane parallel to the xy-plane. An arbitrary solution of (5.1) can be expanded in wave functions as

$$\Phi(\mathbf{r}) = \int_{\mathbb{R}^2} a(\mathbf{k}_\rho) \psi(\mathbf{k}_\rho, \mathbf{r})\, dS(\mathbf{k}_\rho), \tag{5.19}$$

where, writing $\mathbf{r} = \boldsymbol{\rho} + \hat{z}z$ and applying the orthogonality on the xy-plane,

$$a(\mathbf{k}_\rho) = \frac{1}{2\pi} \int_{\mathbb{R}^2} \Phi(\boldsymbol{\rho}) \psi^*(\mathbf{k}_\rho, \boldsymbol{\rho})\, dS(\boldsymbol{\rho}). \tag{5.20}$$

The translational addition theorem for a plane wave is especially simple:

$$e^{i\mathbf{k}\cdot(\mathbf{t}+\mathbf{r})} = e^{i\mathbf{k}\cdot\mathbf{t}} e^{i\mathbf{k}\cdot\mathbf{r}}. \tag{5.21}$$

Formulated for the scalar wave functions defined as in (5.18), the theorem is

$$\psi(\mathbf{k}_\rho, \mathbf{t} + \mathbf{r}) = \alpha(\mathbf{k}_\rho, \mathbf{t}) \psi(\mathbf{k}_\rho, \mathbf{r}), \tag{5.22}$$

where

$$\alpha(\mathbf{k}_\rho, \mathbf{t}) = \psi(\mathbf{k}_\rho, \mathbf{t}). \tag{5.23}$$

By substituting (5.22) into the expansion of Φ^{init}, it is found that $a^{\text{trans}}(\mathbf{k}_\rho)$ is given by

$$a^{\text{trans}}(\mathbf{k}_\rho) = \alpha(\mathbf{k}_\rho, \mathbf{t}) a^{\text{init}}(\mathbf{k}_\rho). \tag{5.24}$$

The vector wave functions in the rectangular system of co-ordinates are obtained by introducing (5.18) in (5.7)–(5.9). Choosing $\mathbf{p} = \hat{z}$ they are

$$\mathbf{L}(\mathbf{k}_\rho, \mathbf{r}) = i\hat{k}e^{i\mathbf{k}\cdot\mathbf{r}}, \tag{5.25}$$

$$\mathbf{M}(\mathbf{k}_\rho, \mathbf{r}) = i\hat{k} \times \hat{z}e^{i\mathbf{k}\cdot\mathbf{r}}, \tag{5.26}$$

$$\mathbf{N}(\mathbf{k}_\rho, \mathbf{r}) = i\hat{k} \times (i\hat{k} \times \hat{z})e^{i\mathbf{k}\cdot\mathbf{r}}, \tag{5.27}$$

where $\hat{k} = \mathbf{k}/k_0$. The wave functions defined as in (5.25)–(5.27) are orthogonal on any plane parallel to the xy-plane. An arbitrary solution of (5.6) can be expanded in wave functions as

$$\mathbf{A}(\mathbf{r}) = \frac{k_0}{i\omega}\int_{\mathbb{R}^2} [a(\mathbf{k}_\rho)\mathbf{L}(\mathbf{k}_\rho, \mathbf{r}) + b(\mathbf{k}_\rho)\mathbf{M}(\mathbf{k}_\rho, \mathbf{r}) + c(\mathbf{k}_\rho)\mathbf{N}(\mathbf{k}_\rho, \mathbf{r})]\, dS(\mathbf{k}_\rho), \tag{5.28}$$

where $a(\mathbf{k}_\rho)$ is as in (5.20) and

$$b(\mathbf{k}_\rho) = \frac{i\omega}{k_0}\frac{1}{2\pi}\int_{\mathbb{R}^2} \mathbf{A}(\boldsymbol{\rho}) \cdot \mathbf{M}^*(\mathbf{k}_\rho, \boldsymbol{\rho})\, dS(\boldsymbol{\rho}), \tag{5.29}$$

$$c(\mathbf{k}_\rho) = \frac{i\omega}{k_0}\frac{1}{2\pi}\int_{\mathbb{R}^2} \mathbf{A}(\boldsymbol{\rho}) \cdot \mathbf{N}^*(\mathbf{k}_\rho, \boldsymbol{\rho})\, dS(\boldsymbol{\rho}). \tag{5.30}$$

It is easy to see that the translational addition theorems for the vector wave functions defined as in (5.25)–(5.27) are

$$\mathbf{M}(\mathbf{k}_\rho, \mathbf{t} + \mathbf{r}) = \beta(\mathbf{k}_\rho, \mathbf{t})\mathbf{M}(\mathbf{k}_\rho, \mathbf{r}), \tag{5.31}$$

$$\mathbf{N}(\mathbf{k}_\rho, \mathbf{t} + \mathbf{r}) = \beta(\mathbf{k}_\rho, \mathbf{t})\mathbf{N}(\mathbf{k}_\rho, \mathbf{r}), \tag{5.32}$$

where

$$\beta(\mathbf{k}_\rho, \mathbf{t}) = \psi(\mathbf{k}_\rho, \mathbf{t}). \tag{5.33}$$

By substituting (5.31) and (5.32) into the expansion of $\mathbf{A}^{\text{init}}$, it is found that $b^{\text{trans}}(\mathbf{k}_\rho)$ and $c^{\text{trans}}(\mathbf{k}_\rho)$ are given by

$$b^{\text{trans}}(\mathbf{k}_\rho) = \beta(\mathbf{k}_\rho, \mathbf{t})b^{\text{init}}(\mathbf{k}_\rho), \tag{5.34}$$

$$c^{\text{trans}}(\mathbf{k}_\rho) = \beta(\mathbf{k}_\rho, \mathbf{t})c^{\text{init}}(\mathbf{k}_\rho). \tag{5.35}$$

The above translations of plane waves are said to be diagonal. In numerical calculations, a^{init}, b^{init} and c^{init} are sampled at discrete values of $\mathbf{k}_\rho$, and these samples are collected in vectors. The corresponding vectors for a^{trans}, b^{trans} and c^{trans} are obtained through multiplications by translation matrices consisting of samples of α and β. These translation matrices are diagonal. This is not the case in other systems of co-ordinates considered next.

5.3 In cylindrical system of co-ordinates

In the cylindrical system of co-ordinates, the separation of variables in (5.1) shows that scalar wave functions finite at the z-axis can be defined as

$$\psi_m(k_\rho, \mathbf{r}) = J_m(k_\rho \rho) e^{im\phi} e^{ik_z z}, \tag{5.36}$$

where $\mathbf{r} = \hat{x}\rho\cos\phi + \hat{y}\rho\sin\phi + \hat{z}z$, and k_ρ is taken as an independent variable, k_z being fixed through the separation equation $k_\rho^2 + k_z^2 = k_0^2$. The radial function J_m is a Bessel function of the first kind. The wave functions defined as in (5.36) are orthogonal on any plane parallel to the xy-plane. An arbitrary solution of (5.1) can be expanded in wave functions as

$$\Phi(\mathbf{r}) = \sum_{m=-\infty}^{\infty} \int_0^\infty a_m(k_\rho) \psi_m(k_\rho, \mathbf{r}) k_\rho \, dk_\rho, \tag{5.37}$$

where writing $\boldsymbol{\rho} = \hat{x}\rho\cos\phi + \hat{y}\rho\sin\phi$ and applying the orthogonality on the xy-plane,

$$a_m(k_\rho) = \frac{1}{2\pi} \int_0^{2\pi} \int_0^\infty \Phi(\boldsymbol{\rho}) \psi_m{}^*(k_\rho, \boldsymbol{\rho}) \rho \, d\rho \, d\phi. \tag{5.38}$$

Now, consider the translational addition theorem for the cylindrical scalar wave functions defined as in (5.36). As given in [18, Sec. 11.3, Eq. (2)], the addition theorem for Bessel functions is

$$J_{m'}(k_\rho \rho') e^{im'\phi'} = \sum_{m=-\infty}^{\infty} J_{m'-m}(k_\rho \tau) e^{i(m'-m)\vartheta} J_m(k_\rho \rho) e^{im\phi}, \tag{5.39}$$

where the geometry is as shown in Fig. 5.2. Since a translation along the z-axis is similar to the translation of a plane wave, the complete theorem is

$$\psi_{m'}(k_\rho, \mathbf{t} + \mathbf{r}) = \sum_{m=-\infty}^{\infty} \alpha_{m,m'}(k_\rho, \mathbf{t}) \psi_m(k_\rho, \mathbf{r}), \tag{5.40}$$

where

$$\alpha_{m,m'}(k_\rho, \mathbf{t}) = \psi_{m'-m}(k_\rho, \mathbf{t}). \tag{5.41}$$

By substituting (5.40) into the expansion of Φ^{init} and interchanging the order of summations, it is found that $a_m^{\text{trans}}(k_\rho)$ are given by

$$a_m^{\text{trans}}(k_\rho) = \sum_{m'=-\infty}^{\infty} \alpha_{m,m'}(k_\rho, \mathbf{t}) a_{m'}^{\text{init}}(k_\rho). \tag{5.42}$$

Vector wave functions in the cylindrical system of co-ordinates are ob-

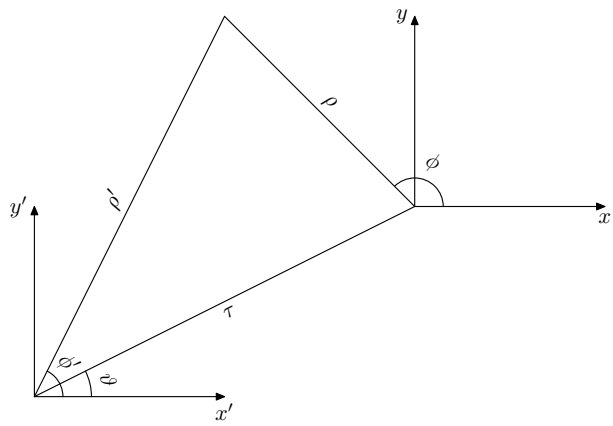

Figure 5.2. Translation of origin in the cylindrical system of co-ordinates.

tained by introducing (5.36) in (5.7)–(5.9). Choosing $\mathbf{p} = \hat{z}k_0/k_\rho$ they are

$$\mathbf{L}_m(k_\rho, \mathbf{r}) = \left\{ \frac{k_\rho}{k_0} \left[\hat{\rho} J'_m(k_\rho \rho) + \hat{\phi} im \frac{J_m(k_\rho \rho)}{k_\rho \rho} \right] + \frac{ik_z}{k_0} \hat{z} J_m(k_\rho \rho) \right\} e^{im\phi} e^{ik_z z}, \tag{5.43}$$

$$\mathbf{M}_m(k_\rho, \mathbf{r}) = \left[\hat{\rho} im \frac{J_m(k_\rho \rho)}{k_\rho \rho} - \hat{\phi} J'_m(k_\rho \rho) \right] e^{im\phi} e^{ik_z z}, \tag{5.44}$$

$$\mathbf{N}_m(k_\rho, \mathbf{r}) = \left\{ \frac{ik_z}{k_0} \left[\hat{\rho} J'_m(k_\rho \rho) + \hat{\phi} im \frac{J_m(k_\rho \rho)}{k_\rho \rho} \right] + \frac{k_\rho}{k_0} \hat{z} J_m(k_\rho \rho) \right\} e^{im\phi} e^{ik_z z}. \tag{5.45}$$

The wave functions defined as in (5.43)–(5.45) are orthogonal on any plane parallel to the xy-plane. An arbitrary solution of (5.6) can be expanded in wave functions as

$$\mathbf{A}(\mathbf{r}) = \frac{k_0}{i\omega} \sum_{m=-\infty}^{\infty} \int_0^\infty [a_m(k_\rho) \mathbf{L}_m(k_\rho, \mathbf{r}) + b_m(k_\rho) \mathbf{M}_m(k_\rho, \mathbf{r}) + c_m(k_\rho) \mathbf{N}_m(k_\rho, \mathbf{r})] k_\rho \, dk_\rho, \tag{5.46}$$

where $a_m(k_\rho)$ are as in (5.38) and

$$b_m(k_\rho) = \frac{i\omega}{k_0} \frac{1}{2\pi} \int_0^{2\pi} \int_0^\infty \mathbf{A}(\boldsymbol{\rho}) \cdot \mathbf{M}_m{}^*(k_\rho, \boldsymbol{\rho}) \rho \, d\rho \, d\phi, \tag{5.47}$$

$$c_m(k_\rho) = \frac{i\omega}{k_0} \frac{1}{2\pi} \int_0^{2\pi} \int_0^\infty \mathbf{A}(\boldsymbol{\rho}) \cdot \mathbf{N}_m{}^*(k_\rho, \boldsymbol{\rho}) \rho \, d\rho \, d\phi. \tag{5.48}$$

Additional translation theorems for the cylindrical vector wave functions can be obtained directly from the scalar theorem: if (5.40) is substituted into (5.7)–(5.9) with $\mathbf{p} = \hat{z}/k_\rho$, it is found that the gradient operator,

cross product and curl operator affect only the wave functions, not the translation coefficients, yielding

$$\mathbf{M}_{m'}(k_\rho, \mathbf{t}+\mathbf{r}) = \sum_{m=-\infty}^{\infty} \beta_{m,m'}(k_\rho, \mathbf{t})\mathbf{M}_m(k_\rho, \mathbf{r}), \tag{5.49}$$

$$\mathbf{N}_{m'}(k_\rho, \mathbf{t}+\mathbf{r}) = \sum_{m=-\infty}^{\infty} \beta_{m,m'}(k_\rho, \mathbf{t})\mathbf{N}_m(k_\rho, \mathbf{r}), \tag{5.50}$$

where

$$\beta_{m,m'}(k_\rho, \mathbf{t}) = \psi_{m'-m}(k_\rho, \mathbf{t}). \tag{5.51}$$

By substituting (5.49) and (5.50) into the expansion of $\mathbf{A}^{\text{init}}$ and interchanging the order of summations, it is found that $b_m^{\text{trans}}(k_\rho)$ and $c_m^{\text{trans}}(k_\rho)$ are given by

$$b_m^{\text{trans}}(k_\rho) = \sum_{m'=-\infty}^{\infty} \beta_{m,m'}(k_\rho, \mathbf{t}) b_{m'}^{\text{init}}(k_\rho), \tag{5.52}$$

$$c_m^{\text{trans}}(k_\rho) = \sum_{m'=-\infty}^{\infty} \beta_{m,m'}(k_\rho, \mathbf{t}) c_{m'}^{\text{init}}(k_\rho). \tag{5.53}$$

The translation matrices obtained by sampling $\alpha_{m,m'}(k_\rho, \mathbf{t})$ and $\beta_{m,m'}(k_\rho, \mathbf{t})$ at discrete values of $\mathbf{k}_\rho$ are block-diagonal.

5.4 In spherical system of co-ordinates

In the spherical system of co-ordinates, the separation of variables in (5.1) shows that scalar wave functions can be defined as

$$\psi_{l,m}(\mathbf{r}) = z_l(k_0 r) Y_{l,m}(\hat{r}), \tag{5.54}$$

where $r = |\mathbf{r}|$, $\hat{r} = \mathbf{r}/r$, $l = 0, 1, \ldots$ and $m = -l, \ldots, l$. The radial function z_l is the spherical Bessel function of the first kind j_l if the wave function is incoming (or locally standing) and the spherical Hankel function of the first kind $h_l^{(1)}$ if the wave is outgoing (or radiating). The angular function $Y_{l,m}$ is the spherical harmonic defined as

$$Y_{l,m}(\hat{r}) = \sqrt{\frac{2l+1}{4\pi}\frac{(l-m)!}{(l+m)!}} P_l^m(\cos\theta) e^{im\phi}, \tag{5.55}$$

where $\hat{r} = \hat{x}\sin\theta\cos\phi + \hat{y}\sin\theta\sin\phi + \hat{z}\cos\theta$, and P_l^m is the associate Legendre function.

The spherical harmonics defined as in (5.55) are orthonormal on a sphere with $\theta \in (0, \pi)$ and $\phi \in [0, 2\pi)$. To find the coefficients for the expansion of a given scalar field in spherical scalar wave functions, the orthogonality

can be applied on any sphere with a radius r provided that $z_l(k_0 r)$ is not zero for any needed l. However, in some cases, for instance, in deriving the translational addition theorems, it is better to get rid of z_l by applying incoming wave and radiation patterns as follows.

A scalar field Φ inside a sphere S due to a source outside S can be expanded in incoming spherical scalar wave functions as

$$\Phi(\mathbf{r}) = \sum_{l=0}^{\infty} \sum_{m=-l}^{l} a_{l,m} \psi_{l,m}^{\text{in}}(\mathbf{r}). \tag{5.56}$$

For instance, a plane wave can be expanded as

$$e^{ik_0 \hat{k}\cdot\mathbf{r}} = 4\pi \sum_{l=0}^{\infty} \sum_{m=-l}^{l} i^l Y_{l,m}{}^*(\hat{k}) \psi_{l,m}^{\text{in}}(\mathbf{r}). \tag{5.57}$$

The above expansion is the counterpart of the following expansion of an incoming spherical scalar wave function in plane waves, given e.g. in [19, Eq. (2.44)],

$$\psi_{l,m}^{\text{in}}(\mathbf{r}) = (-i)^l \frac{1}{4\pi} \int_B Y_{l,m}(\hat{k}) e^{ik_0 \hat{k}\cdot\mathbf{r}}\, d\Omega, \tag{5.58}$$

where the integral is with respect to $\hat{k} = \hat{x}\sin\alpha\cos\beta + \hat{y}\sin\alpha\sin\beta + \hat{z}\cos\alpha$ over

$$B = \{\, \hat{k} \mid \alpha \in (0, \pi),\ \beta \in [0, 2\pi) \,\}. \tag{5.59}$$

An approximate expansion of an arbitrary field Φ in plane waves is obtained by substituting (5.58) into a truncation of (5.56) and interchanging the order of integration and summation, yielding

$$\Phi(\mathbf{r}) \approx \frac{1}{4\pi} \int_B \Phi_0(\hat{k}) e^{ik_0 \hat{k}\cdot\mathbf{r}}\, d\Omega, \tag{5.60}$$

where

$$\Phi_0(\hat{k}) = \sum_{l=0}^{P} \sum_{m=-l}^{l} (-i)^l a_{l,m} Y_{l,m}(\hat{k}), \tag{5.61}$$

which is the incoming wave pattern of Φ. Now, the coefficients are found through Φ_0 by the orthogonality of the spherical harmonics as

$$a_{l,m} = i^l \int_B \Phi_0(\hat{k}) Y_{l,m}{}^*(\hat{k})\, d\Omega. \tag{5.62}$$

A scalar field Φ outside a sphere S due to a source inside S can be expanded in outgoing spherical scalar wave functions as

$$\Phi(\mathbf{r}) = \sum_{l=0}^{\infty} \sum_{m=-l}^{l} a_{l,m} \psi_{l,m}^{\text{out}}(\mathbf{r}). \tag{5.63}$$

In the far zone with $k_0 r \gg 1$ the field can be approximated as

$$\Phi(\mathbf{r}) \approx \frac{e^{ik_0 r}}{ik_0 r} \Phi_\infty(\hat{r}), \tag{5.64}$$

where Φ_∞ is the radiation pattern of Φ defined as

$$\Phi_\infty(\hat{k}) = \lim_{k_0 r \to \infty} \frac{ik_0 r}{e^{ik_0 r}} \Phi(\hat{k}r). \tag{5.65}$$

Applying (5.65) on the both sides of (5.63) yields

$$\Phi_\infty(\hat{k}) = \sum_{l=0}^{\infty} \sum_{m=-l}^{l} (-i)^l a_{l,m} Y_{l,m}(\hat{k}). \tag{5.66}$$

Now, the coefficients are found through Φ_∞ by the orthogonality of the spherical harmonics as

$$a_{l,m} = i^l \int_B \Phi_\infty(\hat{k}) Y_{l,m}{}^*(\hat{k})\, d\Omega. \tag{5.67}$$

An approximate expansion of Φ in terms of Φ_∞, more accurate at a close range than (5.64), is obtained by substituting (5.67) into a truncation of (5.63) and interchanging the order of integration and summation, yielding

$$\Phi(\mathbf{r}) \approx \frac{1}{4\pi} \int_B \Phi_\infty(\hat{k}) T_P(\hat{k}, \mathbf{r})\, d\Omega, \tag{5.68}$$

where

$$T_P(\hat{k}, \mathbf{r}) = 4\pi \sum_{l=0}^{P} \sum_{m=-l}^{l} i^l Y_{l,m}{}^*(\hat{k}) \psi_{l,m}^{\text{out}}(\mathbf{r}). \tag{5.69}$$

The expression in (5.69) is called the Rokhlin translator. It is an important tool in MLFMA discussed in Sec. 7. The Rokhlin translator diverges as $P \to \infty$, the divergence becoming exponential after P exceeds $k_0 r$. This phenomenon is called the low-frequency breakdown of the Rokhlin translator. The physical explanation for the breakdown is that the radiation pattern of a source of a fixed size loses its fine structure as the frequency gets lower. This is due to evanescent waves. As a result, the field close to the source cannot be restored from the radiation pattern through (5.68). Consequently, the expansion works only when $k_0 r$ is not too small compared to P.

Another expansion of Φ in terms of Φ_∞, valid for all $k_0 r$, is obtained with the aid of the following expansion, given e.g. in [20, Eq. (3.13)],

$$\psi_{l,m}^{\text{out}}(\mathbf{r}) = (-i)^l \frac{1}{2\pi} \int_C Y_{l,m}(\hat{k}) e^{ik_0 \hat{k}\cdot\mathbf{r}}\, d\Omega, \tag{5.70}$$

where

$$C = \{\, \hat{k} \mid \alpha \in \Gamma,\ \beta \in [0, 2\pi) \,\}, \tag{5.71}$$

and where

$$\Gamma = \{\, \alpha \mid \alpha \in (0, \pi/2 - i\infty) \,\}. \tag{5.72}$$

The first part of Γ with $\alpha \in (0, \pi/2)$ is related to propagating waves and the second part with $\alpha \in [\pi/2, \pi/2 - i\infty)$ to evanescent waves. For this

reason, (5.70) is called the expansion of an outgoing spherical scalar wave function in inhomogeneous plane waves. An expansion of an arbitrary field Φ in inhomogeneous plane waves is obtained by substituting (5.70) into (5.63) and interchanging the order of integration and summation, yielding

$$\Phi(\mathbf{r}) = \frac{1}{2\pi} \int_C \Phi_\infty(\hat{k}) e^{ik_0 \hat{k}\cdot\mathbf{r}} \, d\Omega, \tag{5.73}$$

where Φ_∞ is as in (5.65) but continued into the complex domain C. While owing to the evanescent waves the expansion in (5.73) works for all $k_0 r$, it is restricted to field points with $z > 0$. This is because the integrand diverges exponentially along $\alpha \in [\pi/2, \pi/2 - i\infty)$ if $z < 0$.

Now, consider the translational addition theorem for the spherical scalar wave functions defined as in (5.54). There are three types of the theorem depending on the types of the initial and translated wave functions. Let them be called out-to-out, in-to-in and out-to-in translations. They are all of the form

$$\psi_{l',m'}(\mathbf{t} + \mathbf{r}) = \sum_{l=0}^{\infty} \sum_{m=-l}^{l} \alpha_{l,m;l',m'}(\mathbf{t}) \psi_{l,m}(\mathbf{r}), \tag{5.74}$$

where $\alpha_{l,m;l',m'}$ are translation coefficients. By substituting (5.74) into the expansion of Φ^{init} and interchanging the order of summations, it is found that the coefficients of Φ^{trans} are given by

$$a_{l,m}^{\text{trans}} = \sum_{l'=0}^{\infty} \sum_{m'=-l'}^{l'} \alpha_{l,m;l',m'}(\mathbf{t}) a_{l',m'}^{\text{init}}. \tag{5.75}$$

A unified derivation based on the radiation and incoming wave patterns yielding the translation coefficients for all the types of the theorem is presented in Publication III. Below, there are some alternative integral expressions for the coefficients useful in the theory of the MLFMA discussed in Section 7. As given in Publication III, Eq. (44), the coefficients of the out-to-out translation are

$$\alpha_{l,m;l',m'}^{\text{out-out}}(\mathbf{t}) = i^{l-l'} \int_B {Y_{l,m}}^*(\hat{k}) Y_{l',m'}(\hat{k}) e^{ik_0 \hat{k}\cdot\mathbf{t}} \, d\Omega. \tag{5.76}$$

The coefficients of the in-to-in translation are similar:

$$\alpha_{l,m;l',m'}^{\text{in-in}}(\mathbf{t}) = i^{l-l'} \int_B {Y_{l,m}}^*(\hat{k}) Y_{l',m'}(\hat{k}) e^{ik_0 \hat{k}\cdot\mathbf{t}} \, d\Omega. \tag{5.77}$$

As given in Publication III, Eq. (51), the coefficients of the out-to-in translation have radiation patterns

$$(\alpha_{l,m;l',m'}^{\text{out-in}})_\infty(\hat{k}) = 4\pi i^{l-l'} {Y_{l,m}}^*(\hat{k}) Y_{l',m'}(\hat{k}). \tag{5.78}$$

Then, (5.68) suggests that the coefficients are

$$\alpha^{\text{out-in}}_{l,m;l',m'}(\mathbf{t}) = i^{l-l'} \int_B Y_{l,m}{}^*(\hat{k}) Y_{l',m'}(\hat{k}) T_{2P}(\hat{k}, \mathbf{t})\, d\Omega. \tag{5.79}$$

Because of the property of $T_{2P}(\hat{k}, \mathbf{t})$, the above expression works only when $k_0 t$ is not too small compared to $2P$. An alternative expression for the coefficients of the out-to-in translation, valid for all $k_0 t$, is obtained by substituting (5.78) into (5.73), yielding

$$\alpha^{\text{out-in}}_{l,m;l',m'}(\mathbf{t}) = 2i^{l-l'} \int_C Y_{l,m}{}^*(\hat{k}) Y_{l',m'}(\hat{k}) e^{ik_0 \hat{k}\cdot\mathbf{t}}\, d\Omega. \tag{5.80}$$

However, this equation is valid only when $\hat{z} \cdot \mathbf{t} > 0$.

Vector wave functions in the spherical system of co-ordinates are obtained by introducing (5.54) in (5.7)–(5.9). Choosing $\mathbf{p} = ik_0\mathbf{r}/\sqrt{l(l+1)}$ they are

$$\mathbf{L}_{l,m}(\mathbf{r}) = \hat{r} z_l'(k_0 r) Y_{l,m}(\hat{r}) + \frac{z(k_0 r)}{k_0 r} \mathbf{V}_{l,m}(\hat{r}), \tag{5.81}$$

$$\mathbf{M}_{l,m}(\mathbf{r}) = z_l(k_0 r) \mathbf{U}_{l,m}(\hat{r}), \tag{5.82}$$

$$\mathbf{N}_{l,m}(\mathbf{r}) = -iz_l'(k_0 r)\mathbf{V}_{l,m}(\hat{r}) - i\frac{z_l(k_0 r)}{k_0 r}\mathbf{V}_{l,m}(\hat{r}) + \frac{z_l(k_0 r)}{k_0 r} i\hat{r}\sqrt{l(l+1)} Y_{l,m}(\hat{r}), \tag{5.83}$$

where $\mathbf{U}_{l,m}$ and $\mathbf{V}_{l,m}$ are vector spherical harmonics defined here as

$$\mathbf{U}_{l,m}(\hat{r}) = \frac{i}{\sqrt{l(l+1)}} \nabla_\Omega Y_{l,m}(\hat{r}) \times \hat{r}, \tag{5.84}$$

$$\mathbf{V}_{l,m}(\hat{r}) = i\hat{r} \times \mathbf{U}_{l,m}(\hat{r}), \tag{5.85}$$

where ∇_Ω is a surface gradient on the unit sphere.

The vector spherical harmonics defined as in (5.84) and (5.85) are orthonormal on a sphere with $\theta \in (0, \pi)$ and $\phi \in [0, 2\pi)$. To find the coefficients for the expansion of a given field in spherical vector wave functions through wave patterns on the unit sphere, just like in the scalar case above, consider $\mathbf{E}$ instead of $\mathbf{A}$. This is because $\mathbf{E}$, unlike $\mathbf{A}$, has transversal radiation and incoming wave patterns.

An electric field $\mathbf{E}$ inside a sphere S due to a source outside S can be expanded in incoming spherical vector wave functions as

$$\mathbf{E}(\mathbf{r}) = k_0 \sum_{l=1}^{\infty} \sum_{m=-l}^{l} [b_{l,m} \mathbf{M}^{\text{in}}_{l,m}(\mathbf{r}) + c_{l,m} \mathbf{N}^{\text{in}}_{l,m}(\mathbf{r})]. \tag{5.86}$$

For instance, a plane wave can be expanded through

$$(\mathbb{I} - \hat{k}\hat{k}) e^{ik_0 \hat{k}\cdot\mathbf{r}} = 4\pi \sum_{l=0}^{\infty} \sum_{m=-l}^{l} i^l [\mathbf{U}_{l,m}{}^*(\hat{k}) \mathbf{M}^{\text{in}}_{l,m}(\mathbf{r}) + \mathbf{V}_{l,m}{}^*(\hat{k}) \mathbf{N}^{\text{in}}_{l,m}(\mathbf{r})]. \tag{5.87}$$

The above expansion is the counterpart of the following expansions of the incoming spherical vector wave functions in plane waves, given e.g. in [20, Eqs. (4.17a) and (4.17b)],

$$\mathbf{M}^{\text{in}}_{l,m}(\mathbf{r}) = (-i)^l \frac{1}{4\pi} \int_B \mathbf{U}_{l,m}(\hat{k}) e^{ik_0 \hat{k}\cdot\mathbf{r}}\, d\Omega, \tag{5.88}$$

$$\mathbf{N}^{\text{in}}_{l,m}(\mathbf{r}) = (-i)^l \frac{1}{4\pi} \int_B \mathbf{V}_{l,m}(\hat{k}) e^{ik_0 \hat{k}\cdot\mathbf{r}}\, d\Omega. \tag{5.89}$$

An expansion of an arbitrary electric field $\mathbf{E}$ in plane waves is obtained by substituting (5.88) and (5.89) into a truncation of (5.86) and interchanging the order of integration and summation, yielding

$$\mathbf{E}(\mathbf{r}) \approx \frac{1}{4\pi} \int_B \mathbf{E}_0(\hat{k}) e^{ik_0 \hat{k}\cdot\mathbf{r}}\, d\Omega, \tag{5.90}$$

where

$$\mathbf{E}_0(\hat{k}) = k_0 \sum_{l=1}^{P} \sum_{m=-l}^{l} (-i)^l [b_{l,m}\mathbf{U}_{l,m}(\hat{k}) + c_{l,m}\mathbf{V}_{l,m}(\hat{k})], \tag{5.91}$$

which is the incoming wave pattern of $\mathbf{E}$. Now, the coefficients are found through $\mathbf{E}_0$ by the orthogonality of the vector spherical harmonics as

$$b_{l,m} = i^l \frac{1}{k_0} \int_B \mathbf{E}_0(\hat{k}) \cdot \mathbf{U}_{l,m}{}^*(\hat{k})\, d\Omega, \tag{5.92}$$

$$c_{l,m} = i^l \frac{1}{k_0} \int_B \mathbf{E}_0(\hat{k}) \cdot \mathbf{V}_{l,m}{}^*(\hat{k})\, d\Omega. \tag{5.93}$$

An electric field $\mathbf{E}$ outside a sphere S due to a source inside S can be expanded in outgoing spherical vector wave functions as

$$\mathbf{E}(\mathbf{r}) = k_0 \sum_{l=1}^{\infty} \sum_{m=-l}^{l} [b_{l,m}\mathbf{M}^{\text{out}}_{l,m}(\mathbf{r}) + c_{l,m}\mathbf{N}^{\text{out}}_{l,m}(\mathbf{r})]. \tag{5.94}$$

In the far zone with $k_0 r \gg 1$ the field can be approximated as

$$\mathbf{E}(\mathbf{r}) \approx \frac{e^{ik_0 r}}{ik_0 r} \mathbf{E}_\infty(\hat{r}), \tag{5.95}$$

where $\mathbf{E}_\infty$ is the radiation pattern of $\mathbf{E}$ defined as

$$\mathbf{E}_\infty(\hat{k}) = \lim_{k_0 r \to \infty} \frac{ik_0 r}{e^{ik_0 r}} \mathbf{E}(\hat{k}r). \tag{5.96}$$

Applying (5.96) on the both sides of (5.94) yields

$$\mathbf{E}_\infty(\hat{k}) = k_0 \sum_{l=1}^{\infty} \sum_{m=-l}^{l} (-i)^l [b_{l,m}\mathbf{U}_{l,m}(\hat{k}) + c_{l,m}\mathbf{V}_{l,m}(\hat{k})]. \tag{5.97}$$

Now, the coefficients are found through $\mathbf{E}_\infty$ by the orthogonality of the vector spherical harmonics as

$$b_{l,m} = i^l \frac{1}{k_0} \int_B \mathbf{E}_\infty(\hat{k}) \cdot \mathbf{U}_{l,m}{}^*(\hat{k})\, d\Omega, \tag{5.98}$$

$$c_{l,m} = i^l \frac{1}{k_0} \int_B \mathbf{E}_\infty(\hat{k}) \cdot \mathbf{V}_{l,m}{}^*(\hat{k})\, d\Omega. \tag{5.99}$$

An approximate formula for $\mathbf{E}$ in terms of $\mathbf{E}_\infty$, more accurate at a close range than (5.95), is obtained by substituting (5.98) and (5.99) in a truncation of (5.94) and interchanging the order of integration and summation, yielding

$$\mathbf{E}(\mathbf{r}) \approx \frac{1}{4\pi} \int_B \mathbf{E}_\infty(\hat{k}) \cdot \mathbb{T}_P(\hat{k}, \mathbf{r})\, d\Omega, \tag{5.100}$$

where

$$\mathbb{T}_P(\hat{k}, \mathbf{r}) = 4\pi \sum_{l=0}^{P} \sum_{m=-l}^{l} i^l [\mathbf{U}_{l,m}{}^*(\hat{k}) \mathbf{M}^{\text{out}}_{l,m}(\mathbf{r}) + \mathbf{V}_{l,m}{}^*(\hat{k}) \mathbf{N}^{\text{out}}_{l,m}(\mathbf{r})]. \tag{5.101}$$

As in the scalar case, the above formulation is valid only when $k_0 r$ is not too small compared to P.

Another formula for $\mathbf{E}$ in terms of $\mathbf{E}_\infty$, valid for all $k_0 r$, is obtained with the aid of the following inhomogeneous plane wave expansions of the outgoing vector spherical wave functions, given e.g. in [20, Eqs. (4.14a) and (4.14b)],

$$\mathbf{M}^{\text{out}}_{l,m}(\mathbf{r}) = (-i)^l \frac{1}{2\pi} \int_C \mathbf{U}_{l,m}(\hat{k}) e^{ik_0 \hat{k} \cdot \mathbf{r}}\, d\Omega, \tag{5.102}$$

$$\mathbf{N}^{\text{out}}_{l,m}(\mathbf{r}) = (-i)^l \frac{1}{2\pi} \int_C \mathbf{V}_{l,m}(\hat{k}) e^{ik_0 \hat{k} \cdot \mathbf{r}}\, d\Omega. \tag{5.103}$$

An inhomogeneous plane wave expansion of an arbitrary $\mathbf{E}$ is obtained by substituting (5.102) and (5.103) into (5.94) and interchanging the order of integration and summation, yielding

$$\mathbf{E}(\mathbf{r}) = \frac{1}{2\pi} \int_C \mathbf{E}_\infty(\hat{k}) e^{ik_0 \hat{k} \cdot \mathbf{r}}\, d\Omega, \tag{5.104}$$

where $\mathbf{E}_\infty$ is as defined in (5.96) but continued into the complex domain C. Again, the above expression is valid only when $\hat{z} \cdot \mathbf{r} > 0$.

Now, consider the translational addition theorem for the spherical vector wave functions defined as in (5.81)–(5.83). As in the scalar case, there are three types of the theorem and they are all of the form

$$\mathbf{M}_{l',m'}(\mathbf{t} + \mathbf{r}) = \sum_{l=1}^{\infty} \sum_{m=-l}^{l} [\beta_{l,m;l',m'}(\mathbf{t}) \mathbf{M}_{l,m}(\mathbf{r}) + \gamma_{l,m;l',m'}(\mathbf{t}) \mathbf{N}_{l,m}(\mathbf{r})], \tag{5.105}$$

$$\mathbf{N}_{l',m'}(\mathbf{t} + \mathbf{r}) = \sum_{l=1}^{\infty} \sum_{m=-l}^{l} [\gamma_{l,m;l',m'}(\mathbf{t}) \mathbf{M}_{l,m}(\mathbf{r}) + \beta_{l,m;l',m'}(\mathbf{t}) \mathbf{N}_{l,m}(\mathbf{r})], \tag{5.106}$$

where $\beta_{l,m;l',m'}(\mathbf{t})$ and $\gamma_{l,m;l',m'}(\mathbf{t})$ are translation coefficients. By substituting (5.105) and (5.106) into the expansion of $\mathbf{E}^{\text{init}}$, changing the order of summation and collecting the terms, it is found that the coefficients of

$\mathbf{E}^{\text{trans}}$ are given by

$$b_{l,m}^{\text{trans}} = \sum_{l'=1}^{\infty} \sum_{m'=-l'}^{l'} [\beta_{l,m;l',m'}(\mathbf{t}) b_{l',m'}^{\text{init}} + \gamma_{l,m;l',m'}(\mathbf{t}) c_{l',m'}^{\text{init}}], \tag{5.107}$$

$$c_{l,m}^{\text{trans}} = \sum_{l'=1}^{\infty} \sum_{m'=-l'}^{l'} [\gamma_{l,m;l',m'}(\mathbf{t}) b_{l',m'}^{\text{init}} + \beta_{l,m;l',m'}(\mathbf{t}) c_{l',m'}^{\text{init}}]. \tag{5.108}$$

A unified derivation based on the radiation and incoming wave patterns yielding the translation coefficients for all the types of the theorem is presented in Publication III. Below, there are some alternative integral expressions for the coefficients. As given in Publication III, Eqs. (56) and (57), the coefficients of the out-to-out translation are

$$\beta_{l,m;l',m'}^{\text{out-out}}(\mathbf{t}) = i^{l-l'} \int_B \mathbf{U}_{l,m}{}^*(\hat{k}) \cdot \mathbf{U}_{l',m'}(\hat{k}) e^{ik_0 \hat{k}\cdot\mathbf{t}} \, d\Omega, \tag{5.109}$$

$$\gamma_{l,m;l',m'}^{\text{out-out}}(\mathbf{t}) = i^{l-l'} \int_B \mathbf{U}_{l,m}{}^*(\hat{k}) \cdot \mathbf{V}_{l',m'}(\hat{k}) e^{ik_0 \hat{k}\cdot\mathbf{t}} \, d\Omega. \tag{5.110}$$

The coefficients of the in-to-in translation are similar. As given in Publication III, Eq. (63), the coefficients of the out-to-in translation have radiation patterns

$$(\beta_{l,m;l',m'}^{\text{out-in}})_\infty(\hat{k}) = 4\pi i^{l-l'} \mathbf{U}_{l,m}{}^*(\hat{k}) \cdot \mathbf{U}_{l',m'}(\hat{k}), \tag{5.111}$$

$$(\gamma_{l,m;l',m'}^{\text{out-in}})_\infty(\hat{k}) = 4\pi i^{l-l'} \mathbf{U}_{l,m}{}^*(\hat{k}) \cdot \mathbf{V}_{l',m'}(\hat{k}). \tag{5.112}$$

Then, (5.68) suggests that the coefficients are given by

$$\beta_{l,m;l',m'}^{\text{out-in}}(\mathbf{t}) = i^{l-l'} \int_B \mathbf{U}_{l,m}{}^*(\hat{k}) \cdot \mathbf{U}_{l',m'}(\hat{k}) T_{2P}(\hat{k}, \mathbf{t}) \, d\Omega, \tag{5.113}$$

$$\gamma_{l,m;l',m'}^{\text{out-in}}(\mathbf{t}) = i^{l-l'} \int_B \mathbf{U}_{l,m}{}^*(\hat{k}) \cdot \mathbf{V}_{l',m'}(\hat{k}) T_{2P}(\hat{k}, \mathbf{t}) \, d\Omega. \tag{5.114}$$

Because of the property of $T_{2P}(\hat{k}, \mathbf{t})$, the above expression works only when $k_0 t$ is not too small compared to $2P$. An alternative expression for the coefficients of the out-to-in translation, which works for all $k_0 t$, is obtained by substituting (5.111) and (5.112) into (5.104), yielding

$$\beta_{l,m;l',m'}^{\text{out-in}}(\mathbf{t}) = 2i^{l-l'} \int_C \mathbf{U}_{l,m}{}^*(\hat{k}) \cdot \mathbf{U}_{l',m'}(\hat{k}) e^{ik_0 \hat{k}\cdot\mathbf{t}} \, d\Omega, \tag{5.115}$$

$$\gamma_{l,m;l',m'}^{\text{out-in}}(\mathbf{t}) = 2i^{l-l'} \int_C \mathbf{U}_{l,m}{}^*(\hat{k}) \cdot \mathbf{V}_{l',m'}(\hat{k}) e^{ik_0 \hat{k}\cdot\mathbf{t}} \, d\Omega. \tag{5.116}$$

However, these are valid only when $\hat{z} \cdot \mathbf{t} > 0$.

It is easy to notice from the above expressions for the translation coefficients $\alpha_{l,m;l',m'}$, $\beta_{l,m;l',m'}$ and $\gamma_{l,m;l',m'}$ that, in general, the coefficients are non-zero for all $l, m; l', m'$. That is, the translation matrices consisting of the coefficients are full matrices.

5.5 In ultra-spherical system of co-ordinates

As a continuation of the above route from plane waves first to cylindrical waves and then to spherical waves, consider now ultra-spherical waves in a p-dimensional space $\mathbb{R}^p$. Although a general analysis becomes difficult when $p > 3$, a certain rotationally symmetric scalar case is formulated in [18, Sec. 4.83]. Accordingly, ultra-spherical scalar wave functions can be defined as

$$\psi_l(r,\theta) = \frac{Z_{l+\frac{p}{2}-1}(k_0 r)}{(k_0 r)^{\frac{p}{2}-1}} C_l^{(\frac{p}{2}-1)}(\cos\theta). \tag{5.117}$$

$C_l^{(\frac{p}{2}-1)}$ is the Gegenbauer polynomial of order $p/2-1$. r is a radial co-ordinate so that $r^2 = x_1^2 + \cdots + x_p^2$ where $x_1, \ldots, x_p$ are the cartesian co-ordinates in $\mathbb{R}^p$. θ is an angular co-ordinate so that $\cos\theta = x_p/r$. The wave functions are rotationally symmetric along the other angles.

Consider a translational addition theorem for the ultra-spherical scalar wave functions defined as in (5.117). According to Gegenbauer's addition theorem [18, Sec. 11.41, Eq. (4)],

$$\begin{aligned}
&\frac{Z_{\frac{p}{2}-1}(k_0\sqrt{t^2+r^2-2tr\cos\vartheta})}{(k_0\sqrt{t^2+r^2-2tr\cos\vartheta})^{\frac{p}{2}-1}} \\
&= 2^{\frac{p}{2}-1}\Gamma\left(\frac{p}{2}-1\right)\sum_{l=0}^{\infty}\left(\frac{p}{2}-1+l\right)\frac{J_{\frac{p}{2}-1+l}(k_0 t)}{(k_0 t)^{\frac{p}{2}-1}}\frac{Z_{\frac{p}{2}-1+l}(k_0 r)}{(k_0 r)^{\frac{p}{2}-1}}C_l^{(\frac{p}{2}-1)}(\cos\vartheta).
\end{aligned} \tag{5.118}$$

This result is exploited in Section 6.4 to derive an integral transform for basis functions for a charge on a ring conductor.

6. Spatial-spectral hybrid method in cylindrical system of co-ordinates

6.1 Hankel transforms

Suppose that a scalar function F can be expanded in the cylindrical system of co-ordinates as

$$F(\mathbf{r}) = \sum_{m=-\infty}^{\infty} F_m(\rho, z) e^{im\phi}, \tag{6.1}$$

$$F_m(\rho, z) = \int_0^{\infty} f_m(k_\rho, z) J_m(k_\rho \rho) k_\rho \, dk_\rho, \tag{6.2}$$

where

$$f_m(k_\rho, z) = \int_0^{\infty} F_m(\rho, z) J_m(k_\rho \rho) \rho \, d\rho, \tag{6.3}$$

$$F_m(\rho, z) = \frac{1}{2\pi} \int_0^{2\pi} F(\mathbf{r}) e^{-im\phi} \, d\phi. \tag{6.4}$$

The integrals in (6.3) and (6.2) form a Hankel transform pair of order m. The expansion formed by (6.1) and (6.2) is a generalisation of the expansion of a scalar field in cylindrical scalar wave functions in (5.37), and the integrals in (6.3) and (6.4) are similar to the integrals in (5.38).

Suppose that a vector function $\mathbf{F} = \hat{\rho} F_\rho + \hat{\phi} F_\phi$ can be expanded as

$$\mathbf{F}(\mathbf{r}) = \sum_{m=-\infty}^{\infty} \mathbf{F}_m(\rho, z) e^{im\phi}, \tag{6.5}$$

$$\mathbf{F}_m(\rho, z) = \int_0^{\infty} \mathbf{f}_m(k_\rho, z) \cdot \mathbb{H}_m(k_\rho \rho) k_\rho \, dk_\rho, \tag{6.6}$$

where

$$\mathbf{f}_m(k_\rho, z) = \int_0^{\infty} \mathbf{F}_m(\rho, z) \cdot \mathbb{H}_m{}^{\mathrm{H}}(k_\rho \rho) \rho \, d\rho, \tag{6.7}$$

$$\mathbf{F}_m(\rho, z) = \frac{1}{2\pi} \int_0^{2\pi} \mathbf{F}(\mathbf{r}) e^{-im\phi} \, d\phi \tag{6.8}$$

and

$$\mathbb{H}_m(k_\rho \rho) = \hat{k}_\rho \left[\hat{\rho} J'_m(k_\rho \rho) + \hat{\phi} im \frac{J_m(k_\rho \rho)}{k_\rho \rho} \right] + \hat{\beta} \left[\hat{\rho} im \frac{J_m(k_\rho \rho)}{k_\rho \rho} - \hat{\phi} J'_m(k_\rho \rho) \right]. \tag{6.9}$$

The integrals in (6.7) and (6.6) form a vector Hankel transform pair of order m. The vector Hankel transform was introduced and its properties are proved in [21]. The expansion formed by (6.5) and (6.7) is related to the expansion of a vector field in cylindrical vector wave functions in (5.46), and the integrals in (6.7) and (6.8) are related to the integrals in (5.47) and (5.48).

6.2 Static Green's function in layered medium

Consider a static Green's function G in a layered medium. Suppose that the medium is layered in the z-direction and invariant in the x- and y-directions as illustrated in Fig. 6.1 and defined in Publication II, Section 2. The solution of G can be greatly simplified by using the Hankel transform defined in Section 6.1. However, the Hankel transform $g(k_\rho, z, z')$ of $G(\mathbf{r}, \mathbf{r}')$ decays slowly as a function of k_ρ if z is close to z', the limiting rate being $1/k_\rho$. A remedy is to divide G, somewhat similarly as in (2.42), into two parts as

$$G = G^{\text{pri}} + G^{\text{sec}}, \tag{6.10}$$

where G^{pri}, as described in Publication II, Section 5, includes the fields of the primary source and the first image sources that are easy to formulate explicitly. The fields of the rest of the infinitely many image sources are included in G^{sec}, which can be formulated with an exponentially decaying Hankel transform g^{sec}. The formulation of G^{sec} is described in Publication II, Section 5. Below, there is an alternative formulation based on an expansion of G^{sec} in cylindrical static wave functions.

Suppose that the field point is in the lth layer with $z_{l,1} < z < z_{l,2}$ and the source point is in the l'th layer with $z_{l',1} < z' < z_{l',2}$. Since G^{pri} includes the primary source, G^{sec} needs only to satisfy the homogeneous Laplace equation and can thus be expanded in cylindrical static wave functions as

$$G^{\text{sec}}(\mathbf{r}, \mathbf{r}') = \sum_{s=1}^{2} \sum_{m=-\infty}^{\infty} \int_0^\infty a_{l,m,s}(k_\rho, \mathbf{r}') \psi_{l,m,s}(k_\rho, \mathbf{r}) k_\rho \, dk_\rho, \tag{6.11}$$

where

$$\psi_{l,m,s}(k_\rho, \mathbf{r}) = J_m(k_\rho \rho) e^{im\phi} Z_{l,s}(k_\rho, z). \tag{6.12}$$

Here, $Z_{l,s}$ consists of hyperbolic functions as defined in Publication II, Eq. (22). Accordingly, $Z_{l,1}$ equals one at the bottom of the layer and zero at the top of the layer, and $Z_{l,2}$ vice versa. If the system of co-ordinates is

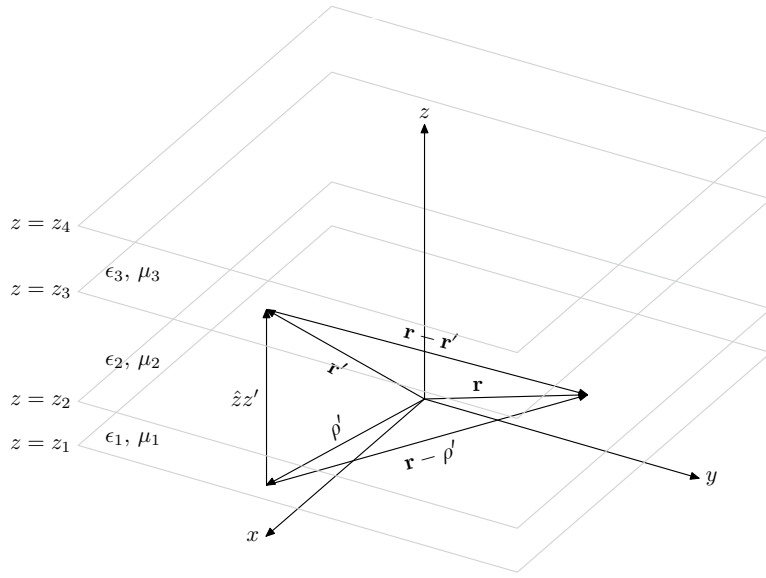

Figure 6.1. System of co-ordinates and layered medium.

translated so that the source comes to the z-axis, the field is rotationally symmetric with respect to the z-axis and (6.11) reduces to

$$G^{\text{sec}}(\mathbf{r} - \boldsymbol{\rho}', \hat{z}z') = \sum_{s=1}^{2} \int_0^\infty a_{l,0,s}(k_\rho, \hat{z}z') \psi_{l,0,s}(k_\rho, \mathbf{r} - \boldsymbol{\rho}') k_\rho \, dk_\rho. \tag{6.13}$$

Now, by virtue of the reciprocity between the field and the source,

$$a_{l,0,s}(k_\rho, \hat{z}z') = \sum_{s'=1}^{2} g^{\text{sec}}(k_\rho, z_{l,s}, z_{l',s'}) Z_{l',s'}(k_\rho, z'), \tag{6.14}$$

where $g^{\text{sec}}(k_\rho, z_{l,s}, z_{l',s'})$ is given in Publication II, Eqs. (25) and (26). Then, substituting (6.14) into (6.13) and restoring the location of the source with the aid of the translational addition theorem (5.40), (6.13) becomes

$$G^{\text{sec}}(\mathbf{r}, \mathbf{r}') = \sum_{s,s'=1}^{2} \sum_{m=-\infty}^{\infty} \int_0^\infty \psi_{l,m,s}(k_\rho, \mathbf{r}) g^{\text{sec}}(k_\rho, z_{l,s}, z_{l',s'}) \psi_{l',-m,s'}(k_\rho, \mathbf{r}') k_\rho \, dk_\rho. \tag{6.15}$$

6.3 MoM system matrix terms in hybrid method

Consider method of moment solutions of the electro- and magnetostatic problems formulated by integral equations as in Sections 3.1 and 3.2 when the geometry consists of concentric ring conductors with rectangular cross-sections and a layered medium as illustrated in Fig. 6.2. When

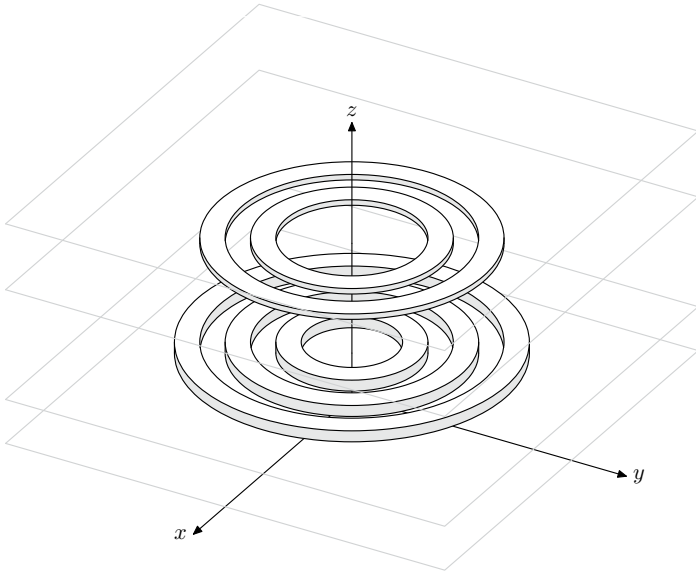

Figure 6.2. Ring conductors in a layered medium.

the Green's function is divided into two parts as described above, also matrix terms (4.6) are divided into corresponding parts as

$$a_{n,n'} = a^{\text{pri}}_{n,n'} + a^{\text{sec}}_{n,n'}. \tag{6.16}$$

Formulas for the matrix terms are given in Publication II, Section 6. Below, there are revised choices for the formulas. The revisions include the extraction of the edge singularity from the basis functions to a weight function and a more explicit use of the vector Hankel transform in the magnetostatic case. The notation is similar to the notation in Publication II, Section 6. In particular, $S_{p,q}$ denotes the qth face of the pth conductor and $L_{p,q}$ a transversal line across the face.

In the electrostatic problem, the first part can be formulated as

$$a^{\text{pri}}_{n,n'} = \int_{S_{p,q}} w_{p,q}(\xi) b_n(\xi) \Phi^{\text{pri}}_{n'}(\mathbf{r})\, dS, \tag{6.17}$$

where

$$\Phi^{\text{pri}}_{n'}(\mathbf{r}) = \int_{S_{p',q'}} G^{\text{pri}}(\mathbf{r}, \mathbf{r}') w_{p',q'}(\xi') b_{n'}(\xi')\, dS'. \tag{6.18}$$

Above, $w_{p,q}$ is a weight function matching with the edge singularity on $S_{p,q}$ and b_n is a polynomial basis function. By using the expansion (6.15), the second part can be formulated as

$$a^{\text{sec}}_{n,n'} = \int_0^\infty \sum_{s,s'=1}^{2} I_{n,s}(k_\rho) g^{\text{sec}}(k_\rho, z_{l,s}, z_{l',s'}) I_{n',s'}(k_\rho) k_\rho\, dk_\rho, \tag{6.19}$$

where

$$I_{n,s}(k_\rho) = 2\pi \int_{L_{p,q}} w_{p,q}(\xi) b_n(\xi) J_0(k_\rho \rho) Z_{l,s}(k_\rho, z) \rho \, d\ell. \tag{6.20}$$

The modes with $m > 0$ are dropped out since the problem is rotationally symmetric. The integral in (6.20) is either the Hankel or Fourier transform of $w_{p,q} b_n$ depending on whether $S_{p,q}$ is a horizontal or vertical face, respectively.

In the magnetostatic problem, the first part can be formulated as

$$a^{\text{pri}}_{n,n'} = \int_{S_{p,q}} \hat{\phi} w_{p,q}(\xi) b_n(\xi) \cdot \mathbf{A}^{\text{pri}}_{n'}(\mathbf{r}) \, dS, \tag{6.21}$$

where

$$\mathbf{A}^{\text{pri}}_{n'}(\mathbf{r}) = \int_{S_{p',q'}} G^{\text{pri}}(\mathbf{r}, \mathbf{r}') \hat{\phi}' w_{p',q'}(\xi') b_{n'}(\xi') \, dS'. \tag{6.22}$$

By using the expansion (6.15) and the vector Hankel transform (6.3), the second part can be formulated as

$$a^{\text{sec}}_{n,n'} = \int_0^\infty \sum_{s,s'=1}^{2} \mathbf{I}_{n,s} \cdot g^{\text{sec}}(k_\rho, z_{l,s}, z_{l',s'}) \mathbf{I}_{n',s'} k_\rho \, dk_\rho, \tag{6.23}$$

where

$$\mathbf{I}_{n,s}(k_\rho) = 2\pi \int_{L_{p,q}} \hat{\phi} w_{p,q}(\xi) b_n(\xi) \cdot \mathbb{H}^{\text{H}}_0(k_\rho \rho) Z_{l,s}(k_\rho, z) \rho \, d\ell. \tag{6.24}$$

6.4 Charge and current on ring conductor

Consider the choice of the weight function w and the basis functions $b_1, b_2, \ldots$ for approximating a surface charge or current on a ring conductor. An ideal choice would be such that:

1. w matches with the correct edge singularity. Then, the unknown function can be expressed by a plain polynomial.

2. $b_1, b_2, \ldots$ constitute a complete and orthogonal set with respect to the inner product with w. This ensures that the approximate solution converges quickly toward the exact solution as the number of basis functions increases.

3. b_1 represents the exact solution in a free space. Then, $b_2, b_3, \ldots$ are just for compensating the disturbance due to the surroundings.

4. The potential due to each b_n in a free space is known. Then, the integrals in (6.18) and (6.22), which are difficult to evaluate numerically, have analytic formulas.

5. The needed integral transforms for wb_n are available in a closed form. Then, the integrations in (6.20) and (6.24) have analytic formulas.

In a case of an indefinitely thin line conductor, all the above requirements could be fulfilled, as shown e.g. in [15]. Now, in the case of a finitely thick ring conductor, the requirements 1, 2 and 5 can be fulfilled by choosing the weight and basis functions as described in Publication I, Section 6, and in Publication II, Section 7. Similar basis functions were already used in [22] and [23] concerning the capacitance of an indefinitely thin ring conductor and in [24] concerning the capacitance of a finite cylinder. Below, a couple of integral results are re-derived to show that they can be seen as results of the addition theorems discussed in Sections 5.3 and 5.5.

Consider the surface charge on an indefinitely thin ring conductor. On such a conductor, the surface charge is known to grow like the inverse of the square root of the distance to the edge when approaching the edge. To find such w and $b_1, b_2, \ldots$ that fulfill the requirements 1, 2 and 5, start with Neumann's addition theorem (5.39) rewritten as

$$J_0(k_\rho\sqrt{r^2+v^2-2rv\cos\theta}) = \sum_{m=0}^{\infty} \epsilon_m J_m(k_\rho r) J_m(k_\rho v)\cos(m\theta), \qquad (6.25)$$

where ϵ_m is Neumann's factor equaling 1 when $m = 0$ and 2 otherwise. Now, applying the orthogonality of cosine functions to (6.25) yields an integral result

$$\int_0^\pi \cos(m\theta) J_0(k_\rho\sqrt{r^2+v^2-2rv\cos\theta})\,d\theta = \pi J_m(k_\rho r) J_m(k_\rho v), \qquad (6.26)$$

which is a special case of "the very important integral" given e.g. in [18, Sec. 12.1]. A change of variables according to $\rho^2 = r^2+v^2-2rv\cos\theta$ turns (6.26) into

$$\frac{1}{rv}\int_{r-v}^{r+v}\left[1-\left(\frac{r^2+v^2-\rho^2}{2rv}\right)^2\right]^{-\frac{1}{2}} T_m\left(\frac{r^2+v^2-\rho^2}{2rv}\right) J_0(k_\rho\rho)\rho\,d\rho = \pi J_m(k_\rho r) J_m(k_\rho v). \qquad (6.27)$$

This provides the Hankel transforms for $wb_1, wb_2, \ldots$ if

$$w(\rho) = \frac{1}{rv}\left[1-\left(\frac{r^2+v^2-\rho^2}{2rv}\right)^2\right]^{-\frac{1}{2}} \qquad (6.28)$$

and

$$b_n(\rho) = T_m\left(\frac{r^2+v^2-\rho^2}{2rv}\right). \qquad (6.29)$$

Also, it is easy to deduce from the orthogonality of cosine functions that $b_1, b_2, \ldots$ are orthogonal with respect to the inner product with (6.28) as

$$\int_{r-v}^{r+v} w(\rho) b_n(\rho) b_{n'}(\rho)\rho\,d\rho = \frac{\pi}{\epsilon_m}\delta_{n,n'}. \qquad (6.30)$$

On a finitely thick conductor with rectangular cross-section, the surface charge is known to grow like the inverse cubic root of the distance to the edge when approaching the edge; see e.g. [13] or [14, Ch. 4]. So, on the top or bottom surface of the conductor, w similar to (6.28) but with an inverse cubic root singularity is

$$w(\rho) = \frac{1}{rv}\left[1 - \left(\frac{r^2 + v^2 - \rho^2}{2rv}\right)^2\right]^{-\frac{1}{3}}. \tag{6.31}$$

$b_1, b_2, \ldots$ orthogonal with respect to the inner product with (6.31) are

$$b_n(\rho) = C_m^{(\frac{1}{6})}\left(\frac{r^2 + v^2 - \rho^2}{2rv}\right), \tag{6.32}$$

where $C_m^{(\frac{1}{6})}$ are Gegenbauer polynomials of order $1/6$. The integral result providing the Hankel transforms for $wb_1, wb_2, \ldots$ with the above w and $b_1, b_2, \ldots$ is given in Publication II, Eq. (42). Also, it is easy to deduce from the orthogonality of Gegenbauer polynomials, see e.g. [25, Tab. 22.2], that $b_1, b_2, \ldots$ are orthogonal with respect to the inner product with (6.31) as

$$\int_{r-v}^{r+v} w(\rho) b_n(\rho) b_{n'}(\rho) \rho \, d\rho = \frac{\pi 2^{\frac{2}{3}} \Gamma(m + \frac{1}{3})}{m!(m + \frac{1}{6})[\Gamma(\frac{1}{6})]^2} \delta_{n,n'}. \tag{6.33}$$

On a vertical surface, the matching weight function and basis functions are

$$w(z) = \frac{1}{(r \pm v)\tau}\left[1 - \left(\frac{z - h}{\tau}\right)^2\right]^{-\frac{1}{3}} \tag{6.34}$$

and

$$b_n(z) = C_m^{(\frac{1}{6})}\left(\frac{z - h}{\tau}\right). \tag{6.35}$$

To obtain the integral result providing the Hankel transform for $wb_1, wb_2, \ldots$ with above w and $b_1, b_2, \ldots$, start with Gegenbauer's addition theorem (5.118) rewritten with $p = 7/3$ as

$$\frac{H_{\frac{1}{6}}^{(1)}(k_\rho \sqrt{h^2 + \tau^2 - 2h\tau\cos\theta})}{(k_\rho \sqrt{h^2 + \tau^2 - 2h\tau\cos\theta})^{\frac{1}{6}}}$$
$$= 2^{\frac{1}{6}}\Gamma\left(\frac{1}{6}\right) \sum_{m=0}^{\infty} \left(\frac{1}{6} + m\right) \frac{H_{\frac{1}{6}+m}^{(1)}(k_\rho h)}{(k_\rho h)^{\frac{1}{6}}} \frac{J_{\frac{1}{6}+m}(k_\rho \tau)}{(k_\rho \tau)^{\frac{1}{6}}} C_m^{(\frac{1}{6})}(\cos\theta). \tag{6.36}$$

Next, take a large argument as $h \to \infty$ yielding

$$e^{ik_\rho \tau \cos\theta} = 2^{\frac{1}{6}}\Gamma\left(\frac{1}{6}\right) \sum_{m=0}^{\infty} i^m \left(\frac{1}{6} + m\right) \frac{J_{\frac{1}{6}+m}(k_\rho \tau)}{(k_\rho \tau)^{\frac{1}{6}}} C_m^{(\frac{1}{6})}(\cos\theta). \tag{6.37}$$

Now, the application of the orthogonality of Gegenbauer polynomials yields

$$\int_0^\pi (\sin\theta)^{\frac{1}{3}} C_m^{(\frac{1}{6})}(\cos\theta) e^{ik_\rho \tau \cos\theta} \, d\theta = \frac{i^m 2^{\frac{5}{6}} \pi \Gamma(m + \frac{1}{3})}{\Gamma(\frac{1}{6}) m!} \frac{J_{\frac{1}{6}+m}(k_\rho \tau)}{(k_\rho \tau)^{\frac{1}{6}}}. \tag{6.38}$$

Finally, combine exponential functions to form hyperbolic functions and performing a change of variables according to $z = h + \tau\cos\theta$ yields

$$\frac{1}{\tau}\int_{h-\tau}^{h+\tau}\left[1-\left(\frac{z-h}{\tau}\right)^2\right]^{-\frac{1}{3}} C_m^{(\frac{1}{6})}\left(\frac{z-h}{\tau}\right)\sinh(k_\rho z)\,dz$$
$$= \frac{2^{\frac{5}{6}}\pi\Gamma(\frac{1}{3}+m)}{\Gamma(\frac{1}{6})m!}\frac{I_{\frac{1}{6}+m}(k_\rho\tau)}{(k_\rho\tau)^{\frac{1}{6}}}\begin{cases}\sinh(k_\rho h), & m \text{ even},\\ \cosh(k_\rho h), & m \text{ odd},\end{cases} \tag{6.39}$$

where $I_{\frac{1}{6}+m}$ is the modified Bessel function of the first kind.

In the considered rotationally symmetric case, the surface current on a ring conductor has only the ϕ-component. Then, the weight function for the current is the same as for the charge, and the basis functions for the current are closely related to those for the charge as explained in Publication I, Section 6.2, and in Publication II, Section 7.2.

6.5 Application to an LC-model of a spiral inductor

In Publication I, an indefinitely thin spiral conductor, such as the one illustrated in Fig. 6.3, is approximated by concentric annular ring conductors, capacitance and inductance matrices of the system consisting of the ring conductors are calculated by using the method described in the paper and partly revised above, and the capacitance and inductance matrix elements are used to construct LC-models for the spiral conductors.

The approximation consists of two consecutive steps: First, a spiral conductor is divided into intervals, for instance, so that each of the intervals corresponds one turn in the spiral conductor, and the current and charge are approximated by constant values at each of the intervals. Then, the radii of curvature are approximated by constant values at each of the intervals. These two steps turn the dynamic electromagnetic problem of the spiral conductor into electro- and magnetostatic problems of the concentric annular ring conductors. Fig. 6.4 illustrates an approximation of a three-turn spiral conductor by three ring conductors.

The capacitances and inductances resulting from solving the electro- and magnetostatic problems, respectively, are then used in an LC-model that approximates the initial dynamic problem. Fig. 6.5 shows the resulting LC-model where each turn is modelled by a π-circuit. The diagonal elements correspond to the self-capacitances and -inductances of the turns while the non-diagonal elements correspond to mutual couplings between the turns.

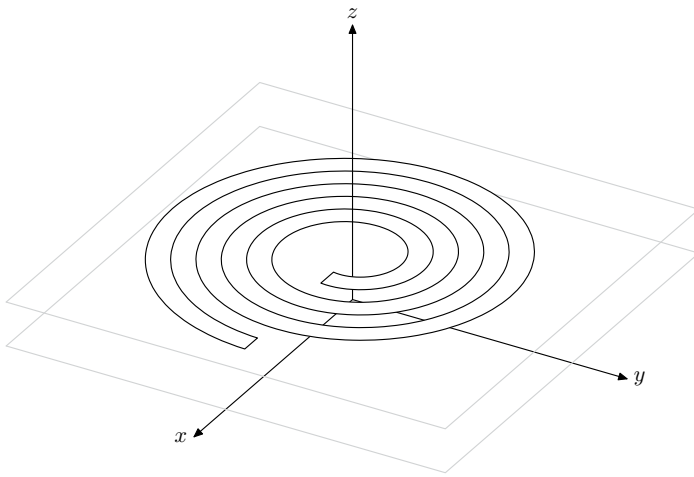

Figure 6.3. Spiral conductor.

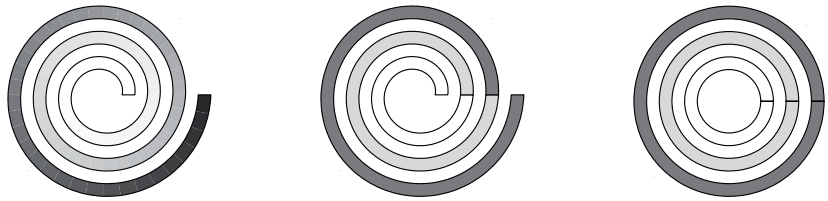

(a) Initial geometry and charge/current

(b) Initial geometry, approximated charge/current

(c) Approximated geometry and charge/current

Figure 6.4. Consecutive steps in approximating a three-turn spiral conductor and continuous charge/current on it by three concentric ring conductors and step-wise constant charge/current.

The generalised method presented in Publication II enables similar analysis of structures consisting of finitely thick conductors with comparable accuracy.

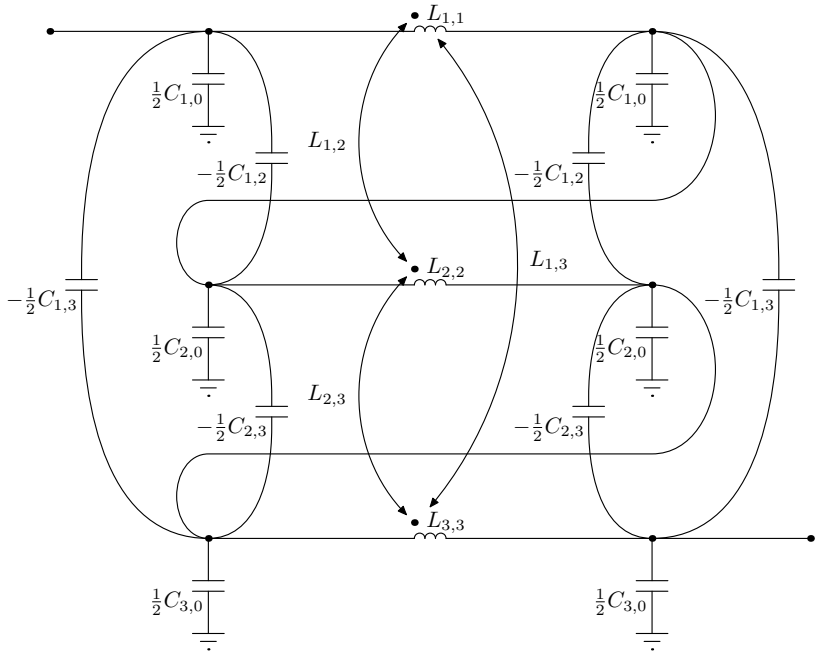

Figure 6.5. LC-model for a three-turn spiral conductor consisting of three cascaded and also parallel-coupled π-circuits. The capacitances $C_{1,0}$, $C_{2,0}$ and $C_{3,0}$ between the rings and the ground are of the form $C_{n,0} = C_{n,1} + C_{n,2} + C_{n,3}$.

7. Multilevel fast multipole algorithm

7.1 Overview of algorithm with expansions in wave functions

Consider an iterative solution of a matrix equation of the form of (4.5) obtained by discretising an integral equation. Iterative schemes repeatedly apply a matrix-vector multiplication with the system matrix A. This multiplication equals calculating the field due to the source expanded in the basis functions with the prevailing iterated values of the expansion coefficients in the vector x and testing the field by the test functions. An application of a numerical integration scheme turns the basis and test functions into point sources located in the integration nodes. Consequently, the calculation is reduced to computing sums of the following form for each node point $\mathbf{r}_n$:

$$\sum_{n'} G(\mathbf{r}_n, \mathbf{r}_{n'}) q_{n'}, \tag{7.1}$$

where G is the Green's function defined as in (2.41), $q_{n'}$ is the amplitude of a point source at $\mathbf{r}_{n'}$ and the summation goes through all the sources except those related to the basis function whose support includes the point $\mathbf{r}_n$. If N is the total number of point sources, the operation count in evaluating (7.1) is proportional to N^2. This is too large for a practical calculation if N is large.

The multilevel fast multipole algorithm (MLFMA), explained e.g. in [26], [27] and [28], is for carrying out the above extremely simple but laborious task in a complex but a lot more efficient way, with the operation count proportional to N in the low-frequency regime and to $N \log N$ in the high-frequency regime. To start with, the summation in (7.1) is divided into two parts as

$$\sum_{n'} G(\mathbf{r}_n, \mathbf{r}_{n'}) q_{n'} = \sum_{n' \in \text{ near}} G(\mathbf{r}_n, \mathbf{r}_{n'}) q_{n'} + \sum_{n' \in \text{ far}} G(\mathbf{r}_n, \mathbf{r}_{n'}) q_{n'}. \tag{7.2}$$

The first summation on the right-hand-side of (7.2) contains sources near to $\mathbf{r}_n$ and is calculated in the ordinary 'slow way'. The second summation contains the rest of the sources, which are farther from $\mathbf{r}_n$, and is calculated by using the MLFMA.

The MLFMA applies a hierarchical system, which can be set up as follows: First, all the sources are enclosed in a cube. Then, the cube is subdivided into eight subcubes called children, the former cube being called a parent. Each of these child cubes is again subdivided into eight new child cubes, which are assigned to a level H, and this process is recursively continued, building an octree structure with levels $H, H-1, H-2, \ldots$, until the last cube at each branch of the octree encloses only a few sources. All the empty cubes emerging in the process are ignored. Two cubes at the same level are called neighbours if their boundaries share a point, and a cube is considered as a neighbour to itself. If two cubes are not neighbours, they are called non-nearby to each other. For every cube an interaction list is defined, which includes all the non-nearby cubes whose parents are neighbours of the parent of the initial cube. In addition, denoting the side length of a cube at a level h by s_h, the levels are categorised into two classes calling the lower levels $h = 0, -1, -2, \ldots$ with $k_0 s_h < 2\pi$ the sub-wavelength levels and the remaining higher levels $h = 1, 2, \ldots$ the super-wavelength levels. A two-level example of the hierarchical system is illustrated in Fig. 7.1.

The algorithm consists of two passes; let them be called the aggregation pass and the disaggregation pass. In the aggregation pass, the field due to the sources in each cube at each level is collectively represented by truncated expansion in outgoing spherical wave functions, i.e., in the fields of multipoles. For instance, the outgoing field from a cube Q_i with the centre at $\mathbf{c}_i$ is represented as

$$\Phi^{\text{from } Q_i}(\mathbf{r}) \approx \sum_{l=0}^{P_h} \sum_{m=-l}^{l} a_{l,m}^{\text{from } Q_i} \psi_{l,m}^{\text{out}}(\mathbf{r} - \mathbf{c}_i), \tag{7.3}$$

where the truncation point P_h depends on the level and the desired accuracy. For a childless cube, i.e., the last cube at a branch of the octree, the coefficients of the expansion are obtained from

$$a_{l,m}^{\text{from } Q_i} = ik_0 \sum_{n'} \psi_{l,m}^{\text{in}\ *}(\mathbf{r}_{n'} - \mathbf{c}_i) q_{n'} \tag{7.4}$$

owing to the expansion of G in spherical wave functions,

$$G(\mathbf{r}, \mathbf{r}') \approx ik_0 \sum_{l=0}^{P_h} \sum_{m=-l}^{l} \psi_{l,m}^{\text{out}}(\mathbf{r}) \psi_{l,m}^{\text{in}\ *}(\mathbf{r}'), \tag{7.5}$$

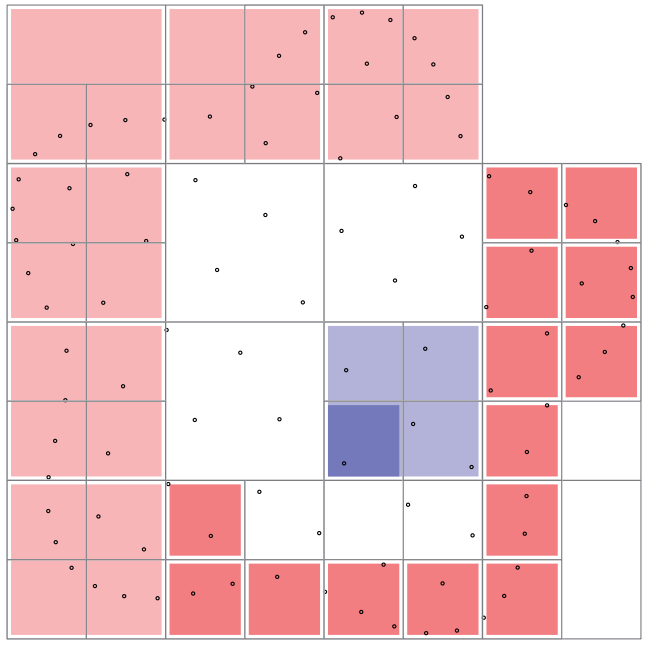

(a)

(b)

Figure 7.1. A two-level example of the hierarchical system of the MLFMA: (a) the division into cubes, and (b) the octree (or, in fact, a quadtree in this two-dimensional example). The black dots represent source points. The small, dark blue cube is a child of the large, light blue cube and, vice versa, the light blue cube is the parent of the dark blue cube. The small, dark red cubes belong to the interaction list of the dark blue cube, and the large, light red cubes belong on the interaction list of the light blue cube. The clear cubes are neighbours of the blue cubes.

given e.g. in [19, Eq. (2.42)]. For a cube with children, the coefficients are obtained by superposing translated coefficients of its children as

$$a_{l,m}^{\text{from } Q_i} = \sum_{j \,\in\, \text{children}} a_{l,m}^{\text{from } Q_j,\, \text{trans}}, \tag{7.6}$$

where

$$a_{l,m}^{\text{from } Q_j,\, \text{trans}} = \sum_{l'=0}^{P_{h-1}} \sum_{m'=-l'}^{l'} \alpha_{l,m;l',m'}^{\text{out-out}}(\mathbf{c}_i - \mathbf{c}_j) a_{l',m'}^{\text{from } Q_j,\, \text{init}}, \tag{7.7}$$

where $\alpha_{l,m;l',m'}^{\text{out-out}}(\mathbf{c}_i - \mathbf{c}_j)$ are the out-to-out translation coefficients given in (5.76).

In the disaggregation pass, the field inside each cube at each level due to the sources in all non-nearby cubes is represented by a truncated expansion in incoming spherical wave functions. For instance, the incoming field to the cube Q_i is represented as

$$\Phi^{\text{to } Q_i}(\mathbf{r}) \approx \sum_{l=0}^{P_h} \sum_{m=-l}^{l} a_{l,m}^{\text{to } Q_i} \psi_{l,m}^{\text{in}}(\mathbf{r} - \mathbf{c}_i). \tag{7.8}$$

The coefficients of the expansion are composed of two parts as

$$a_{l,m}^{\text{to } Q_i} = \sum_{j \,\in\, \text{IAL}} a_{l,m}^{\text{from } Q_j,\, \text{trans}} + a_{l,m}^{\text{to } Q_k,\, \text{trans}}. \tag{7.9}$$

The first part emerges from the coefficients of the outgoing fields from the cubes in the interaction list of Q_i translated to the coefficients of incoming fields as

$$a_{l,m}^{\text{from } Q_j,\, \text{trans}} = \sum_{l'=0}^{P_h} \sum_{m'=-l'}^{l'} \alpha_{l,m;l',m'}^{\text{out-in}}(\mathbf{c}_i - \mathbf{c}_j) a_{l',m'}^{\text{from } Q_j,\, \text{init}}, \tag{7.10}$$

where $\alpha_{l,m;l',m'}^{\text{out-in}}(\mathbf{c}_i - \mathbf{c}_j)$ are the out-to-in translation coefficients given in (5.79) or, alternatively, in (5.80). The second part emerges from the coefficients of the incoming field to the parent cube distributed to Q_i as

$$a_{l,m}^{\text{to } Q_k,\, \text{trans}} = \sum_{l'=0}^{P_{h+1}} \sum_{m'=-l'}^{l'} \alpha_{l,m;l',m'}^{\text{in-in}}(\mathbf{c}_i - \mathbf{c}_k) a_{l',m'}^{\text{to } Q_k,\, \text{init}}, \tag{7.11}$$

where $\alpha_{l,m;l',m'}^{\text{in-in}}(\mathbf{c}_i - \mathbf{c}_k)$ are the in-to-in translation coefficients given in (5.77). Finally, in the lasts cubes at the branches of the octree the field is evaluated at the points $\mathbf{r}_n$ from (7.8). Fig 7.2 illustrates a few examples of the above translations.

Now, is the above complex algorithm any faster than a simple calculation through (7.1)? To examine operation counts, denote the average number of non-empty children of a division cube by b. For a volume source

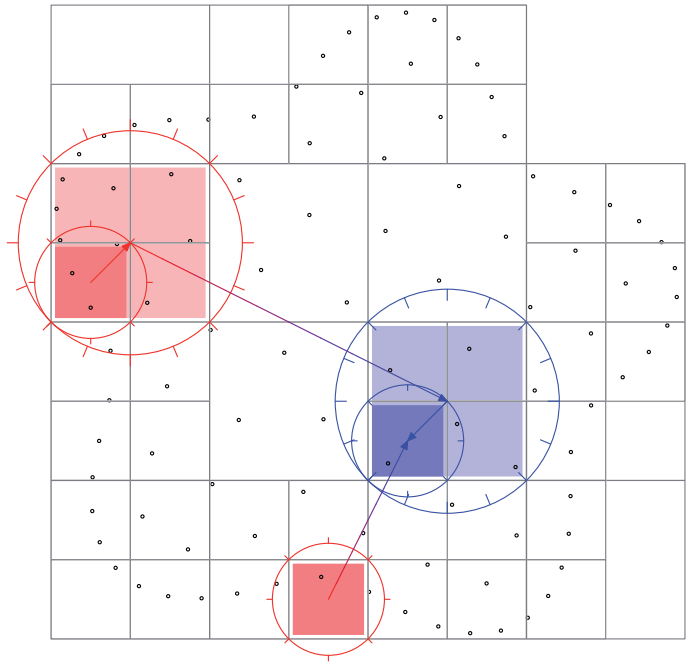

(a)

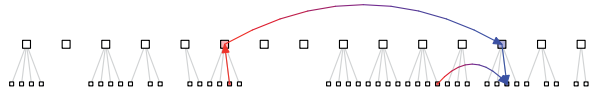

(b)

Figure 7.2. Examples of translations in the two-level MLFMA hierarchical system introduced in Fig. 7.1: (a) in the division cube structure, and (b) in the octree. The red circles with outward rays represent outgoing fields from the red cubes, and the blue circles with inward rays represent incoming fields to the blue cubes. The red arrow represents an out-to-out translation, the arrows turning from red to blue represent out-to-in translations, and the blue arrow represents an in-to-in translation.

distribution, b is close to eight, while for a surface source distribution, b equals roughly four. Then, at a level h there are approximately b^{H-h+2} non-empty division cubes in total. Assuming that most of the branches of the octree are of equal lengths, the lowest level L can be defined so that the average number of point sources per division cube is $N/b^{H-L+2} \sim 1$. Then, $H - L + 2 \sim \log_b N$. If the operation count for a procedure per division cube at a level h equals c_h, the total operation count for the procedure through the aggregation or disaggregation pass equals approximately

$$\sum_{h=L}^{H} b^{H-h+2} c_h. \tag{7.12}$$

In particular, for each of the above translations by full translation matrices per division cube at a level h, $c_h \sim P_h^4$. At the sub-wavelength levels, P_h is approximately the same at every level, as is reasoned e.g. in [27] and [28], and as can also be seen in Publication IV, Table I. That is, $P_h \approx P_0$. Thus, the total operation count through the sub-wavelength levels is proportional to

$$\sum_{h=L}^{0} b^{H-h+2} P_0^4 \sim N P_0^4. \tag{7.13}$$

Therefore, the dependency of the operation count on N is lowered from N^2 to N. At the super-wavelength levels, P_h approximately doubles when going from a level $h-1$ to a level h. That is, $P_h \approx 2P_{h-1} \approx 2^h P_0$. Thus, the total operation count through the super-wavelength levels is proportional to

$$\sum_{h=1}^{H} b^{H-h+2} (2^h P_0)^4 \sim \begin{cases} N^{\frac{4}{3}} P_0^4 & \text{if } b = 8, \\ N^2 P_0^4 & \text{if } b = 4. \end{cases} \tag{7.14}$$

Hence, for a volume source distribution, the dependency of the operation count on N lowers from N^2 to $N^{\frac{4}{3}}$, but for a surface source distribution, the algorithm does not provide virtually any improvement. Moreover, the factor P_0^4 appearing in the counts is in practice so large that it cancels out the lowering in the dependency on N. As suggested in [29] and [27, Sec. 5.3.6] and reviewed in Publication III, Sec. 6, the operation count per a division cube can be lowered to $c_h \sim P_h^3$ by implementing the translations with sequential rotation, axial translation and rotation back. Then, the total operation count through the sub-wavelength levels lowers to $N P_0^3$ and through the super-wavelength levels to

$$\sum_{h=1}^{H} b^{H-h+2} (2^h P_0)^3 \sim \begin{cases} N \log_8 N P_0^3 & \text{if } b = 8, \\ N^{\frac{3}{2}} P_0^3 & \text{if } b = 4. \end{cases} \tag{7.15}$$

It is seen that for a volume source distribution, the dependency on N already reaches $N \log_8 N$ which is typically considered the theoretical limit of MLFMA. It is, however, later found that for a volume source distribution, the dependency can be lowered further to N, which is also noticed at least in [30]. For a surface source distribution, the dependency is still $N^{3/2}$. Also, the factor P_0^3 is still quite large, at least if a high accuracy is required.

As a conclusion, the above algorithm with expansions in spherical wave functions and full translation matrices is not yet a 'fast algorithm'. At the sub-wavelength levels and for the volume source distribution at the super-wavelength levels, it can be assumed to be faster than a simple calculation through (7.1) if N is large enough. However, the ultimate efficiency of the MLFMA comes with wave patterns and diagonal translations, which are discussed next.

7.2 Diagonal translations with wave patterns

As explained in Section 5.4, the coefficients of the expansion of a field in spherical wave functions are essentially the same as the coefficients of the expansion of a radiation or incoming wave pattern of the field in spherical harmonics. Furthermore, besides these coefficients, the wave pattern can equally well be stored as its values, or samples, at appropriate points on the unit sphere B defined in (5.59) or the complex surface C defined in (5.71). When applied to the coefficients, the translations in (7.7), (7.10) and (7.11) equal multiplications by full matrices, but when applied to the samples, these translation matrices become diagonal and multiplications by them faster.

Consider the out-to-out translation in (7.7). The coefficients of the translation can be expressed as in (5.76). By substituting (5.76) into (7.7) and interchanging the order of integration and summation, the translation can be reformulated as

$$\begin{aligned} a_{l,m}^{\text{trans}} &= \sum_{l'=0}^{P_{h-1}} \sum_{m'=-l'}^{l'} \alpha_{l,m;l',m'}^{\text{out-out}}(\mathbf{t}) a_{l',m'}^{\text{init}} \\ &= \sum_{l'=0}^{P_{h-1}} \sum_{m'=-l'}^{l'} \left[i^{l-l'} \int_B Y_{l,m}{}^*(\hat{k}) Y_{l',m'}(\hat{k}) e^{ik_0 \hat{k}\cdot\mathbf{t}} \, d\Omega \right] a_{l',m'}^{\text{init}} \\ &= i^l \int_B e^{ik_0 \hat{k}\cdot\mathbf{t}} \left[\sum_{l'=0}^{P_{h-1}} \sum_{m'=-l'}^{l'} (-i)^{l'} a_{l',m'}^{\text{init}} Y_{l',m'}(\hat{k}) \right] Y_{l,m}{}^*(\hat{k}) \, d\Omega, \end{aligned} \tag{7.16}$$

where $\mathbf{t} = \mathbf{c}_i - \mathbf{c}_j$ for short. The result of (7.16) can be divided into three consecutive steps as

$$\Phi_\infty^{\text{init}}(\hat{k}) = \sum_{l=0}^{P_{h-1}} \sum_{m=-l}^{l} (-i)^l a_{l,m}^{\text{init}} Y_{l,m}(\hat{k}), \tag{7.17}$$

$$\Phi_\infty^{\text{trans}}(\hat{k}) = e^{ik_0 \hat{k}\cdot\mathbf{t}} \Phi_\infty^{\text{init}}(\hat{k}), \tag{7.18}$$

$$a_{l,m}^{\text{trans}} = i^l \int_B \Phi_\infty^{\text{trans}}(\hat{k}) Y_{l,m}{}^*(\hat{k})\, d\Omega. \tag{7.19}$$

In the above steps, first in (7.17), the coefficients $a_{l,m}^{\text{init}}$ are transformed into samples of the initial radiation pattern $\Phi_\infty^{\text{init}}$ on B with the origin at $\mathbf{c}_j$. Then in (7.18), the origin is translated to $\mathbf{c}_i$ resulting in the samples of the translated radiation pattern $\Phi_\infty^{\text{trans}}$. This translation equals a multiplication of the sample vector by a diagonal translation matrix. Finally in (7.19), the samples of $\Phi_\infty^{\text{trans}}$ are transformed back into coefficients $a_{l,m}^{\text{trans}}$. The integral in (7.19) over the unit sphere B is most efficiently and accurately evaluated by using the Gaussian rule with $P_h + 1$ points in the α-direction and the trapezoidal rule with $2P_h + 1$ points in the β-direction. These rules define the appropriate sampling points for the radiation patterns.

The out-to-in translation (7.10) is diagonalised in a similar way by expressing the translation coefficients as in (5.79):

$$\begin{aligned} a_{l,m}^{\text{trans}} &= \sum_{l'=0}^{P_h} \sum_{m'=-l'}^{l'} \alpha_{l,m;l',m'}^{\text{out-in}}(\mathbf{t}) a_{l',m'}^{\text{init}} \\ &= \sum_{l'=0}^{P_h} \sum_{m'=-l'}^{l'} \left[i^{l-l'} \int_B Y_{l,m}{}^*(\hat{k}) Y_{l',m'}(\hat{k}) T_{2P_h}(\hat{k}, \mathbf{t})\, d\Omega \right] a_{l',m'}^{\text{init}} \\ &= i^l \int_B T_{2P_h}(\hat{k}, \mathbf{t}) \left[\sum_{l'=0}^{P_h} \sum_{m'=-l'}^{l'} (-i)^{l'} a_{l',m'}^{\text{init}} Y_{l',m'}(\hat{k}) \right] Y_{l,m}{}^*(\hat{k})\, d\Omega, \end{aligned} \tag{7.20}$$

where $\mathbf{t} = \mathbf{c}_i - \mathbf{c}_j$ for short. Divided into three consecutive steps, the result of (7.20) reads

$$\Phi_\infty^{\text{init}}(\hat{k}) = \sum_{l=0}^{P_h} \sum_{m=-l}^{l} (-i)^l a_{l,m'}^{\text{init}} Y_{l,m'}(\hat{k}), \tag{7.21}$$

$$\Phi_{0,B}^{\text{trans}}(\hat{k}) = T_{2P_h}(\hat{k}, \mathbf{t}) \Phi_\infty^{\text{init}}(\hat{k}), \tag{7.22}$$

$$a_{l,m}^{\text{trans}} = i^l \int_B \Phi_{0,B}^{\text{trans}}(\hat{k}) Y_{l,m}{}^*(\hat{k})\, d\Omega. \tag{7.23}$$

Here, $\Phi_{0,B}^{\text{trans}}$ is the incoming wave pattern of the field Φ^{trans} on B with the origin at $\mathbf{c}_i$. The translation in (7.22) equals a multiplication of the sample vector by a diagonal translation matrix. The integral in (7.23) can be evaluated by using similar points as in (7.19). However, for the

translation in (7.22), $\Phi_\infty^{\text{init}}$ must be interpolated to the double size because T_{2P_h} is of order $2P_h$.

The in-to-in translation (7.11) is diagonalised similarly as the out-to-out translation in (7.7).

The above derivation of the diagonal translations in the super-wavelength levels is somewhat similar than the one given in [31].

Due to the property of (5.79), the diagonalisation of the out-to-in translation in (7.20) works only when $\mathbf{t}$ is not too short in wavelengths, i.e., at the super-wavelength levels. At the sub-wavelength levels, the out-to-in translation can be diagonalised by expressing the translation coefficients by using the alternative expression given in (5.80):

$$\begin{aligned} a_{l,m}^{\text{trans}} &= \sum_{l'=0}^{P_h} \sum_{m'=-l'}^{l'} \alpha_{l,m;l',m'}^{\text{out-in}}(\mathbf{t}) a_{l',m'}^{\text{init}} \\ &= \sum_{l'=0}^{P_h} \sum_{m'=-l'}^{l'} \left[i^{l-l'} \int_C Y_{l,m}{}^*(\hat{k}) e^{ik_0 \hat{k}\cdot\mathbf{t}} Y_{l',m'}(\hat{k})\, d\Omega \right] a_{l',m'}^{\text{init}} \\ &= i^l \int_C e^{ik_0\hat{k}\cdot\mathbf{t}} \left[\sum_{l'=0}^{P_h} \sum_{m'=-l'}^{l'} (-i)^{l'} a_{l',m'}^{\text{init}} Y_{l',m'}(\hat{k}) \right] Y_{l,m}{}^*(\hat{k})\, d\Omega. \end{aligned} \tag{7.24}$$

Divided into three consecutive operations, the result of (7.24) reads

$$\Phi_\infty^{\text{init}}(\hat{k}) = \sum_{l=0}^{P_h} \sum_{m=-l}^{l} (-i)^l a_{l,m'}^{\text{init}} Y_{l,m'}(\hat{k}), \tag{7.25}$$

$$\Phi_{0,C}^{\text{trans}}(\hat{k}) = e^{ik_0\hat{k}\cdot\mathbf{t}} \Phi_\infty^{\text{init}}(\hat{k}), \tag{7.26}$$

$$a_{l,m}^{\text{trans}} = i^l \int_C \Phi_{0,C}^{\text{trans}}(\hat{k}) Y_{l,m}{}^*(\hat{k})\, d\Omega. \tag{7.27}$$

Here, $\Phi_{0,C}^{\text{trans}}$ is the incoming wave pattern of the field Φ^{trans} on C. The translation in (7.26) equals a multiplication of the sample vector by a diagonal translation matrix. The integral in (7.27) over the complex domain C can be evaluated by using the integration rule introduced in [32] and also described in [33] in the α-direction and the trapezoidal rule in the β-direction.

The above diagonal out-to-in translation at the sub-wavelength levels was first introduced in [34].

The out-to-out and in-to-in translations at the sub-wavelength levels are treated similarly as at the super-wavelength levels.

At the sub-wavelength levels, the operation counts in the diagonalised translations are $c_h \sim P_0^2$, and the total operation counts are proportional to NP_0^2. At the super-wavelength levels, the operation counts in the diagonalised translations are proportional to $c_h \sim (2^h P_0)^2$. Then, the total

operation counts are proportional to

$$\sum_{h=1}^{H} b^{H-h+2}(2^h P_0)^2 \sim \begin{cases} NP_0^2 & \text{if } b = 8, \\ N \log_4 NP_0^2 & \text{if } b = 4. \end{cases} \tag{7.28}$$

So, the diagonalised translations are fast also at the super-wavelength levels. However, the transforms between the coefficients and samples are slow, as explained and corrected next.

7.3 Interpolation and anterpolation

In the aggregation pass, the size of a division cube doubles between two consecutive levels. Because of this, at the super-wavelength levels, also the number of required terms in the expansion of the field of the source enclosed by a division cube in outgoing wave functions increases. For the corresponding samples of the radiation pattern, this equals interpolation. Respectively, in the disaggregation pass, the size of a division cube halves and the number of required terms in the expansion of the field inside a division cube in incoming wave functions decreases between two consecutive levels. For the corresponding samples of the incoming wave pattern, this equals anterpolation. In addition, as mentioned, the out-to-in translation requires the radiation pattern to be interpolated into a double size compared to the storage size. At the sub-wavelength levels, the number of required terms in the expansion of the field in wave functions does not vary because of the dominance of the evanescent waves. However, interpolations and anterpolations are still needed if the translations are performed for the wave patterns. This is because the required sampling points are located differently on C at different levels.

Since the interpolation and anterpolation are just zero-padding or truncation, respectively, for coefficients whereas the translations are diagonal for samples, it might sound a good idea to alternate between the two representations throughout the algorithm. The bottleneck, however, would then be the transforms, such as (7.17) and (7.19), between the representations. That is to say, although it is easy to use the Fast Fourier transform (FFT) for computing the Fourier transforms in the β-direction with an operation count proportional to $P_h^2 \log_2 P_h$, it is difficult to find a fast algorithm for computing the Legendre transforms in the α-direction. The operation count for computing the transforms by direct multiplication by a transformation matrix is proportional to P_h^3. There are two asymptotically

faster algorithms presented in [35] for computing the Legendre transform with operation counts proportional to $P_h^{5/2} \log P_h$ and $P_h^2 (\log P_h)^2$, but the prefactors for these algorithms seem to be noticeable larger than for the FFT. When $c_h \sim P_h^3$, the total operation count through the sub-wavelength levels is proportional to NP_0^3 and through the super-wavelength levels to

$$\sum_{h=1}^{H} b^{H-h+2} (2^h P_0)^3 \sim \begin{cases} N \log_8 N P_0^3 & \text{if } b = 8, \\ N^{\frac{3}{2}} P_0^3 & \text{if } b = 4. \end{cases} \tag{7.29}$$

This would throw away the benefit obtained by the diagonal translations. Therefore, to take advantage of the diagonal translations, the interpolations and anterpolations must be implemented some other way without interchanging to coefficients.

Most of the broadband multilevel fast multipole algorithms, for instance, the algorithms described in [36] and [37], apply expansions in wave functions at the sub-wavelength levels and samples of wave patterns at the super-wavelength levels. At the sub-wavelength levels, the out-to-out and in-to-in translations are performed for coefficients by the 'rotation - diagonal translation - rotation back' -procedure, as explained e.g. in [27, Sec. 5.3.6]. The out-to-in translation is performed by transforming the coefficients to samples, translating the samples diagonally and then transforming the samples back to coefficients, like described in (7.25)–(7.27). The interpolations and anterpolations are performed for the coefficients by zero-padding and truncation, respectively. At the super-wavelength levels, all the translations are performed for samples diagonally. In the algorithm described in [36], the interpolations and anterpolations are performed by using a local interpolator. In the algorithm described in [37], the interpolations and anterpolations are performed by using the FFT in the β-direction and a one-dimensional fast multipole method in the α-direction.

An algorithm presented in [38] and reviewed in [33] and Publication IV applies an alternative expansion at the super-wavelength levels that enables performing the interpolations and anterpolations of the wave patterns by a full use of the FFT. In addition, in Publication IV is presented a novel method that enables the use of the wave patterns and almost a full use of the FFT also at the sub-wavelength levels. These alternative expansions are briefly described next.

7.4 Alternative expansions enabling full use of the FFT

Besides expansions in spherical harmonics, wave patterns can also be expanded in exponential functions, as presented in [38]. For instance, a radiation pattern Φ_∞ can be expanded as

$$\Phi_\infty(\alpha,\beta) = \sum_{l=-P_h}^{P_h} \sum_{m=-P_h}^{P_h-1} u_{l,m} e^{i(l\alpha+m\beta)}, \tag{7.30}$$

where

$$u_{l,m} = \frac{1}{(2\pi)^2} \int_0^{2\pi} \int_0^{2\pi} \Phi_\infty(\alpha,\beta) e^{-i(l\alpha+m\beta)}\, d\alpha\, d\beta. \tag{7.31}$$

The integrals in (7.31) can be evaluated by using equally spaced sampling points in both the α- and β-directions. This means that transforms between the samples of Φ_∞ and the coefficients $u_{l,m}$ can be performed by using the FFT in both directions, and the interpolations and anterpolations can be performed by zero-padding and truncation, respectively. This is faster than the interpolations and anterpolations with the expansions in spherical harmonics. Although the double integration in (7.31) goes over the unit sphere twice, due to the 'sphericality' defined in [38], the samples of the wave pattern need to be stored only on a half of the integration domain, i.e., on the unit sphere B. Thanks to the full use of the FFT, the operation counts in (7.30) and (7.31) at level h are $c_h \sim P_h^2 \log_2 P_h$. Then, the total operation count through the super-wavelength levels is proportional to

$$\sum_{h=1}^{H} b^{H-h+2} (2^h P_0)^2 \log_2(2^h P_0) \sim \begin{cases} N P_0^2 \log_2 P_0 & \text{if } b = 8, \\ N (\log_4 N)^2 P_0^2 & \text{if } b = 4. \end{cases} \tag{7.32}$$

Another alternative method for expanding wave patterns, enabling almost a full use of the FFT at the sub-wavelength levels, is presented in Publication IV. Accordingly, a wave pattern, for instance, a radiation pattern Φ_∞, is firstly expanded in the β-direction in exponential functions as

$$\Phi_\infty(\alpha,\beta) \approx \sum_{m=-P_h}^{P_h} U_m(\cos\alpha) e^{im\beta}, \tag{7.33}$$

where

$$U_m(\cos\alpha) = \frac{1}{2\pi} \int_0^{2\pi} \Phi_\infty(\alpha,\beta) e^{-im\beta}\, d\beta. \tag{7.34}$$

Since U_m are essentially expansions in the associate Legendre functions of order m, they can be decomposed as

$$U_m(\cos\alpha) = [1 - (\cos\alpha)^2]^{|m|/2} V_m(\cos\alpha), \tag{7.35}$$

where V_m are polynomials of order $P_h - |m|$. These polynomials are then expanded as

$$V_m(\cos\alpha) = \sum_{j=0}^{P_h-|m|} v_{j,m}(\cos\alpha)^j, \tag{7.36}$$

where $v_{j,m}$ are the eventual coefficients of the complete expansion. So, if $v_{j,m}$ are known, Φ_∞ is obtained through (7.36), (7.35) and (7.33); and vice versa, if Φ_∞ is known at a proper set of sampling points, $v_{j,m}$ are obtained through (7.34) and the transposes of (7.35) and (7.36).

It is clear that the integral in (7.34) can be calculated by using a trapezoidal rule with $2P_h + 1$ sampling points, and so equally spaced points are proper sampling points in the β-direction. But how should the sampling points be chosen in the α-direction? In principle, the transpose of (7.36) can be calculated, provided that V_m is known at least at $P_h + 1$ distinct sampling points. To perform the out-to-in translation at a sub-wavelength level with wave patterns, V_m is required at sampling points along Γ defined in (5.72). With such sampling points, however, the calculations of (7.36) and its transpose are slow. On the other hand, fast transforms would surely be provided if V_m was sampled at equally spaced sampling points along $[0, 2\pi)$, as in the transforms (7.30) and (7.31), but those sampling points would not enable the evaluation of V_m along Γ. Evaluating a sampled function on points other than the initial sampling points corresponds to an interpolation or extrapolation, and in the above case, the initial sampling points would be too far from the target points. Fast transforms and possibility to extrapolate onto Γ are both provided if $\cos\alpha$ is fixed onto a circle on a complex plane according to $\cos\alpha = \varrho e^{i\gamma}$ where ϱ is a level-dependent constant and $\gamma \in [0, 2\pi)$. Then, (7.36) becomes

$$V_m(\varrho e^{i\gamma}) = \sum_{j=0}^{P_h-|m|} v_{j,m}\varrho^j e^{ij\gamma}, \tag{7.37}$$

where

$$v_{j,m} = \varrho^{-j}\frac{1}{2\pi}\int_0^{2\pi} V_m(\varrho e^{i\gamma})e^{-ij\gamma}\,d\gamma, \tag{7.38}$$

which can be calculated by using a trapezoidal rule with $P_h + 1$ sampling points. Fig. 7.3 shows how these new paths at different levels compare to the path Γ. The same thing is shown in a different way in Publication IV, Fig. 5.

If the wave patterns are sampled at the sampling points suggested above, the transforms between the coefficients and samples can be performed by three consecutive fast operations: FFT, multiplication by a diagonal

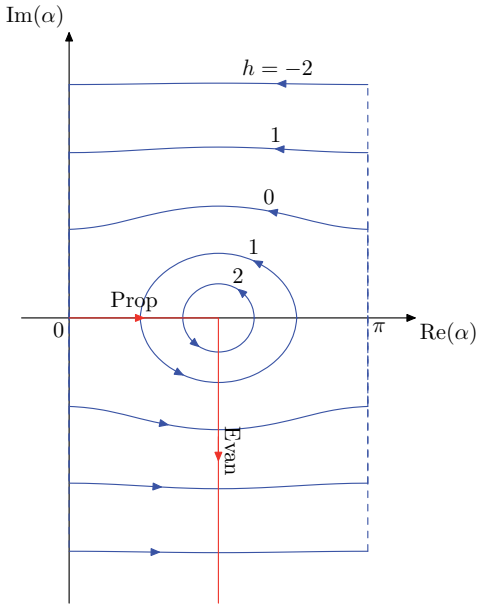

Figure 7.3. Illustrative paths on the complex α-plane defined by $\cos\alpha = \varrho e^{i\gamma}$ when $k_0 s_h = 2^h\pi$, $h = -2, -1, 0, 1, 2$, and $\gamma \in [0, 2\pi)$ (blue paths) in comparison to Γ (red path).

matrix and another FFT. Then, the interpolations and anterpolations between the levels can be performed by zero-padding or truncating the coefficients, while the out-to-out and in-to-in translations can be performed by multiplying the sample vectors by diagonal translation matrices. To perform the out-to-in translation, the radiation pattern needs to be evaluated in the α-direction along Γ. This can be done by extrapolating through (7.36) and its transpose. The work of this operation is proportional to P_h^3. So, this operation is not fast. Moreover, the extrapolation works at the sub-wavelength levels but loses its accuracy at the super-wavelength levels. This is because greater values of $k_0 s_h$ force ϱ to be reduced so small that the extrapolation onto the interval $(0, \pi/2)$ corresponding to the propagating waves is no longer successful.

7.5 Error control

Since the MLFMA rests fundamentally on truncated expansions in spherical wave functions, it suffers from truncation errors. However, these errors can be controlled through the truncation points of the expansions. In addition, the use of numerical integration generates integration errors,

but in general they can be kept negligible by choosing sampling points properly. The use of the Rokhlin translator at too low levels with too high accuracy requirements could generate severe integration errors, but this can be avoided by using the alternative methods at the lower levels.

As an example of determining a truncation point, consider the basic MLFMA described in Sections 7.1–7.3. For this algorithm, the proper truncation point P_h at a level h is such that the field outside a cube Q_i due to the source inside Q_i can be evaluated from the expansion in (7.3) with the required accuracy for any possible source point $\mathbf{r}'$ and observation point $\mathbf{r}$. It can be determined by studying the error in approximating the Green's function by the expansion in (7.5):

$$\left| G(\mathbf{r},\mathbf{r}') - ik_0 \sum_{l=0}^{P_h} \sum_{m=-l}^{l} \psi_{l,m}^{\text{out}}(\mathbf{r}) \psi_{l,m}^{\text{in}\ *}(\mathbf{r}') \right| / |G(\mathbf{r},\mathbf{r}')| < 10^{-d}, \tag{7.39}$$

where d is the required number of accurate digits. The convergence of the expansion is the slower the longer $\mathbf{r}'$ and the shorter $\mathbf{r}$. So, the worst case is when $\mathbf{r}'$ is at a corner of $Q_i$so that $|\mathbf{r}'| = \sqrt{3}s_h/2$ and $\mathbf{r}$ is in the closest non-nearby cube located so that $|\mathbf{r}| = 3s_h/2$. Roughly speaking, P_h must then be slightly larger than $\sqrt{3}\,ks_h/2$. However, the exact values are easily calculated from (7.39), and they can then be tabulated. In Publication IV the truncation points for different expansions are calculated and tabulated by using the same idea.

After the truncation point P_h has been fixed, the proper sampling points required for the diagonal translations can be defined.

7.6 Application to a scattering model of a pine tree

In Publication V, the scattering of the electromagnetic plane wave by the top of a pine tree is modelled by using the MoM and the solution is sped up by using the MLFMA presented in Publication IV and overviewed above.

The top of the pine tree is modelled by a collection of dielectric cylinders, in each of which the electric susceptibility χ is assumed constant. The problem is formulated by the volume integral equation (3.17). So, the unknown of the problem is the electric field $\mathbf{E}$ inside the trunk and the needles. $\mathbf{E}$ is expanded in simple piece-wise constant basis functions as

$$\mathbf{E}(\mathbf{r}) \approx \sum_{n'=1}^{N} \mathbf{E}_{n'} b_{n'}(\mathbf{r}), \tag{7.40}$$

where $b_{n'}$ equals unity inside the n'th cylinder and is zero elsewhere. Substituting (7.40) into (3.17) yields

$$\sum_{n'=1}^{N}\left[\mathbf{E}_{n'}b_{n'}(\mathbf{r})-\chi_{n'}(k_0^2\mathbb{I}+\nabla\nabla)\cdot\int_{V_{n'}}G(\mathbf{r},\mathbf{r}')\mathbf{E}_{n'}\,dV'\right]=\mathbf{E}^{\text{inc}}(\mathbf{r}). \tag{7.41}$$

This equation is tested by the delta functions defined in (4.34), resulting in a set of equations

$$\mathbf{E}_n-\sum_{n'=1}^{N}\mathbb{A}_{n,n'}\cdot\mathbf{E}_{n'}=\mathbf{E}_n^{\text{inc}},\quad n=1,\ldots,N, \tag{7.42}$$

where $\mathbf{E}_n=\mathbf{E}(\mathbf{r}_n)$, $\mathbf{E}_n^{\text{inc}}=\mathbf{E}^{\text{inc}}(\mathbf{r}_n)$ and $\mathbb{A}_{n,n'}=\mathbb{A}_{n'}(\mathbf{r}_n)$ where

$$\mathbb{A}_{n'}(\mathbf{r})=\chi_{n'}(k_0^2\mathbb{I}+\nabla\nabla)\int_{V_{n'}}G(\mathbf{r},\mathbf{r}')\,dV'. \tag{7.43}$$

Because of the complicated geometry with a lot of small details and the coarse discretisation, N in (7.42) is large. So, to solve the system it is necessary to use an iterative method together with the MLFMA. To that end, the summation in (7.42) is divided into two parts as

$$\sum_{n'=1}^{N}\mathbb{A}_{n,n'}\cdot\mathbf{E}_{n'}=\sum_{n'\,\in\,\text{near}}\mathbb{A}_{n,n'}\cdot\mathbf{E}_{n'}+\sum_{n'\,\in\,\text{far}}\mathbb{A}_{n,n'}\cdot\mathbf{E}_{n'}, \tag{7.44}$$

in analogy to the division in (7.1). Furthermore, in the latter summation on the right-hand-side of (7.44), the field point is sufficiently far from the source point so that $\mathbb{A}_{n,n'}$ can be evaluated from the approximate expression

$$\mathbb{A}_{n'}(\mathbf{r})\approx\chi_{n'}k_0^2V_{n'}\mathbb{G}(\mathbf{r},\mathbf{r}_{n'}), \tag{7.45}$$

and the summation becomes

$$\sum_{n'\,\in\,\text{far}}\mathbb{A}_{n,n'}\cdot\mathbf{E}_{n'}\approx\sum_{n'\,\in\,\text{far}}\chi_{n'}k_0^2V_{n'}\mathbb{G}(\mathbf{r}_n,\mathbf{r}_{n'})\cdot\mathbf{E}_{n'}. \tag{7.46}$$

This summation is calculated by using the MLFMA.

8. Conclusions

In the introduction, the thesis was divided into two main topics: the first one is about solving selected electromagnetic problems formulated by integral equations, and the second one is about exploiting translational addition theorems for wave functions. From the point of view of the results, the thesis can be divided into two resulting methods: the first one is the spatial-spectral hybrid method for calculating the capacitances and inductances of ring conductors in a layered medium, and the second one is the broadband version of the MLFMA with novel expansions of wave patterns at the sub-wavelength levels.

The spectral method presented in Publication I applies the Hankel transform, or equivalently, expansions in cylindrical static wave functions to simplify the solution of the static Green's function in a layered medium. In addition, the method uses physical and compact expansions of the surface charge and current in basis functions on indefinitely thin ring conductors. Consequently, the method provides efficient and accurate calculations of the capacitances and inductances of indefinitely thin ring conductors in a layered medium. As an application of the method, Publication I demonstrates a quasi-static analysis of a spiral microstrip inductor. To that end, Publication I introduces a two-step approximation where a spiral conductor is approximated by a system of ring conductors and the dynamic electromagnetic field is approximated by electro- and magnetostatic fields. As shown by a numerical test, the approximation works surprisingly well throughout the practical frequency band of a spiral inductor and even further.

The spatial-spectral hybrid method presented in Publication II introduces two improvements to the above purely spectral method: firstly, it uses a two-step calculation of MoM system matrix entries where singular free-space terms are calculated in the spatial domain and non-singular

image source terms in the spectral domain; secondly, it applies similar physical and compact expansions of the surface charge and current in basis functions as the earlier method but allows ring conductors of arbitrary thickness.

The bottle neck in the above spatial-spectral hybrid method in terms of both the efficiency and accuracy is the calculation of the integrals in Publication II, Eqs. (32) and (38), or equivalently, the integrals in (6.18) and (6.22). Due to the singularity of the Green's function, these integrals need a special treatment when the field is calculated on or near to the support of the basis function. The calculation could be improved by finding analytic formulae for the potentials due to the basis functions in a free space. This equals the requirement 4 in Section 6.4. For an indefinitely thin ring conductor when the field point is at the same height with the source point, this can be done by the integral results derived in [39]. Also, as mentioned in Publication II, Section 9, the edge singularity of the surface charge or current on a finite thick conductor changes if the top or bottom face of the conductor touches an interface between two medium layers. In that case, the weight function and the related basis functions with the strictly correct edge singularity could be obtained by using Jacobi polynomials, defined e.g. in [25, Sec. 22]. A yet more ambitious goal would be to formulate a new, natural set of basis functions for a ring geometry satisfying also the requirement 3 in Section 6.4. This would require a definition of a new system of co-ordinates, similar to a toroidal system but with an elliptical cross-section. Finally, the method could be generalised to an analysis of ring conductors around different axes or to a similar analysis of dynamic problems. Both of the above generalisations would require an analysis of higher ϕ-modes of the charge and current and also currents with a ρ-component.

The derivation of the translational addition theorems for the spherical wave functions presented in Publication III, besides providing a unified and transparent derivation of the theorems through the wave patterns, serves also as a supporting study for the development of the MLFMA. As emphasised in Section 7.2, the results of Publication III, some of them reformulated in Section 5.4, give a nice additional view for the translations and their diagonalisations in the MLFMA.

As a subsequent step after the spherical wave functions, it would be interesting to study the addition theorems for ultra-spherical wave functions. Even though there might not be as many direct applications for the

ultra-spherical wave functions as for the spherical ones, the addition theorems for them might provide some useful integral results, like the one in (6.38), which yields the Fourier transform for the basis functions for the surface charge on a finitely thick strip conductor.

The broadband version of the MLFMA presented in Publication IV differs from the traditional approaches in that it applies diagonal translations together with such expansions of wave patterns that interpolations and anterpolations can be performed almost exclusively by the FFT throughout the algorithm at the sub-wavelength levels as well as the super-wavelength levels. The traditional approaches apply ordinary expansions in spherical wave functions at the sub-wavelength levels and because of that either out-to-out and in-to-in translations or interpolations and anterpolations are slower, at least in theory. Comparing the practical performance of two different versions of the MLFMA is quite difficult. For practical comparisons, one would need to implement both the rival version as well as the own version on the same platform with the same care and devotedness. On the other hand, while one can always make theoretical analyses on operation counts, as was done in Section 7, they can never include effects of all the details of a complex MLFMA. Although such analyses give limits for the dependency of the operation counts on the number of unknowns, N, and the number of expansion modes at the sub-wavelength levels, P_0, the multiplying constant is much more difficult to determine. Nevertheless, since relying almost exlusively on the FFT, the broadband version of the MLFMA presented in this thesis has at the sub-wavelength levels operation counts with respect to P_0 proportional to $P_0^2 \log_2 P_0$ while for the traditional approaches the counts are proportional to P_0^3. This must eventually pay off when P_0 is large, which happens when a high accuracy is required. Another contribution of Publication IV is the rigorous, numerical determination of the minimum number of expansion modes, P_h, at different levels h so that the expansions still yield the required accuracy.

The presented broadband version of the MLFMA is applied in Publication V in the solution of the scattering of the electromagnetic plane wave by the top of a pine tree. To the best knowledge of the author, such a detailed solution of the scattering from a pine tree is the first one. A similar solution without the MLFMA is applied in [40] in the solution of the scattering by a pine shoot.

Bibliography

[1] I. Lindell and A. Sihvola, *Sähkömagneettinen kenttäteoria: 1. Staattiset kentät*. Otatieto, 1995.

[2] A. Sihvola and I. Lindell, *Sähkömagneettinen kenttäteoria: 2. Dynaamiset kentät*. Otatieto, 1995.

[3] J. A. Stratton, *Electromagnetic Theory*. McGraw-Hill, 1941.

[4] J. D. Jackson, *Classical Electrodynamics*, 3rd ed. Wiley, 1998.

[5] W. K. H. Panofsky and M. Phillips, *Classical Electricity and Magnetism*, 2nd ed. Addison-Wesley, 1962.

[6] E. Kreyszig, *Introductory Functional Analysis with Applications*. Wiley, 1989.

[7] R. F. Harrington, *Field computation by Moment Methods*. Macmillan, 1968.

[8] R. Harrington, "Origin and development of the method of moments for field computation," *Antennas and Propagation Society Magazine*, pp. 31–36, 1990.

[9] I. Lindell, *Sähkömagnetiikan likimääräismenetelmät*.

[10] C. H. Chen and C.-D. Lien, "The variational principle for non-self-adjoint electromagnetic problems," *IEEE Trans. Microwave Theory Tech.*, vol. 28, no. 8, pp. 878–886, 1980.

[11] A. F. Peterson, D. R. Wilton, and R. E. Jorgenson, "Variational nature of Galerkin and non-Galerkin moment method solutions," *IEEE Trans. Antennas Propagat.*, vol. 44, no. 4, pp. 500–503, 1996.

[12] D. G. Dudley, "Comments on 'variational nature of Galerkin and non-Galerkin moment method solutions'," *IEEE Trans. Antennas Propagat.*, vol. 45, no. 6, pp. 1062–1063, 1997.

[13] J. Meixner, "The behaviour of electromagnetic fields at edges," *IEEE Trans. Antennas Propagat.*, vol. 20, no. 4, pp. 442–446, 1972.

[14] J. V. Bladel, *Singular Electromagnetic Fields and Sources*. Wiley, 1996.

[15] J. C.-E. Sten, "Focal image charge singularities for the dielectric elliptic cylinder," *Electrical Engineering (Archic für Elektrotechnik)*, vol. 79, no. 1, pp. 9–15, 1996.

[16] S. M. Rao, D. R. Wilton, and A. W. Glisson, "Electromagnetic scattering by surfaces of arbitrary shape," *IEEE Trans. Antennas Propagat.*, vol. 30, no. 3, pp. 409–418, 1982.

[17] L. N. Trefethen and D. Bau, *Numerical Linear Algebra*. SIAM, 1997.

[18] G. N. Watson, *A Treatise on the Theory of Bessel Functions*, 2nd ed. Cambridge University Press, 1944.

[19] D. Colton and R. Kress, *Inverse Acoustic and Electromagnetic Scattering Theory*, 2nd ed. Springer, 1998.

[20] A. J. Devaney and E. Wolf, "Multipole expansions and plane wave representations of the electromagnetic field," *J. Math. Phys.*, vol. 15, no. 2, pp. 234–244, 1974.

[21] W. C. Chew and J. A. Kong, "Resonance of nonaxial symmetric modes in circular microstrip disk antenna," *J. Math. Phys.*, vol. 21, no. 10, pp. 2590–2598, 1980.

[22] G. Miano, G. Panariello, F. Schettino, and L. Verolino, "Ring capacitance in microstrip," *Journal of Electrostatics*, vol. 46, no. 1, pp. 49–57, 1999.

[23] G. Panariello, F. Schettino, and L. Verolino, "Capacitance of an annular ring between two conducting plates," *Electrical Engineering (Archiv für Elektrotechnik)*, vol. 82, no. 1, pp. 11–15, 1999.

[24] S. Falco, G. Panariello, F. Schettino, and L. Verolino, "Capacitance of a finite cylinder," *Electr. Eng.*, vol. 85, pp. 177–182, 2003.

[25] M. Abramowitz and I. A. Stegun, Eds., *Handbook of Mathematical Functions*. Dover Publications, 1970.

[26] R. Coifman, V. Rokhlin, and S. Wandzura, "The fast multipole method for the wave equation: a pedestrian prescription," *IEEE Antennas Propag. Mag.*, vol. 35, no. 3, pp. 7–12, 1993.

[27] W. C. Chew, J.-M. Jin, E. Michielssen, and J. Song, Eds., *Fast and Efficient Algorithms in Computational Electromagnetics*. Artech House, 2001.

[28] N. A. Gumerov and R. Duraiswami, *Fast Multipole Methods for the Helmholtz Equation in Three Dimensions*. Elsevier, 2004.

[29] J.-S. Zhao and W. C. Chew, "Applying matrix rotation to the three-dimensional low-frequency multilevel fast multipole algorithm," *Microw. Opt. Technol. Lett.*, vol. 26, no. 2, pp. 105–110, 2000.

[30] I. B. J. De Zaeytijd and A. Franchois, "An efficient hybrid MLFMA-FFT solver for the volume integral equation in case of sparse 3D inhomogeneous dielectric scatterers," *J. Comput. Phys.*, vol. 227, pp. 7052–7068, 2008.

[31] W. C. Chew, S. Koc, J. M. Song, and E. Michielssen, "A succinct way to diagonalize the translation matrix in three dimensions," *Microw. Opt. Technol. Lett.*, vol. 15, no. 3, pp. 144–147, 1997.

[32] N. Yarvin and V. Rokhlin, "Generalized Gaussian quadratures and singular value decompositions of integral operators," *SIAM J. Comput.*, vol. 20, no. 2, pp. 699–718, 1998.

[33] H. Wallén and J. Sarvas, "Translation procedures for broadband MLFMA," *Progress in Electromagnetics Research*, vol. PIER 55, pp. 47–78, 2005.

[34] L. J. Jiang and W. C. Chew, "Low-frequency fast inhomogeneous plane-wave algorithm (LF-FIPWA)," *Microwave Opt. Tech. Lett.*, vol. 40, no. 2, pp. 117–122, Jan. 2004.

[35] M. J. Mohlenkamp, "A fast transform for spherical harmonics," *J. Fourier Analy. Applicat.*, vol. 5, no. 2/3, pp. 159–184, 1999.

[36] L. J. Jiang and W. C. Chew, "A mixed-form fast multipole algorithm," *IEEE Trans. Antennas Propag.*, vol. 53, no. 12, pp. 4145–4156, 2005.

[37] H. Cheng, W. Y. Crutchfield, Z. Gimbutas, L. F. Greengard, J. F. Ethridge, J. Huang, V. Rokhlin, N. Yarvin, and J. Zhao, "A wideband fast multipole method for the Helmholtz equation in three dimensions," *J. Comput. Phys.*, vol. 216, pp. 300–325, 2006.

[38] J. Sarvas, "Performing interpolation and anterpolation entirely by fast Fourier transform in the 3-D multilevel fast multipole algorithm," *SIAM J. Numer. Anal.*, vol. 41, no. 6, pp. 2180–2196, 2003.

[39] A. Gervois and H. Navelet, "Integrals of some three Bessel functions and legendre functions. II," *J. Math. Phys.*, vol. 26, no. 4, pp. 645–655, 1985.

[40] T. Manninen, A. Penttilä, and K. Lumme, "C-band scattering simulation of a Scots pine shoot," *Waves Random Complex Media*, vol. 17, no. 1, pp. 85–98, 2007.

Aalto-DD 89/2011

ISBN 978-952-60-4301-2 (pdf)
ISBN 978-952-60-4300-5
ISSN-L 1799-4934
ISSN 1799-4942 (pdf)
ISSN 1799-4934

Aalto University
School of Electrical Engineering
Department of Radio Science and Engineering
www.aalto.fi

BUSINESS +
ECONOMY

ART +
DESIGN +
ARCHITECTURE

SCIENCE +
TECHNOLOGY

CROSSOVER

DOCTORAL
DISSERTATIONS